CHAPTER 27

Energy Sources and Storage - Primary Sources

The progressive proliferation of embedded and distributed generation with renewable energy sources has spurred research into alternative energy sources and storage methods. Although this chapter is mainly concerned with primary sources, namely fuel cells and photovoltaic cells, their energy and power density capabilities can only be put into context by considering conventional energy sources, specifically, the hydrocarbons.

In electrical terms, primary and secondary energy sources are defined as follows.

Primary source is not a reversible energy source. During energy discharging, the original states are permanently changed as electrical energy is released until the original energy reactants, or any one of them, are depleted. A primary cell can be used only once.

Secondary source is reversible and the original states can be reconstituted by the application of an electrical potential which injects energy into the source. A secondary cell can source and sink energy many times.

27.1 Hydrocarbon attributes

Table 27.1 shows that the energy density associated with the hydrocarbons dwarfs all other common sources such as batteries and supercapacitors. The table highlights why petrol is so firmly entrenched, while the limitations of hydrogen are made apparent. Although hydrogen offers 3 times more energy than petrol for a giving reactant weight, its volume per kg is grossly in excess of that of petrol. One mole of hydrogen H_2 occupies 22.4 litres and weight just 2 grams. Thus the energy per unit volume for petrol is 2500 times more than that for hydrogen. Table 10.2a presents the basic properties of hydrogen.

Pressurising hydrogen mitigates the volume limitation somewhat, but liquefaction is at an impractical temperature of 20K, with a density of 0.07g/cm^3 (only helium has a lower boiling point). Pressure helps minimally since the boiling point rises to only 43K at 13 bar, with minimal temperature increase for higher pressures. On the other hand, propane has a boiling point of -42°C, but can be liquefied at 21°C and 13bar, with a gain in energy density.

The expansion ratio for hydrogen is 1:850, that is, at atmospheric temperature and pressure, hydrogen gas occupies 850 times the volume as in its liquid state. The ratio is 1:240 at 250 bar and atmospheric temperature, but cannot approach the liquid ratio at much higher pressures, as shown in Table 27.2b. Basically, hydrogen has a poor molecular packing density. A cubic metre of water contains 111kg of hydrogen, whereas a cubic metre of liquid hydrogen contains only 71kg of hydrogen. In fact, water (111kg) contains more kg/m^3 of hydrogen that methanol (100kg) and a similar weight of hydrogen as in heptane (113kg). The energy stored, in Joules, is given by mass times specific energy (calorific value).

Thus, in summary, the specific energy of pure hydrogen (the energy per kilogram) is higher than any other fuel at better than 120 MJ/kg. However, its energy density (energy per m^3) is very low, that is, it is difficult to get a large mass of hydrogen into a small volume, as shown in table 27.2. Cryo-adsorption of hydrogen into graphite at low temperature and pressures up to 5MPa, or the use of metal hydrides, provide higher hydrogen storage densities, as shown in table 27.2b.
Table 27.1, in conjunction with figure 27.1, show that both batteries and super capacitors fall significantly short of the energy that can be released from hydrocarbons, on an equivalent volume and weight basis.

Table 27.1: Energy properties of hydrocarbons and alternative energy sources

Fuel Type	Fuel	CO_2 kg/kWh	Calorific Value				Density	
			MJ/kg	kWh/kg	MJ/Litre	MJ/m^3	kg/m^3	Litres/kg
solid	charcoal		30	10	-	6250	208	-
	coal	0.32	25	8	-	37500	1500	-
	wood		16	5.4	-	8000	400-700	-
	dung cake		7	2.3	-	5000	700	-
liquid	kerosene	0.27	48	15	35	44000	820	0.73
	petrol		50	16	48	37000	751	1.36
	diesel		45	15	39	38200	850	1.19
	ethanol		30	10	30	23700	789	1.00
gas	bio gas		38	12		46	1.2	
	butane(LPG)	0.23	50	16	29	30000	600	1.72
	butane gas		50	16	29	125	2.5	
	methane		55	18	0.9kJ/mol	39	0.668	
	hydrogen		150	49	5.6	13	0.0838	11,126
battery	Lithium-ion	0	1.3	0.2				
	Lead acid	0	0.1	0.04				
capacitor	double layer	0	0.1	0.02				
fuel cell	hydrogen	0	120	26	11 STP			
PV cell		0						
Flywheel	FES	0		0.13				
fusion	U_{235}	0	8×10^7	2.5×10^7	1.5×10^9			

Table 27.2a: Hydrogen: high gravimetric energy density but low volumetric energy density

Hydrogen property	unit	value
relative atomic mass	u	1.00794
density	kg/Nm^3	0.0899
specific HHV energy	MJ/kg	142.0
specific LHV energy	MJ/kg	120.0
HHV energy density	MJ/Nm^3	11.7
LHV energy density	MJ/Nm^3	9.9
boiling point	K (°C)	20.268 (–252.88)
melting point	K (°C)	14.025 (–259.13)
critical point	K (°C)	33.250 (–239.90)

Table 27.2b: Hydrogen: high gravimetric energy density but low volumetric energy density

Energy carrier	Form of hydrogen Storage 120 MJ/kg		Energy density by weight	Energy density by volume
			kWh/kg	kWh/l
Hydrogen	gas	20 MPa	33.3	0.53
	gas	24.8 MPa	33.3	0.64
	gas	30 MPa	33.3	0.75
	liquid	-253°C	33.3	2.36
	metal hydride		0.58	3.18
fusion	U_{235}		2.5×10^{7}	4.7×10^{9}

Comparisons

The Ragone plot in figure 27.1 shows the energy storage and power handling capacity of some alternative storage techniques. Energy and power densities, in steady-state, are related by *Energy* = *Power* × *time*.

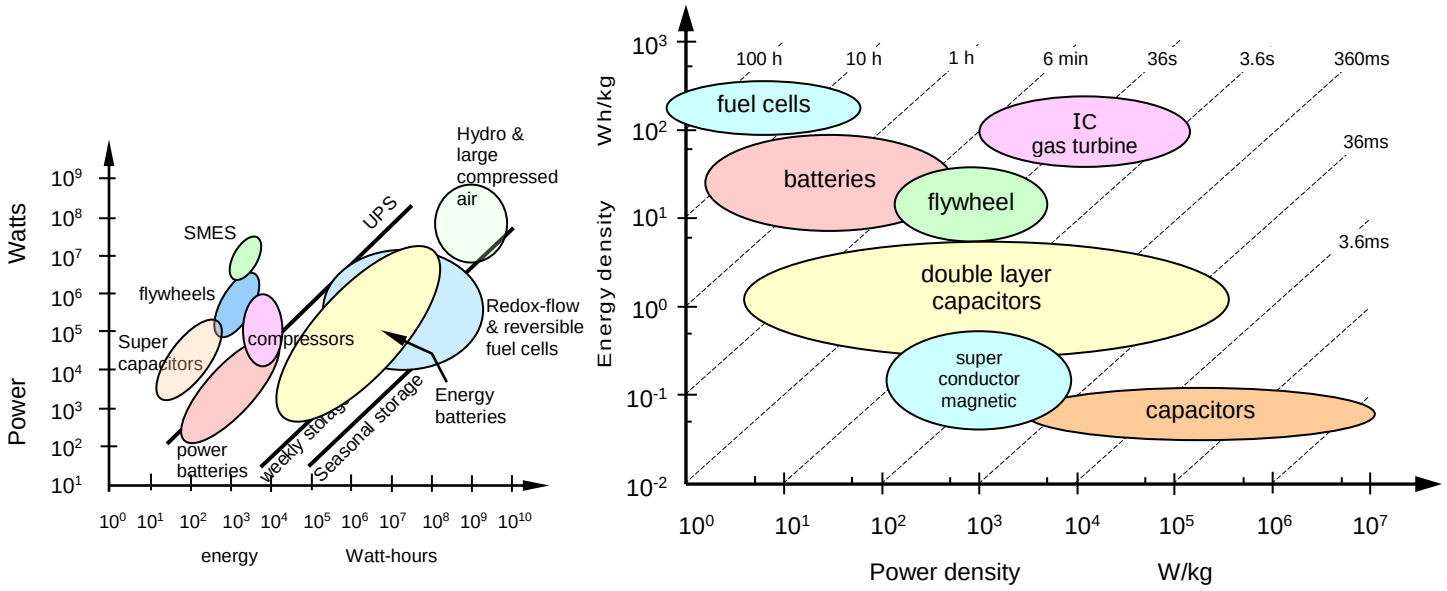

Figure 27.1. *Gravimetric energy and power densities of common energy sources.*

27.2 The fuel cell

The fuel cell is similar to a battery, in function and appearance. It produces electricity directly, using chemicals.

A fuel cell is a solid-state electrochemical device that consists of two electrodes, an anode and cathode, sandwiched around an electrolyte, with a catalyst membrane between each electrode and the electrolyte, which enhances ionization of the fuel molecules. The oxidant oxygen, usually from air, passes over the cathode electrode and typically hydrogen fuel over the anode, generating electricity, and water and heat by-products. An ion-conducting membrane separates the anode and cathode, allowing the reaction to take place without affecting the electrodes.

The fuel cell relies on a basic oxidation/reduction reaction, as with a battery, but the reaction takes place on the fuel rather than on the electrodes. As long as fuel is supplied and oxidized old fuel is disposed of, the cell will continue to generate energy, both electrical power and heat. Since conversion of the fuel to energy takes place via an electrochemical process, not combustion, the process is clean - no CO_2, quiet and highly efficient - two to three times more efficient than fuel combustion.

How the fuel cell operates

The fuel cell process can be divided into three stages; two of these stages involve the chemical reactions at each electrode and the third is ion conduction through the electrolyte.

(i) At the hydrogen electrode - anode
The reaction at the anode involves the release of electrons from the hydrogen fuel that will then be conducted by the electrode to the electrical load. The hydrogen arrives at the anode as a diatomic gas $2H_2$ where each adsorbed hydrogen molecule ionizes into four hydrogen protons, H^+ and four electrons, e^-. The rate of this process is increased with the aid of a catalyst. Because the chemical reaction at this electrode produces positive ions, it is the anode. The negatively charged electrons are then forced to flow from the conductive electrode (anode) to an external electrical load before re-entering the fuel cell at the cathode (that is, electrons diffuse naturally from a high concentration to a low concentration of electrons). However, the hydrogen ions may or may not conduct through the electrolyte since this depends on the pH and type of electrolyte used, meaning the hydrogen ions may have to temporarily remain at the anode in a receptive state.

(ii) At the oxygen electrode - cathode
Meanwhile, oxygen molecules O_2 are diffusing through to the catalytic surface of the cathode electrode which facilitates the separation of the adsorbed oxygen molecule (oxygen bonds are broken) into oxygen atoms which are held momentarily in a receptive state on the active catalyst. The entering electrons diverted externally from the anode bypassing the electrolyte, the oxidant, and cathode electrode together causes another reaction to occur where negative ions and products are produced. If H^+ ions are the free moving ions (because of the acid electrolyte used), they are attracted to the negative ions generated at the cathode and conduct through the acid electrolyte and product $2H_2O$, along with heat. If however, H^+ ions are not able to travel through the electrolyte, then the cathode produced free moving negative ions move through the alkali electrolyte to combine with the H^+ ions to complete the process at the anode.

(iii) Through the electrolyte medium
The electronically-insulated (does not conduct free electrons) electrolyte serves as the physical barrier preventing the fuel and oxidant gas streams from directly mixing, allowing only the appropriate ions to move freely through the layer. This requires that one of the reactants must be able to form the ionized specie needed to complete the process and form the primary by-product, water.

Fuel cells that use hydrogen can be thought of as an electrochemical devices that perform the reverse of electrolysis, where passing an electric current through water splits it up into hydrogen and oxygen. In the fuel cell, hydrogen and oxygen are joined together to produce water and electricity.
Although the majority of fuel cells use hydrogen as the fuel, some fuel cells work off methane, and a few use liquid fuels such as methanol.

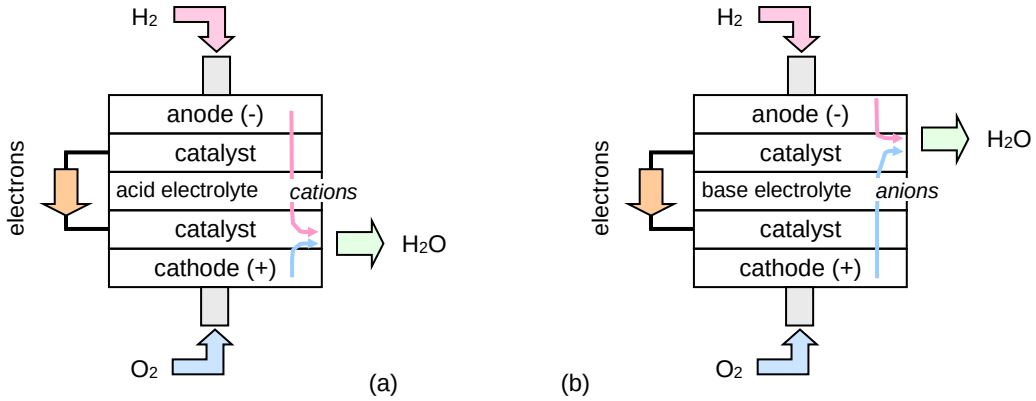

Figure 27.2. *Pictorial representation of a fuel cell with electrolyte conduction of: (a) cations and (b) anions.*

Two basic ion operating mechanism are possible. The first involves cations passing through an acid electrolytic membrane from anode to cathode, while the second mechanism involves anions passing through an alkali membrane in the opposite direction, namely from the cathode to the anode. The ion conducting membrane is non-conducting to electrons.

- ***Cation conduction***: Pressurised hydrogen H_2 gas fuel is fed into the anode of the fuel cell. The pressure forces the H_2 through the catalyst. When an H_2 molecule comes in contact with the platinum catalyst, it splits into two H^+ ions (protons) and two electrons e^-, which take different paths to the cathode. The catalyst increases the rate of this splitting process. The electrolyte membrane does not pass electrons. The electrons conduct externally from the anode, creating a current that can be utilized in an external circuit, then return to the cathode-side of the fuel cell where they are reunited with the hydrogen plus oxygen ions forming a molecule of water, as illustrated in figure 27.2a.

Meanwhile, on the cathode-side of the fuel cell, oxygen gas O_2 (or air) is being forced through the catalyst, where it is encouraged to form two oxygen atoms. Each of these atoms has a strong negative charge. This negative charge attracts two H^+ ions, protons, at the anode side through the membrane, where they combine with an oxygen atom and two of the electrons from the external circuit to form a water molecule H_2O, plus heat energy.

- ***Anion conduction***: The operating principle of an anion conducting cell is illustrated in figure 27.2b. Oxygen supplied at the cathode (air electrode) reacts with incoming electrons from the external circuit to form oxide ions, which migrate to the anode (fuel electrode) through the anion conducting electrolyte. At the anode, anions combine with hydrogen ions (and/or carbon monoxide) in the fuel to form water (and/or carbon dioxide), liberating electrons. Electrons (electricity) flow from the anode through the external circuit to the cathode.

In principle, fuel cells can operate on many reactant combinations but most fuel cells actually operate on a narrow range of fuels in combination with oxygen from the air. As considered in section 27.9, fuels range from pure hydrogen gas, liquid alcohols and other liquid or gaseous hydrocarbons to metals and solid carbon. For the fuel cell types restricted to operating only on pure hydrogen, it is necessary to involve systems that generate hydrogen. Electrolysis and fuel reforming technologies generate hydrogen, but storage at useful energy densities is problematic. Several types of fuel cell can be operated directly on readily available fuels such as methanol, ethanol, and natural gas, thereby dispensing with the infrastructure issues of hydrogen. Traditionally these fuels come predominantly from fossil sources, but they are also increasingly available from renewable bio-sources. Since the fuel cell relies on electro-chemistry and not combustion, emissions are lower than emissions from the cleanest fuel combustion processes.
Fuel cells can be made in a wide range of sizes, from a few watts to MW. The potential power generated by a fuel cell stack depends on the number and size of the individual fuel cells that comprise the stack and the surface area of the membrane. Since the single fuel cell produces only about 0.7V, many separate fuel cells must be series connected to form a high-voltage fuel-cell stack. Bipolar plates are used to judiciously connect one fuel cell to another and are subjected to both oxidizing and reducing conditions and potentials. An issue with bipolar plates is stability. Metallic bipolar plates corrode, and the by-products of corrosion (iron and chromium ions) decrease the effectiveness of fuel cell membranes and electrodes. Low-temperature fuel cells use lightweight metals, graphite, and carbon plus high temperature thermoset composites, as bipolar plate material.

The fuel cell offers a unique combination of benefits. In addition to low or zero emissions, benefits include high efficiency and reliability, multi-fuel capability, sighting flexibility, durability, scalability, and ease of maintenance. Fuel cells operate silently, so they reduce noise pollution as well as air pollution and the waste heat from a fuel cell can be used to provide domestic hot water or space heating.

There are several different types of fuel cells, each using a different chemistry. Fuel cells are usually classified by their operating temperature and the type of electrolyte used.

The materials for the cell components are selected based on suitable electrical conducting properties required of these components to perform their intended cell functions:

- adequate chemical and structural stability at high temperatures encountered during cell operation as well as during cell fabrication;
- minimal reactivity and interdiffusion among different components; and
- matching thermal expansion among different components.

27.3 Materials and cell design

Like the battery, the fuel cell has few component parts although the materials may be sophisticated, involving rare earth transitional metals, high temperature composite ceramics, cermets, etc. The basic fuel cell component parts are:

- Electrodes;
- Catalysts;
- Electrolyte;
- Interconnects; and their
- Stack construction.

27.3.1 Electrodes

Fuel cell electrodes serve three functions:

- To ensure a stable interface between the reactant gas and the electrolyte;
- To catalyze the electrode reactions; and
- To conduct electrons from or to the reaction sites

An electrode forms part of the three-phase boundary, where the electrolyte, electrode, and gas all come together.

i. Cathode

The ***cathode*** is the positive electrode of the fuel cell because it is the electrode where negative ions are produced. It has etched channels that distribute the oxygen to the surface of the catalyst. It also conducts the electrons received from the external circuit to the catalyst, where they can recombine with the hydrogen ions and oxygen to form water. An integral part of the cathode is the metallic interconnect, a bipolar plate, which forms an integral part of the anode of the adjacent cell, when cells are series connected to give higher voltage output.

The oxidant gas is air or oxygen at the cathode, and the electrochemical reduction of oxygen requires a series of elementary reactions and involves the receipt of multiple electrons. The cathode must meet the requirements of:

- high catalytic activity and high surface area for oxygen molecule dissociation and oxygen reduction;
- high electronic conductivity;
- chemical and dimensional stability in environments encountered during cell fabrication and cell operation;
- thermal expansion match with other cell components;
- compatibility and minimum reactivity with the electrolyte and the interconnection; and
- must have a stable, porous microstructure so that gaseous oxygen can readily diffuse through the cathode to the cathode/electrolyte interface.

ii. Anode

The ***anode*** is the negative electrode of the fuel cell because it is the electrode where positive ions are produced. It conducts away the electrons that are released from the hydrogen molecules so that they can be used in an external electrical circuit. An integral part of the anode is the metallic interconnect, a bipolar plate, which form parts of the cathode of an adjacent series cell. It has channels etched into it that disperse the hydrogen gas uniformly over the surface of the catalyst.

The properties of the anode must include:

- an excellent catalyst (in the case of high temperature fuel cells) with a large surface area for the oxidation of fuel (hydrogen, carbon monoxide);
- stable in the reducing environment of the fuel;
- electronically conducting;
- have sufficient porosity to allow the transport of the fuel to and the transport of the products of fuel oxidation away from the electrolyte/anode interface where the fuel oxidation reaction takes place;
- matching thermal expansion coefficient with that of the electrolyte and interconnect;
- integrity of porosity for gas permeation;
- chemical stability with the electrolyte and interconnect;
- applicability to use with versatile fuels and impurities; and
- cost effective is a commercialization factor.

27.3.2 Catalyst

The ***catalyst*** facilitates and speeds up the rate of the ionization reaction of oxygen at the cathode and hydrogen at the anode. It is usually made of platinum for low temperature cells and nickel at higher temperatures. The catalyst is rough and porous so that the maximum surface area can be exposed to the hydrogen or oxygen. The catalyst faces the electrolyte and must be able to conduct electrons to/from the electrode.

The effectiveness of the catalyst is paramount to fuel cell operation. Platinum is sufficiently reactive in bonding H and O intermediates as is required to facilitate the electrode process, then effectively releases the intermediate to form the final product. For example, the anode process requires Pt sites to bond H atoms when the H_2 molecule reacts, and these Pt sites release the H atom as $H^+ + e^-$, as shown in the two equations:

$$H_2 + 2Pt \rightarrow 2Pt{-}H$$

$$2Pt{-}H \rightarrow 2Pt + 2H^+ + 2e^-$$

Platinum can be oxidized which is a problem because it compete with hydrogen oxidation, reducing the half-cell potential:

$$Pt + H_2O \leftrightarrow PtOH + H^+ + e^-$$

$$Pt + H_2O \leftrightarrow PtO + 2H^+ + 2e^-$$

$$½O_2 + 2H^+ + 2e^- \rightarrow H_2O$$

Hydrocarbon fuels, like CH_3OH, tend to poison the anode platinum catalyst with COH and CO species. The poisoning can be prevented by the addition of Ruthenium, Ru.

$$Ru + H_2O \rightarrow RuOH + H^+ + e^-$$

$$Pt_xCO + RuOH \rightarrow CO_2 + H^+ + e^- + xPt + Ru$$

Catalytic reduction action also occurs on the cathode:

$$O_2 + 2Pt \rightarrow 2Pt{-}O$$

$$2Pt{-}O \rightarrow 2Pt + 2O^{2-} - 4e^-$$

The reaction effectiveness is dependant on temperature and platinum surface area. At lower temperature reactions, platinum particles are used, 2 nanometres in diameter, resulting in a large Pt area that is accessible to the gas molecules. At elevated temperatures, over 400°C, transition metals, Ni and oxides NiO, become effective, low cost catalysts, that can also act as the electrode.

$$NiO + CO_2 \rightarrow Ni^{2+} + CO_3^{2-}$$

At higher again temperatures no catalyst is necessary.

Reduction of oxygen at the cathode is less efficient than the catalytic action on hydrogen at the anode. In lower temperature fuel cell, various nanoparticle platinum alloys (AuPt and Pt_3Ni-III) are used to increase the O_2 reduction reaction activity. The tolerance to poisoning and the affects of an acidic environment are factors to be overcome with semi-formed alloy catalysts.

27.3.3 Electrolyte

In terms of chemistries, there are two main types of fuel cells, depending on the pH of the electrolyte. Common to all electrolytes is that they must not conduct free electrons.

- Acid electrolyte which allows H^+ hydrogen ion (proton) migration and free movement through the electrolyte from the anode to the cathode, producing water at the cathode, while conversely
- Alkaline electrolyte which allows anion migration, for example, OH^- hydroxyl ion migration through the electrolyte from the cathode to the anode, producing excess water at the anode.

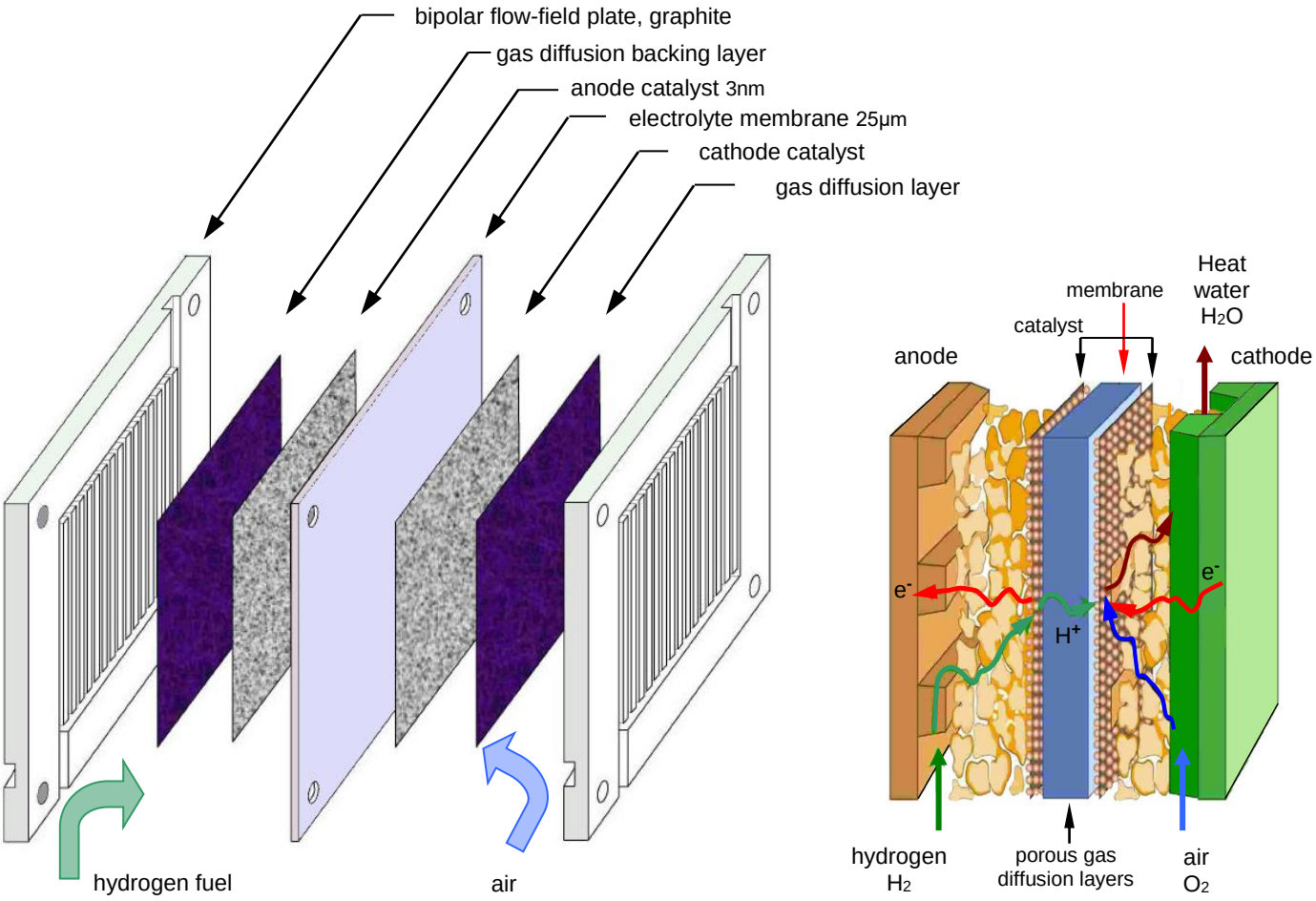

Figure 27.3. *The parts of a fuel cell/Membrane/electrode assembly with backing layers. Enlarged cross-section of a membrane/electrode assembly showing structural details.*

The ***electrolyte*** is either a solid (< 200°C) or a liquid (> 200°C), depending on the operating temperature. The electrolyte can be acidic or alkali and must pass ions but importantly, the electrolyte does not conduct free electrons and does not react with reactant ions. There are several criteria that the electrolyte has to meet. The electrolyte must be:

- dense and leak tight;
- stable in reducing and oxidising environments;
- a good ionic conductor at operating temperatures;
- non-electron conductor;
- thin to reduce ionic resistance;
- extended in area for maximum current capacity;
- thermal shock resistant; and
- economically processable.

27.3.4 Interconnect

Since a single cell only produces a voltage of less than 1V and power around 1W/cm^2, many cells are electrically connected together in a cell stack to obtain higher voltage and power. To connect multiple cells together, an interconnection is used in stacks. The requirements of the interconnection are the most severe of all cell components and include:

- high, nearly 100 percent electronic conductivity, not only through the bulk material but also in in-situ-formed oxide scales;
- strong adhesion between the as-formed oxide scale and the underlying alloy substrate;
- resistance to corrosion and surface stability in both oxidizing and reducing atmospheres at the cell operating temperature since it is exposed to dual atmospheres, with air (or oxygen) on the cathode side and fuel on the anode side;
- low permeability for oxygen and hydrogen to minimize direct combination of oxidant and fuel during cell operation;
- chemical compatibility with other materials in contact with the interconnect, such as seals and cell materials;
- mechanical reliability and durability at the cell operating temperature;
- a thermal expansion coefficient close to that of other stack components, mainly the cathode and the electrolyte (particularly for stacks using a rigid seal design); and
- non-reactivity chemical compatibility with other cell materials.

Suitable metallic alloy interconnects offer advantages such as improved manufacturability, significantly lower raw material and fabrication costs, and higher electrical and thermal conductivity.

27.3.5 Stack design

In the case of planar cell stacks, an effective seal must be provided to isolate air from the fuel. The seal must have a thermal expansion match to the fuel cell components, must be electrically insulating, and must be chemically stable under the operational conditions of the stack. Also, the seal should:

- exhibit no deleterious interfacial reactions with other cell components;
- be stable under both the high temperature oxidizing and reducing operational conditions;
- be created at a low enough temperature to avoid damaging cell components (under 850^{o}C for some materials); and
- should not migrate or flow from the designated sealing region during sealing or cell operation.

In addition, the sealing system should be able to withstand thermal cycling between the cell operation temperature and room temperature. Sealing is more of a problem with cells which operate at higher temperatures, where different sealing approaches include rigid, bonded seals (for example, glass-ceramics and brazes), compliant seals (for example viscous glasses), and compressive seals (for example, mica-based composites); multiple sealants may also be used in any given stack design between different cell components.

27.4 Fuel cell chemistries

The two chemical ion mechanisms involving anions and cations, will be discussed in terms of:

- an acid electrolyte and transfers cations, protons, H^+, through the electrolyte, producing water at the cathode and
- an alkaline electrolyte and transfers anions (OH^-, CO_3^{2-}, O^{2-}) through the electrolyte, producing water at the anode.

27.4.1 Proton H^+ cation conducting electrolyte: e.g. PEMFC, DMFC, PAFC

The acidic electrolytic Fuel Cell utilises one of the simplest reactions of any fuel cell. In low temperature PEMFC and DMFC Fuel Cells, the electrolyte is a flexible acidic membrane that when saturated offers a number of desirable features:

- highly chemical resistant;
- mechanically strong, when only 50μm thick;
- acidic;
- highly water absorptive;
- good proton conductor, H^+ cation, when saturated, but not flooded;
- electrically insulating, high resistance to electrons; and
- non-diffusive the gas molecules, no H_2 and O_2 crossover.

Chemistry

In both acid electrolyte and solid polymer fuel cells, the electrolyte conducts mobile H^+ ions, protons, generated at the anode. It is these H^+ ions that are key to the (half cell) reactions within the cell.
At the anode, hydrogen gas is readily ionised, producing free electrons and H^+ ions:

$$2H_{2(g)} \rightarrow 4H^+ + 4e^- \qquad E^o_{½\,cell} = 0.0\text{V} \qquad \mathrm{d}E^o_{½\,cell}/dT = 0\text{V/K} \tag{27.1}$$

The electrons from the anode conduct through the external circuit connected to the fuel cell, to the cathode. The H^+ ions migrate or permeate through the electrolyte, and also reach the cathode.
At the cathode, the H^+ ions and electrons react with the oxygen atoms, producing water. At the cathode, the oxygen undergoes a two-step indirect reduction reaction. The stable H_2O_2 intermediate is undesirable as it lowers the cell voltage and H_2O_2 attacks and corrodes the carbonaceous electrodes commonly used in lower temperature cells.

$$\begin{aligned} O_2 + 2H^+ + 2e^- &= H_2O_2 \\ H_2O_2 + 2H^+ + 2e^- &= 2H_2O \end{aligned} \tag{27.2}$$

Overall cathode half reaction:

$$O_{2\,(g)} + 4H^+ + 4e^- \rightarrow 2H_2O \qquad E^o_{½\,cell} = 1.23\text{V} \qquad \mathrm{d}E^o_{½\,cell}/dT = -0.85\text{mV/K} \tag{27.3}$$

This movement of ions through the electrolyte, and movement of electrons through the external circuit, is illustrated in the diagram in figure 27.4a. Water produced at the cathode must be continually removed.

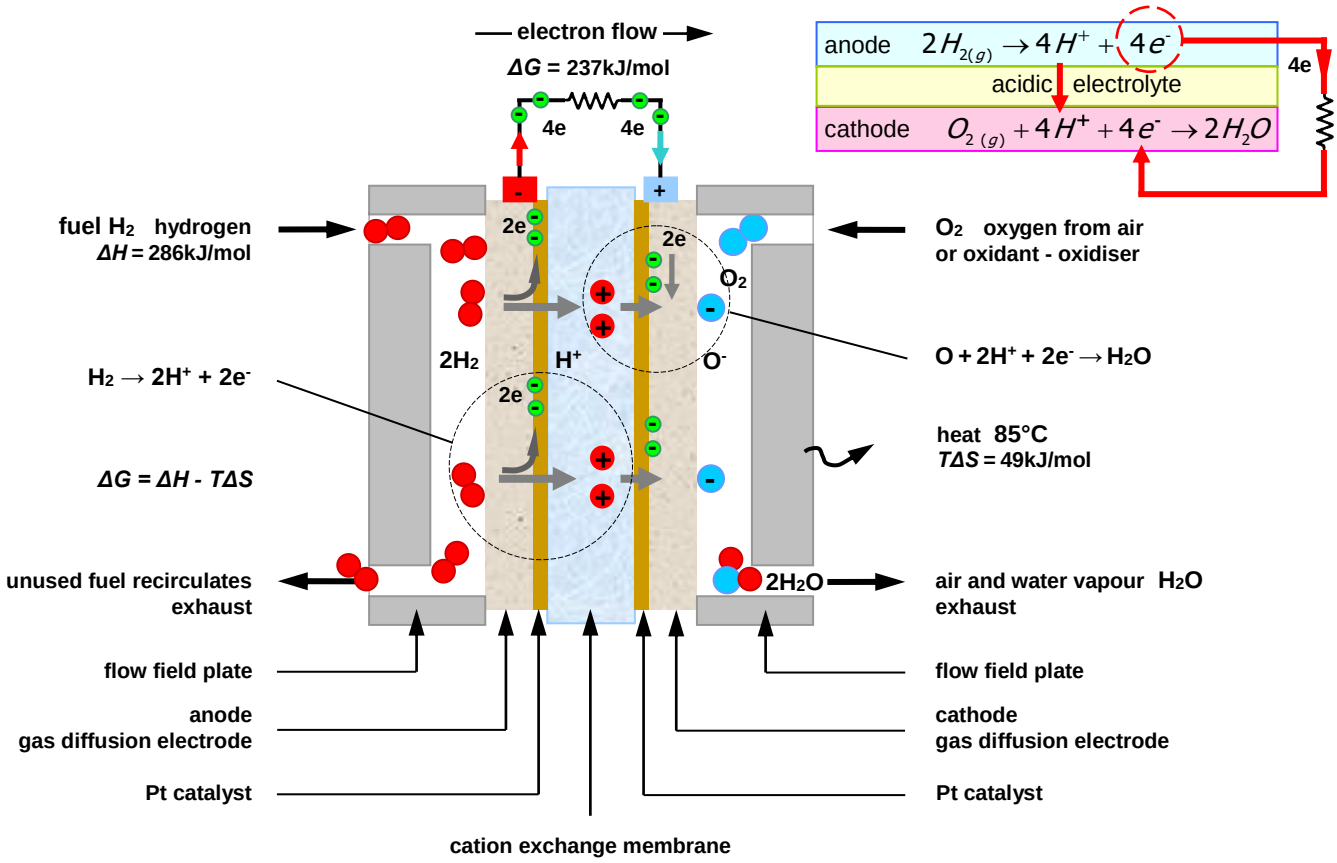

Figure 27.4. *The chemistry mechanisms of an acidic electrolyte fuel cell.*

The net fuel cell reaction, which is exothermic, is the algebraic summation of the half-cell reactions:

$$2H_{2(g)} + O_{2(g)} \rightarrow 2H_2O + energy \qquad E^o_{cell} = 1.23V \qquad (27.4)$$

The chemistry of the fuel cell gives E^o_{cell} = 1.23 - 0 = 1.23V. Standard tables give the enthalpy as 285.15kJ/mol and the number of electrons per H_2, as n = 2. The dissociation kinetics of O_2 and H_2 improve with increased temperature but the cell potential decreases with temperature.

Positive ions are produced at the anode and negative ions are produced at the cathode. The water molecules are always produced at the cathode, the production of which exceeds that which may be required (if any) at the anode.

The H^+ cations, as found in the Polymer Exchange Membrane Fuel Cell - PEMFC, Direct Methanol Fuel Cell – DMFC, and the Phosphoric Acid Fuel Cell – PAFC; all behave the same within the fuel cell. That is, equations (27.1) to (27.4) are applicable to the three cation fuel cells presented.

27.4.2 Anion (OH^-, CO_3^{2-}, O^{2-}) conducting electrolyte: e.g. AFC, MCFC, SOFC

The important feature of an alkali is that there is an excess of anions, X^- ions, generated at the cathode, and these are key to the reactions within the alkali electrolyte fuel cell. An electric current is produced as a result the half-cell reaction at each electrode.
At the anode, hydrogen gas reacts with the X^- ions, anions which have migrated through the electrolyte, producing water, and releasing electrons. The reaction is:

$$2H_{2(g)} + 4X^-_{(aq)} \rightarrow 4H_20_{(l)} + 4e^- \qquad (27.5)$$

The electrons leave the fuel cell at the anode, passing through the external electrical circuit connected to the fuel cell, and reach the cathode. At the cathode the entering electrons react with the incoming oxygen, and water, producing more X^- ions to replenish those used at the anode.

$$O_{2(g)} + 2H_2O + 4e^- \rightarrow 4X^-_{(aq)} \qquad (27.6)$$

The X^- ions move through the electrolyte, and the electrons move round the external circuit. The complementary movement of ions and electrons is illustrated in the diagram in figure 27.5a. The net reaction, which is exothermic, is the algebraic half-cell reaction summation:

$$2H_{2(g)} + O_{2(g)} \rightarrow 2H_2O + energy \qquad (27.7)$$

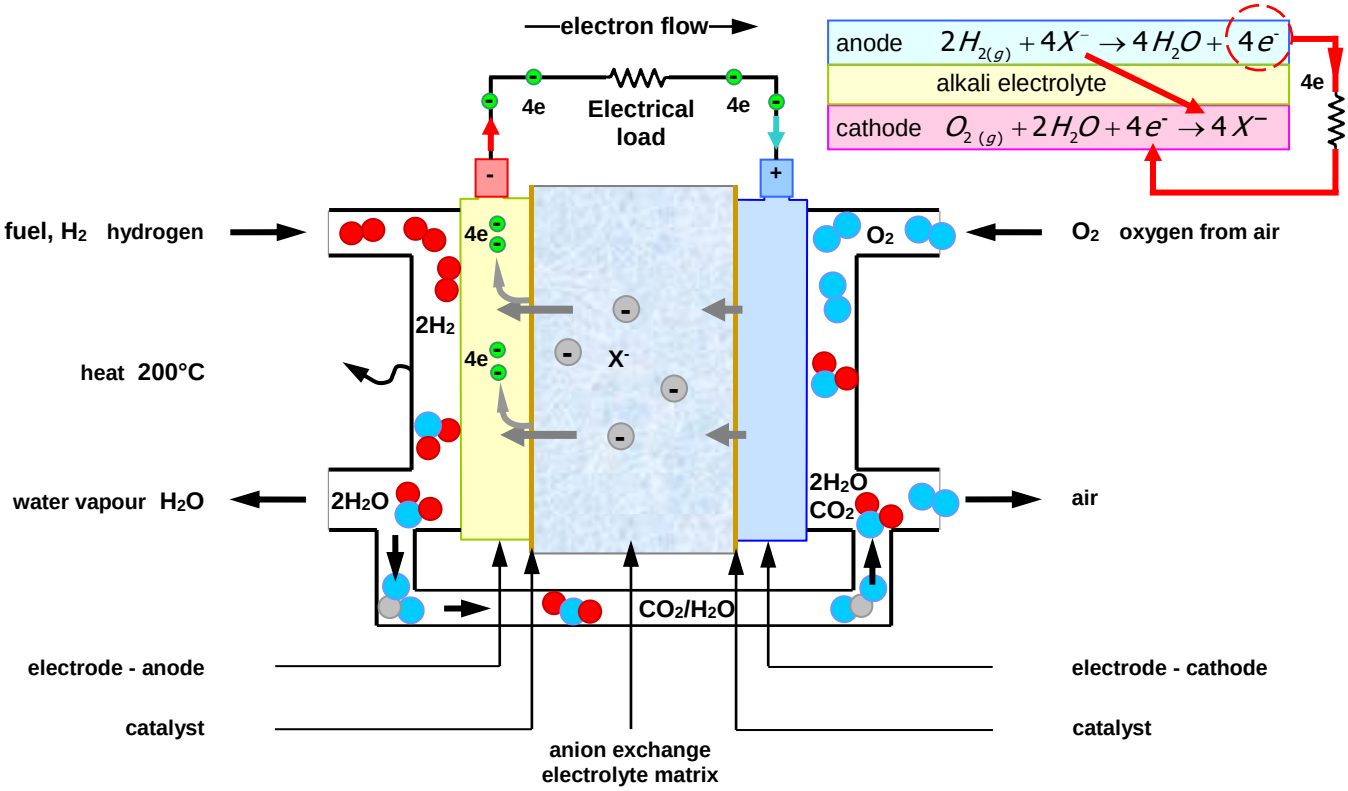

Figure 27.5. *The chemistry mechanisms of an alkaline electrolyte fuel cell.*

Positive ions are produced at the anode and negative ions are produced at the cathode. Water molecules are always produced at the anode, and at a faster rate than those (if any) being consumed at the cathode.
Anions, such as OH^-, CO_3^{2-} and O^{2-} as found in the Alkaline Fuel Cell - AFC, Molten Carbonate Fuel Cell - MCFC, and Solid Oxide Fuel Cell - SOFC, behave similarly within the fuel cell, as given by equations (27.5) to (27.7).

27.5 Six main fuel cells

Some of the main types of fuel cells, with increasing operating temperature, include:

- **Low-temperature Fuel Cell types** (<200°C)
  - *Polymer exchange membrane fuel cell* (PEMFC) - H^+
  - *Alkaline fuel cell* (AFC) - OH^-
  - *Direct-methanol fuel cell* (DMFC) - H^+
- **High-temperature Fuel Cell types** (>200°C)
  - *Phosphoric-acid fuel cell* (PAFC) - H^+
  - *Molten-carbonate fuel cell* (MCFC) - CO_3^{2-}
  - *Solid oxide fuel cell* (SOFC) - O^{2-}

27.6 Low-temperature fuel cell types

27.6.1 Polymer exchange membrane fuel cell (PEMFC) (Proton Exchange Membrane FC)

The PEMFC has a high power density and a relatively low operating temperature (ranging from 60 to 80°C). The low operating temperature means that the fuel cell can warm-up and begin to generate electricity quickly, resulting in less wear on system components, leading to better durability. Cells do not use corrosive fluids like some fuel cells. However, it requires a noble-metal catalyst (typically platinum) to separate the hydrogen's electrons and protons, adding to system cost. The platinum catalyst is also hyper-sensitive to CO poisoning, making it necessary to employ an external reactor to reduce CO in the fuel gas if the hydrogen is derived from an alcohol or hydrocarbon fuel. Platinum/ruthenium catalysts are more resistant to CO. The slow kinetics of oxygen at the cathode also necessitates the use of a catalyst.
Higher-density liquid fuels such as methanol, ethanol, natural gas, liquefied petroleum gas, and gasoline can be used for fuel, but the system must have an external fuel processor to reform the methanol to hydrogen. Reforming releases minimal carbon dioxide.
The PEMFC has a high power density, high efficiency, and can adapt to varying demands. It promises a high conversion efficiency of over 60% and an energy density of 120 W/Kg, with 2kW/l and 2W/cm^2.
The PEM fuel cell is currently favoured for electric motor vehicles. Other applications include air conditioning and domestic sized electronic equipment.
Key features are:

- Fast start-up, rapid transient power response, high power density, compact
- H^+ via polymer (ionomer) membrane electrolyte, Pt, 50°C to 150°C, H_2 at < 5 atm.
- Sensitive to impurities, CO, sulphur species, and NH_3
- Anode and cathode gas sealing is simpler with a solid electrolyte therefore cheaper, no orientation restrictions, and low corrosion leads to a longer cell and stack life.
- Portable applications, 50 to 500kW – automotive, small stationary auxiliary power units
- Overall reaction ΔH = -286.0kJ/mol, with n = 2.

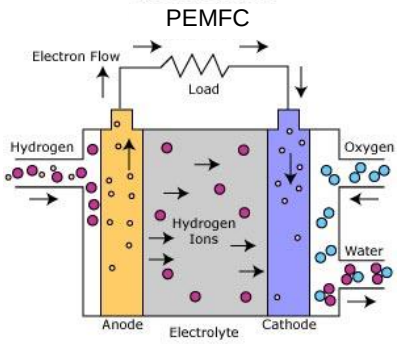

Anode Reactions: $2H_{2(g)} \xrightarrow{Pt} 4H^+ + 4e^-$ $E^o_{½cell} = 0.0V$

Cathode Reactions: $O_{2(g)} + 4H^+ + 4e^- \xrightarrow{Pt} 2H_2O$ $E^o_{½cell} = 1.229V$

Overall Cell Reactions: $2H_{2(g)} + O_{2(g)} \rightarrow 2H_2O$ $E^o_{cell} = 1.229V$

As shown in figure 27.3 for the PEMFC case, which is typical of the basic physical structure, there are four basic elements of the fuel cell:

- The ***anode*** is the negative electrode and conducts the electrons that are released from the hydrogen molecules so that they can be used in an external electrical circuit. The carbon or metal interconnect, which makes electrical contact to the anode carbon sheet, has channels etched into it that disperse the hydrogen gas uniformly over the back surface of the catalyst layer.

- The ***cathode*** is the positive electrode and also has etched channels that distribute the oxygen to the back surface of the catalyst layer. It also conducts the electrons received from the external circuit to the catalyst, where they can recombine with the hydrogen ions and oxygen to form water. The carbon or metal interconnect, like the anode interconnect, makes electrical contact to the cathode carbon sheet.
- The ***electrolyte*** is the proton exchange membrane. This specially treated organic material is a thin, 50μm, flexible plastic (poly-perfluorosulphonic acid) film, which only conducts positively charged ions when it is saturated with water. The membrane must be hydrated (by absorbing water) in order to function and remain stable. Importantly, the membrane blocks electrons. Being a solid, membrane helps minimise gas crossover.
- The ***catalyst*** is usually made of platinum nanoparticles thinly coated onto carbon paper or cloth, which is the effective anode or cathode. The catalyst is rough and porous so that the maximum platinum surface area can be exposed to the hydrogen or oxygen. The platinum-coated side of the carbon sheet, the catalyst, faces the polymer membrane.

The backing layers

The fuel cell anode and cathode assemblies are designed to maximize the current that can be obtained from an electrode and catalyst assembly. The backing layers on which the catalyst is deposited, are usually made of a porous carbon paper or carbon cloth, typically 100 to 300 μm thick, that can conduct the electrons and effectively diffuse reactant gas ions created and reacted in the platinum catalyst. The platinum catalyst particles are deposited 50μm thick on one side of each backing layer; the side that faces the electrolytic.

Diffusion refers to the flow of gas molecules from a region of high concentration, the outer side of the backing layer where the gas is flowing by in the flow fields, to a region of low concentration, the inner side of the backing layer next to the catalyst layer where the gas is consumed by the reaction. The porous structure of the backing layers allows the gas to spread out as it diffuses so that when it penetrates the backing, the gas will be in contact with the entire surface area of the catalyzed membrane.

The backing layers also assist in water management during the operation of the fuel cell. An effective backing material allows the correct amount of water vapour to reach the membrane/electrode assembly to keep the membrane humidified. The backing material also allows the liquid water produced at the cathode to leave the cell to avoid flooding. The backing layers are often wet-proofed with Teflon to ensure that most of the pores in the carbon cloth (or carbon paper) do not become saturated with water, which would prevent the rapid gas diffusion necessary for a good rate of reaction, from occurring at the electrodes.

The solid organic polymer electrolyte membrane

The polymer electrolyte membrane is essentially PTFE containing a fraction of pendant sulphonic acid groups. (Nomenclature: 'sulphonic acid group' usually refers to the un-dissociated SO_3H group, where as 'sulphonate' refers to the ionised SO_3^- group after the proton has dissociated). The ion-containing component is normally given in terms of equivalent weight (that is, number of grams of dry polymer per mole of acidic groups). The useful equivalent weight for Nafion ranges from 800-1500 g/mol.
The length of and the precise nature of the side chains vary between different brands of polymer. Common to all is the PTFE based fluorocarbon 'backbone' of the polymer that has several desirable properties:

- PTFE is hydrophobic - this means the hydrophilic sulphonate groups are effectively repelled by the chains and cluster together;
- PTFE is extremely resilient to chemical attack – the environment within the membrane is hostile and acidic. Hydrocarbon-based polymers would tend to degrade rapidly; and
- PTFE is a thermoplastic with high mechanical strength – meaning very thin membranes can be produced, reducing the thickness of each cell and increasing the power density of the stack.

As shown in figure 27.6, the thin permeable electrolyte sheet of poly-perflourosulphonic acid consists of three distinct regions.

- A Teflon-like fluorocarbon backbone of hundreds of repeating chains -
$$-CF_2-CF-CF_2-$$
- Side chains connecting the molecular backbone to the third region -
$$O-CF_2-CF-O-CF_2-CF_2-$$
- Ion clusters of sulphonic acid ions -
$$SO_3^-H^+$$

When the membrane becomes hydrated, the hydrogen ions become mobile and bond to water molecules as they move from one SO_3^- site to another in the acid molecule.

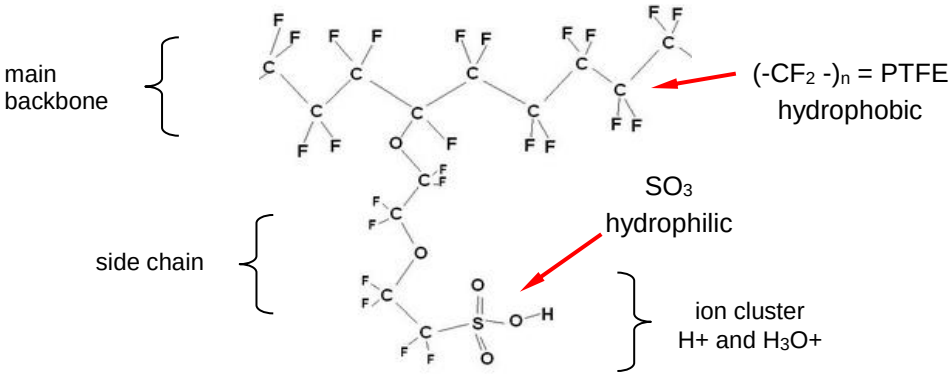

Figure 27.6. *A PTFE fluorocarbon (NAFION) used for the PEM fuel cell electrolyte.*

*27.6.2 **Alkaline fuel cell*** (AFC)

This is one of the oldest designs for fuel cells, with modest cell efficiencies of nearly 70%. The AFC is susceptible to contamination, so requires pure hydrogen and oxygen. It is also expensive, which is hampering commercialization.

Key features are:

- Fast start-up, but bulky, 10kW to 100kW
- OH^- via liquid or polymer electrolyte, KOH, non-Pt, 80°C to 160°C, gas or liquid fuels
- Susceptible to carbon contamination by K_2CO_3 formation, needs pure H_2 and O_2
- Portable, small stationary/transport, space vehicles, submarines
- Overall reaction ΔH = -286.0kJ/mol, with n = 2.

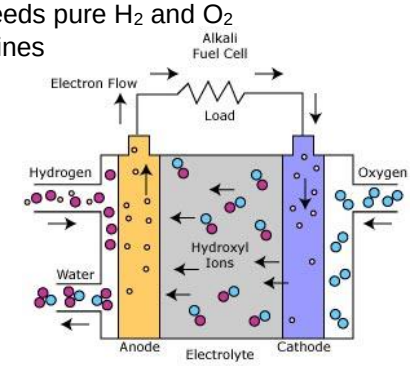

The anode half-cell reaction involves two stages.

$$2H_2 \xrightarrow{Ni} 4H^+ + 4e^-$$

$$4H^+ + 4OH^- \xrightarrow{Ni} 4H_2O$$

The overall cell reactions are:

Anode Reaction: $2H_{2(g)} + 4OH^- \xrightarrow{Ni} 4H_2O + 4e^-$ $E^o_{½cell}$ = -0.83V

Cathode Reaction: $O_{2(g)} + 2H_2O + 4e^- \xrightarrow{Ni} 4OH^-$ $E^o_{½cell}$ = 0.401V

Overall Net Reaction: $2H_{2(g)} + O_{2(g)} \rightarrow 2H_2O$ E^o_{cell} = 1.231V

The chemistry of this fuel cell gives E^o_{cell} = 0.401 - -0.83 = 1.231V. Standard tables give the enthalpy as 286kJ/mol and the number of electrons per H_2, as n = 2. Water removal is needed to maintain reaction.

These fuel cells use an alkali solution of potassium hydroxide KOH in water as the electrolyte and can use a variety of non-precious metals as a catalyst at the anode and cathode. High-temperature AFCs operate at temperatures between 100°C and 250°C, with newer AFC designs operating at temperatures below 100°C. Concentration of electrolyte, KOH, which is contained in an asbestos matrix, decreases to 50% at lower temperatures. Electro-catalyst can by Ni, Ag, metal oxides, spinels, and noble metals.

Aqueous alkaline solutions do not reject CO_2. Thus a disadvantage of this fuel cell type is that it is readily poisoned by carbon dioxide CO_2, which reacts to produce K_2CO_3 that irreversibly blocks the pores in the cathode. The levels of CO_2 in the air affect cell operation, making it necessary to purify both the hydrogen and oxygen used in the cell. This purification process is costly. This susceptibility to catalyst poisoning affects the cell's lifetime and precludes the use of platinum as a catalyst.

*27.6.3 **Direct-methanol fuel cell*** (DMFC)

The methanol fuel cell is an optimised PEMFC but is not as efficient. The efficiency is low due to the permeation of neutral methanol and water through the sulphonated organic hydrocarbon polymer membrane (e.g. Nafion), termed crossover. The low-temperature oxidation of methanol to hydrogen ions and carbon dioxide requires more active platinum catalyst, which makes these fuel cells expensive.

Other catalysts are Ni, Ag, metal oxides, spinels and noble metals. The thin proton exchange membrane is covered on both sides with a sparse layer of platinum-based catalyst.
DMFC do not use hydrogen fuel, but more convenient liquid methanol. The anode catalyst draws H_2 from liquid methanol, thus eliminating the need for a fuel reformer. They are less efficient but offer compact and convenient designs suitable for future consumer electronics applications and in automotive areas because the fuel is convenient. One litre of methanol can theoretically provide 5kWh, but 1.7kWh outputs are typical.
Key features are:

- Use with liquid alcohol - methanol canisters, compact, no reforming
- Methanol is liquid from -97°C to 65°C, with ×10 the energy/litre of highly compressed H_2
- H^+ via polymer electrolyte, Pt or alternatives (Ru), 90°C to 100°C
- Cell efficiency of 40% and increases with temperature
- Small portable, battery replacement in mobile phones and laptops, small transport
- Overall reaction ΔH = -726.6kJ/mol, with n = 6.

Direct Methanol

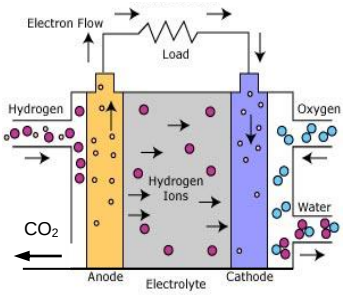

Anode Reaction: $2CH_3OH + 2H_2O \xrightarrow{Pt/Ru} 2CO_{2(g)} + 12H^+ + 12e^-$ $E^o_{½cell} = 0.2V$

Cathode Reaction: $3O_{2(g)} + 12H^+ + 12e^- \xrightarrow{Pt} 6H_2O$ $E^o_{½cell} = 1.23V$

Overall Cell Reaction: $2CH_3OH + 3O_{2(g)} \rightarrow 2CO_{2(g)} + 4H_2O$ $E^o_{cell} = 1.214V$

Note that H_2O is required at the anode, with an excess over the anode requirement being produced at the cathode.

27.7 High-temperature fuel cell types (well in excess of 100°C)

27.7.1 Phosphoric-acid fuel cell (PAFC)

The liquid phosphoric-acid fuel cell has potential for use in small stationary power-generation systems up to 10MW with 50% cell efficiency and better than 80% efficiency if steam produces cogeneration, CHP. It operates at a higher temperature than polymer exchange membrane fuel cells, so it has a longer warm-up time, restricting its application areas, and it must be continuously operated since H_3PO_4 electrolyte effloresces irreversibly and solidifies at 40°C. A silicon carbide matrix is used to retain the concentrated H_3PO_4 electrolyte and highly dispersed Platinum and Pt alloy anode catalysts particles. CO_2 does not affect the electrolyte or cell performance, which can therefore be operated with reformed fossil fuel. Simple construction, low electrolyte volatility, and long-term stability are additional advantages.
Key features are:

- First commercially available, best suited to large size
- H^+ via liquid or polymer electrolyte, Pt, 150-250°C, with near 100% concentration H_3PO_4
- Carbon paper electrodes Pt coated, Pt unaffected by CO (<1½%) or CO_2 impurities in H_2
- Sulphur must be removed from petrol if used
- Medium-large scale stationary, large mobile applications
- Overall reaction ΔH = -286.0kJ/mol, with n = 2

Phosphoric acid fuel cell

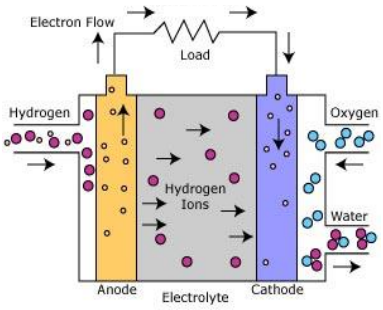

Anode Reaction: $2H_{2(g)} \xrightarrow{Pt} 4H^+ + 4e^-$ $E^o_{½cell} = 0.0V$

Cathode Reaction: $O_{2\,(g)} + 4H^+ + 4e^- \xrightarrow{Pt} 2H_2O$ $E^o_{½cell} = 1.229V$

Overall Cell Reaction: $2H_{2(g)} + O_{2(g)} \rightarrow 2H_2O$ $E^o_{cell} = 1.229V$

Water must be continually removed from the cathode side.

27.7.2 Molten-carbonate fuel cell (MCFC)

Like the SOFC, this fuel cell is suited to large stationary power generators, up to 100MW. They operate at 600°C, so can generate superheated steam that can be used to generate more power, CHP. Typical cell efficiency is 55%, and 85% with high-pressure steam heat capture. Because of high operating temperatures, reforming to H_2 of natural gas fuel occurs internally and the cells are not prone to CO and CO_2 poisoning. They have a lower operating temperature than solid oxide fuel cells, which means they do not need such exotic materials (sheet stainless steel is used in the construction), which makes the design less expensive.

The electrolyte is molten alkaline carbonate salt mixture (lithium carbonate and potassium carbonate - 62 m/o Li_2CO_3 and 38 m/o K_2CO_3 (62/38 Li/K), or lithium carbonate and sodium carbonate) suspended in a porous, chemically inert ceramic matrix of beta-alumina solid electrolyte. The high temperature results in high ion mobility through the liquid electrolyte. The cathode is supplied with carbon dioxide and the fuel is normally fossil fuel or natural gas.

Key features are:

- CO_3^{2-} via liquid electrolyte,
  non-Pt uses nickel based catalyst, 600-800°C
- Fuel flexibility, longer start-up
- CO_2 and O_2 must be delivered to the cathode
- Long term electrode corrosion by CO_3^{2-} electrolyte
- Wide range of fuels, H_2, natural gas, CO, propane, diesel, etc.
- Utilities, industrial, military applications
- Overall reaction ΔH = -247.9kJ/mol, with n = 2.

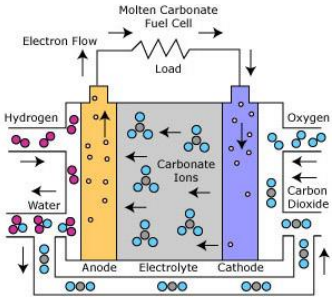

The reactions using CO and H_2, derived from internal CH_4 reforming conversion (see equations (27.8) to (27.9)), are:

Anode Reaction: principal reaction $\quad 2H_{2(g)} + 2CO_3^{2-} \xrightarrow{Ni} 2H_2O + 2CO_{2(g)} + 4e^-$ $\quad E^o_{½cell} = 1.11V$

Cathode Reaction: $\quad O_2 + 2CO_{2(g)} + 4e^- \xrightarrow{NiO} 2CO_3^{2-}$

Overall Cell Reaction: $\quad 2H_{2(g)} + O_{2(g)} + 2CO_{2(cathode)} \rightarrow 2H_2O + 2CO_{2(anode)}$ $\quad E^o_{cell} = 1.07V$

Anode Reaction: minor reaction $\quad 2CO_3^{2-} + 2CO_{(g)} \xrightarrow{Ni} 4CO_{2(g)} + 4e^-$

Cathode Reaction: $\quad O_{2(g)} + 2CO_{2(g)} + 4e^- \xrightarrow{NiO} 2CO_3^{2-}$

Overall Cell Reaction: $\quad O_{2(g)} + 2CO_{(g)} + 2CO_{2(cathode)} \rightarrow 4CO_{2(anode)}$ $\quad E^o_{cell} = 1.04V$

The cathode reaction is the same for both cases. Note that CO_2 is required at the cathode, with that CO_2 being produced at the anode, with an excess at the anode with CO fuel. Water removal is needed.

27.7.3 Solid oxide fuel cell (SOFC)

These fuel cells are best suited for large-scale stationary power generators for providing electricity to factories or towns. The two construction types are planar and tubular, both having a cell efficiency of typically 60%. Of primary importance is the fact that SOFCs require no liquid electrolyte, with associated corrosion and electrolyte management problems.

Figure 27.7 shows the principal components of the tubular solid oxide fuel cell. Air is channelled into the cell stack and through the centre of each tube. The innermost layer of the tube is the cell cathode and is surrounded by the electrolyte (middle layer). Fuel flows over the outer layer that serves as the anode.

Bundles of tubes are joined together into modules to make a fuel cell stack. The modular nature of fuel cells is a strength, because power plants can add modules as needed, keeping the unused capacity to a minimum.

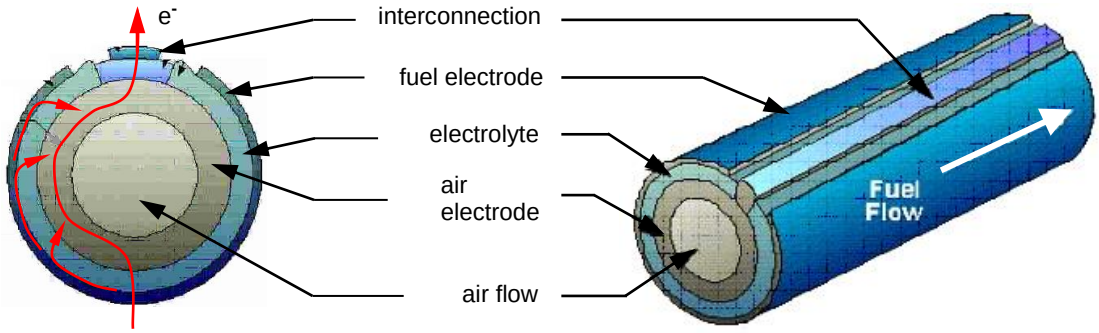

Figure 27.7. *Tubular solid oxide fuel cell construction.*

The SOFC operates at high temperatures, between 700 and 1,000°C, which introduces a reliability problem, because parts of the fuel cell can fail due to repeated on-off thermal cycling. However, solid oxide fuel cells are stable when in continuous use. The high-temperature high-quality wastes for CHP, integrated with secondary gas turbines improve the system efficiency to over 80%.

The high temperature enables them to tolerate relatively impure fuels, such as from coal gasification or gasses from industrial processes, due to internal reforming. Adversely, more expensive and exotic construction materials are required.
To operate at such high temperatures, the electrolyte is a thin, 40μm, solid ceramic material (solid oxide) that is conductive to oxygen ions, O^{2-}. The anode is made form Ni-ZrO_2 cermet, 150μm thick, while the cathode is made from lanthanum strontium manganite. High temperature cell interconnects are made from 100μm conductive ceramics, lanthanum and yttrium chromites doped with Mg, Sr and Ca. Metallic alloys can be used with operating temperatures below 800°C.

Key features are:

- Fuel flexibility
- CHP increases system efficiency
- O^{2-} via conducting non-porous hard ceramic electrolyte of ZrO_2, no catalyst, 500-1000°C
- Sulphur products must be removed by using a zinc absorbent or active carbon bed
- Thick, electrically conducting nickel cermet anode used to strengthen and support the cells
- Planar construction requires 8 hour warm-up while tubular construction requires minutes
- Small to large scale stationary; portable emerging, mobile applications - auxiliary power units
- Overall H_2 reaction ΔH = -286.0kJ/mol, with n = 2.
- Overall CO reaction ΔH = -283.1kJ/mol, with n = 2.
- Overall CH_4 reaction ΔH = -890.8kJ/mol, with n = 8, reformation and water-gas shift phases.

Anode Reaction: $2H_2 + 2O^{2-} \rightarrow 2H_2O + 4e^-$

Cathode Reaction: $O_2 + 4e^- \rightarrow 2O^{2-}$

Overall Cell Reaction: $2H_{2(g)} + O_{2(g)} \rightarrow 2H_2O$ $\quad E^o_{cell} = 1.23V$

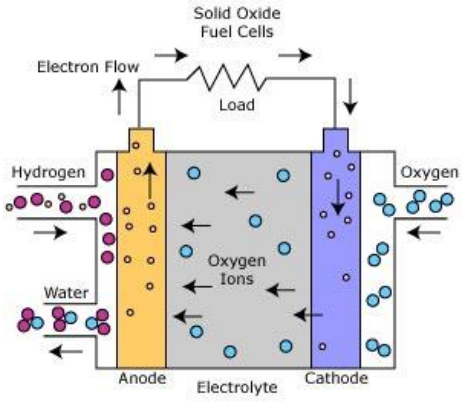

Anode Reaction: $2CO + 2O^{2-} \rightarrow 2CO_2 + 4e^-$

Cathode Reaction: $O_2 + 4e^- \rightarrow 2O^{2-}$

Overall Cell Reaction: $2CO_{(g)} + O_{2(g)} \rightarrow 2CO_2$ $\quad E^o_{cell} = 1.066V$

Anode Reaction: $CH_4 + 4O^{2-} \rightarrow 2H_2O + CO_2 + 8e^-$

Cathode Reaction: $2O_2 + 8e^- \rightarrow 4O^{2-}$

Overall Cell Reaction: $CH_{4(g)} + 2O_{2(g)} \rightarrow 2H_2O + CO_{2(g)}$ $\quad E^o_{cell} = 1.060V$

The disadvantage of using hydrocarbon fuels is the possible formation of coke, C, on the anode.

The cathode reaction is the same for the different anode-side fuel cases. Water removal with all fuels.
Reduction of the SOFC operating temperature by 200°C or more allows use of a broader set of materials, is less demanding on the seals and the balance-of-plant components, simplifies thermal management, aids in faster start up and cool down, and results in less degradation of cell and stack components. Because of these advantages, development of SOFCs capable of operating in the temperature range of 650 to 800°C is in progress. However, at lower temperatures, electrolyte conductivity and electrode kinetics decrease significantly; requiring alternative cell materials and designs.

SOFC components

Electrolyte
Yttrium-doped zirconium oxide ($ZrO_2 + Y_2O_3$, YSZ) is the most widely used material for the electrolyte in SOFCs because of its adequate ionic conductivity, chemical stability, and mechanical strength. The only drawback of stabilized YSZ is the low ionic conductivity in the lower cell operation temperature regime, below about 750°C. This problem is resolved by decreasing the thickness of the YSZ electrolyte or other materials replace the yttrium. Scandium-doped zirconium oxide has higher conductivity than YSZ but the high cost of scandium and detrimental ageing effects in scandium doped zirconium oxide make it less attractive. Gadolinium or samarium doped cerium oxide CeO_2 materials possess higher oxide ion conductivity than zirconium based materials. However, cerium oxide (ceria) based materials, under reducing conditions at high temperatures, exhibit significant electron conductivity and dimensional change. Operation at temperatures below 600°C overcomes this cerium oxide problem. A mixture,

containing among others gallium oxide, has proved a good oxide ion conducting electrolyte. However, it has two drawbacks: uncertain cost of gallium, and oxide uncertain chemical and mechanical stability.

Cathode

The **cathode** material is important because the oxidation reaction determines the efficiency of the fuel cell. The stringent electrochemical and mechanical requirements greatly restrict the number of suitable cathode candidate materials. Lanthanum manganite $LaMnO_3$, which, when substituted with low valence elements such as calcium or strontium Sr, $La_{0.8}Sr_{0.2}MnO_3$, has good electron conductivity. Additionally, it possesses adequate electrocatalytic activity, a reasonable thermal expansion match to YSZ, and stability in the SOFC cathode electrochemical operating environment.

SOFCs cathodes operating at 650 to 800^{o}C typically contain transition metals such as cobalt, iron, and/or nickel. These materials offer higher oxide ion diffusion rates and exhibit faster oxygen reduction kinetics at the cathode/electrolyte interface compared with high-temperature lanthanum manganite. However, the thermal expansion coefficient of cobaltites is much higher than that of the YSZ electrolyte, and the electrical conductivities of ferrites and nickelites are low. The improved cathodic performance deteriorates during the cell lifetime as a result of chemical or microstructural instability. Since these materials are reactive toward YSZ, a thin layer, generally of a cerium oxide based material, is used to reduce the chemical reaction between the cathode and YSZ. The polarization resistance depends on the microstructural grain size of the ionic conductor in the composite electrode and the volume fraction of porosity.

Anode

Nickel-YSZ composites (or Ni-ZrO_2 cermet) are the most commonly used SOFC anode materials. Nickel is an excellent catalyst for fuel oxidation; however, it possesses a high thermal expansion coefficient, and exhibits coarsening of microstructure due to metal aggregation through grain growth at cell operation temperatures. YSZ in the anode constrains nickel aggregation and prevents sintering of the nickel particles, decreases the effective thermal expansion coefficient bringing it closer to that of the electrolyte, and provides better adhesion of the anode with the electrolyte. Anode nickel is the catalyst for hydrogen oxidation and the electrical current conductor. It is also highly active for the steam reforming of methane. This catalytic property is exploited in the internal reforming SOFCs that can operate on fuels composed of mixtures of methane and water. Although nickel is an excellent hydrogen oxidation and methane-steam reforming catalyst, it also catalyzes the formation of carbon from hydrocarbons under reducing conditions. Unless sufficient amounts of steam are present along with the hydrocarbon to remove carbon from the nickel surface, the anode may be destroyed. As a result, even when using methane as the fuel, relatively high steam-to-carbon ratios are needed to suppress this detrimental reaction. Unfortunately, due to the high catalytic activity of nickel for hydrocarbon cracking, this approach does not work for higher hydrocarbons, and it is generally not possible to operate nickel-based anodes on higher hydrocarbon-containing fuels without pre-reforming with steam or oxygen. Additives to the Ni+YSZ cermet, such as 5% ceria or 1% molybdena inhibit the susceptible of nickel to become coated with a carbon layer when reacting with carbon based fuels, which could prevent further reaction. Nevertheless, nickel-YSZ composite remains the most commonly utilized anode material for SOFCs and is satisfactory for cells operating on clean, reformed fuel.

Advanced SOFC designs place additional constraints on the anode, such as tolerance of oxidizing environments and/or the ability to tolerate significant quantities of sulphur and/or hydrocarbon species in the fuel stream. Alternative anode materials, include cerium oxide or strontium titanate/cerium oxide mixtures, but the benefits obtained in terms of sulphur, hydrocarbon and/or redox tolerance are counterbalanced by other limitations, such as the difficulty of integrating such materials with existing cell and stack fabrication processes and materials. Copper based anodes can be used at intermediate temperatures (<800^{o}C).

Interconnect

Doped lanthanum chromite is used as the interconnection for cells which operate at about 1000^{o}C.

In cells intended for operation at lower temperatures (<800^{o}C), it is possible to use oxidation-resistant metallic materials for the interconnection. Ferritic stainless steel alloys in this family offer:

- a protective and conductive chromium-based oxide scale,
- appropriate thermal expansion behaviour,
- ease of manufacturing, and
- low cost.

Although these alloys demonstrate improved performance over traditional compositions, several critical issues remain:

- chromium oxide scale evaporation and subsequent poisoning of cathodes;
- scale electrical resistivity in the long term;
- corrosion and spalling under interconnect exposure conditions; and
- compatibility with the adjacent components such as seals and electrical contact layers.

In mitigation, some surface coatings are applied onto the metallic interconnects to minimize scale growth, electrical resistance, and chromium volatility.

Stack design

Stack design has focused on planar and tubular design cells. The planar SOFC may be in the form of a circular disk fed with fuel from the central axis, or it may be in the form of a square plate fed from the edges. The tubular SOFC may be of a large diameter (>15mm), or of much smaller diameter (<5 mm), the so-called microtubular cells. Also, the tubes may be flat and joined together to give higher power density and easily printable surfaces for depositing the electrode layers. One of the inherent advantages of tubular cell bundles is that the air and the fuel are naturally isolated because the tubes are closed at one end.

The sealing materials and concepts for planar SOFCs is an important issue for the long-term performance stability and lifetime of planar SOFC.

The main advantage of tubular cells over planar cells is that they do not require any high temperature seals to isolate the oxidant from the fuel, and this stabilises the performance of tubular cell stacks over long periods of time. However, their areal power density is much lower (about 0.2W/cm^2) than planar cells (up to 2W/cm^2 for single cells and at least 0.5W/cm^2 for stacks) and manufacturing costs are higher. The volumetric power density is also lower for tubular cells than for planar cells.

High temperature cell operation has three mitigating advantages:

- Reduced need for precious metal, platinum, catalyst and less poisoning
- Reforming of fossil fuel to hydrogen can be performed internally
- The steam produced by the fuel cell can be channelled into turbines to generate more electricity. This process is called co-generation of heat and power (CHP) and improves the overall system efficiency.

27.8 Fuel cell summary

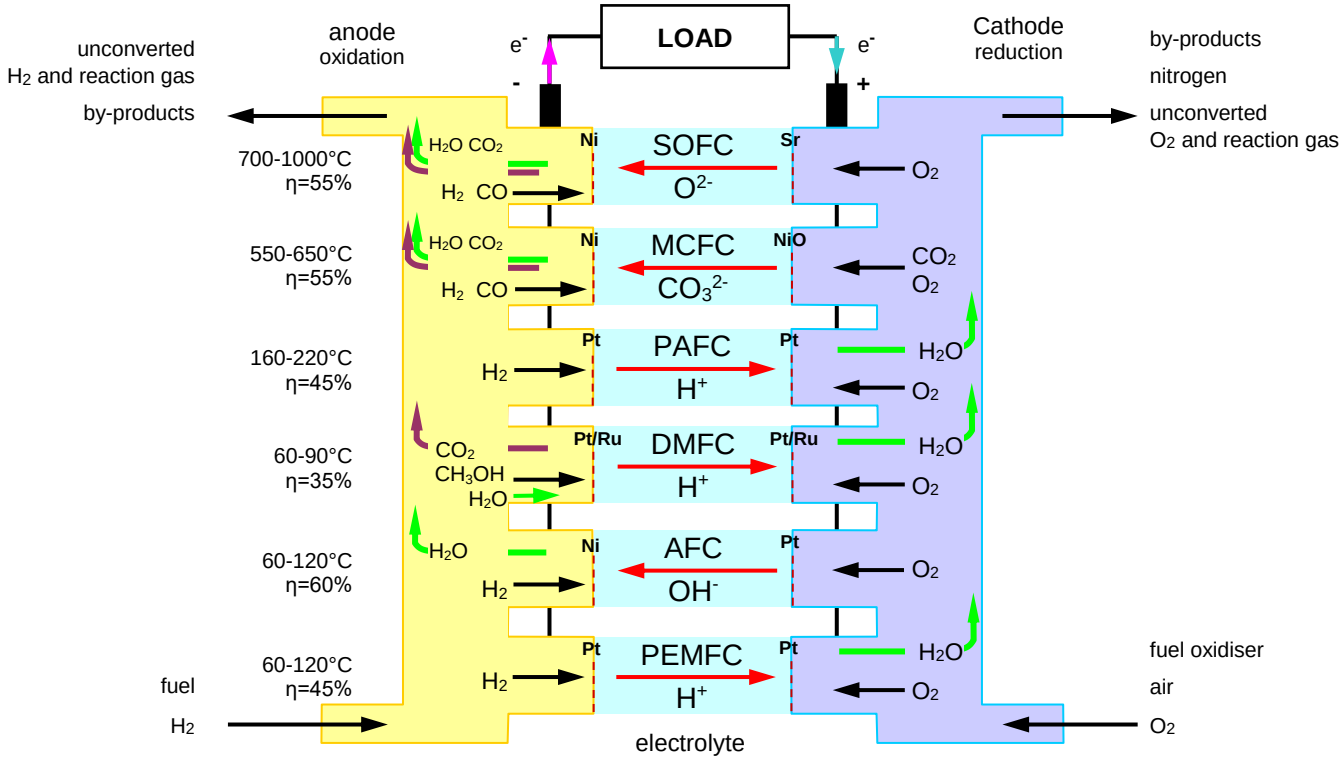

Figure 27.8. *The mechanisms of a fuel cell.*

Gibbs thermodynamic efficiency is $\eta_G = \Delta G/\Delta H = 1 - T\Delta S/\Delta H = \Delta EIt/\Delta H$

Electrochemical reactions in fuel cells

Fuel Cell	Anode Reaction	Cathode Reaction	Overall Reaction
Proton Exchange	$2H_2 \rightarrow 4H^+ + 4e^-$	$O_2 + 4H^+ + 4e^- \rightarrow 2H_2O$	$2H_2 + O_2 \rightarrow 2H_2O(l)$
Alkaline	1) $2H_2 \rightarrow 4H^+ + 4e^-$ 2) $4H^+ + 4(OH)^- \rightarrow 4H_2O$	$O_2 + 2H_2O + 4e^- \rightarrow 4(OH)^-$	$2H_2 + O_2 \rightarrow 2H_2O(l/g)$
Phosphoric Acid	$2H_2 \rightarrow 4H^+ + 4e^-$	$O_2 + 4H^+ + 4e^- \rightarrow 2H_2O$	$2H_2 + O_2 \rightarrow 2H_2O(g)$
Molten Carbonate	1) $2H_2 \rightarrow 4H^+ + 4e^-$ 2) $4H^+ + 2CO_3^{-2} \rightarrow 2H_2O + 2CO_2$	$O_2 + 2CO_2 + 4e^- \rightarrow 2CO_3^{-2}$	$2H_2 + O_2 \rightarrow 2H_2O(g)$
	1) $CH_4 + H_2O \rightarrow CO + 3H_2$ (reformation) 2) $CO + H_2O \rightarrow CO_2 + H_2$ (water-gas shift) 3) $4H_2 + CO_2 \rightarrow CO_2 + 8H^+ + 8e^-$ 4) $CO_2 + 8H^+ + 4CO_3^{-2} \rightarrow 5CO_2 + 4H_2O$	$2O_2 + 4CO_2 + 8e^- \rightarrow 4CO_3^{-2}$	$CH_4 + 2O_2 \rightarrow 2H_2O(g) + CO_2(g)$
Solid Oxide	1) $2H_2 \rightarrow 4H^+ + 4e^-$ 2) $4H^+ + 2O^{-2} \rightarrow 2H_2O$	$O_2 + 4e^- \rightarrow 2O^{-2}$	$2H_2 + O_2 \rightarrow 2H_2O(g)$
	1) $CH_4 + H_2O \rightarrow CO + 3H_2$ (reformation) 2) $CO + H_2O \rightarrow CO_2 + H_2$ (water-gas shift) 3) $4H_2 + CO_2 \rightarrow CO_2 + 8H^+ + 8e^-$ 4) $CO_2 + 8H^+ + 4O^{-2} \rightarrow CO_2 + 4H_2O$	$2O_2 + 8e^- \rightarrow 4O^{-2}$	$CH_4 + 2O_2 \rightarrow 2H_2O(g) + CO_2(g)$

27.9 Fuels

The choice of fuel depends on the application requirement, and the local fuel infrastructure, which influences fuel cell type, system cost, complexity, reformer requirements, etc.
Anode-side fuels:

- Hydrogen, H_2 (direct or via fuel reformer) — all FC
- Methanol, Ethanol, CH_3OH, C_2H_5OH — PEMFC, DMFC, AFC, SOFC
- Methane, C_2H_6 — SOFC, MCFC
- Carbon Monoxide, CO — SOFC, MCFC
- Hydrides, MH — AFC
- Coal — SOFC, AFC
- Metals — SOFC
- Sugars — biological-FC
- Other fuels - hydrazine, formic acid — DMFC

The chemical and consequential electrical properties of these anode-side fuel cells at 25°C are listed in Table 27.3, whilst the effects of anode fuel impurities on the different fuel cells are listed in Table 27.4.

Cathode-side fuels:
Suitable oxidants are air, pure oxygen 0_2, and hydrogen peroxide H_20_2. (see table 27.9) The use of oxygen can produce up to 30% more power than air. Undesirably, hydrogen peroxide gives a lower half-cell potential than oxygen, and is more reactive on the cell components.

H_2O_2 contains oxygen in a state of oxidation midway between molecular oxygen and water.

$$H_2O_2 \rightarrow O_2 + 2H^+ + 2e^- \qquad E_o = -0.682\ V$$
$$H_2O_2 + 2H^+ + 2e^- \rightarrow 2H_2O \qquad E_o = 1.776\ V$$

For the perhydroxyl ion (HO_2^-):

$$OH^- + HO_2^- \rightarrow O_2 + H_2O + 2e^- \qquad E_{Bo} = 0.084\ V$$
$$3OH^- \rightarrow HO_2^- + H_2O + 2e^- \qquad E_{Bo} = -0.87\ V$$

Table 27.3: Alternative anode-side (hydrogen-rich) fuels

Fuel Cells	Anode fuel	Cathode fuel	Enthalpy ΔH	Electrons/H_2 n	Theoretical voltage	Practical voltage	Power density
@ 25°C			kJ/mol		V	V	A-hr/kg
Carbon monoxide	CO	$1½0_2$	283.1	2	1.066		
Hydrogen	H_2	$½0_2$	286.0	2	1.229	0.7	26,000
Hydrazine	N_2H_4	0_2	622.4	4	1.560	0.7	2,100
Methanol	CH_3OH	$1½0_2$	726.6	6	1.214	0.8	1,400
Methane	CH_4	20_2	890.8	8	1.060		
Propane	C_3H_8	50_2	2221.1	20	1.093		

Table 27.4: Fuel constituents impact on fuel cell performance

Gas species	PEFC	AFC	DMFC	PAFC	MCFC	SOFC
H_2	fuel	fuel	fuel	fuel	fuel	fuel
CO	poison < 50ppm reversible	poison	poison	poison > ½%	fuel via shift	fuel via shift
CH_4	diluent	Poison/ diluent	fuel	diluent	diluent	fuel
CO_2, H_2O	diluent	poison	diluent	diluent	diluent	diluent
S (H_2S, COS)	poison cumulative irreversible	poison	poison	poison < 50 ppm reversible	poison < 0.5 ppm reversible	poison < 1 ppm reversible

27.10 Fuel reformers

Low-temperature fuel cells, less than 200ºC, generally operate on pure hydrogen as the anode fuel. The transformation of fossil fuels to hydrogen is called fuel reforming. Coal, oil, and natural gas contain hydrocarbons, molecules consisting of hydrogen and carbon. A reformer splits the hydrogen from the carbon in a hydrocarbon, relatively easily. Three basic technical processing approaches can be used to recover hydrogen from hydrocarbons.

- Thermal Reforming Processes
- Electrolysis Processes
- Photolytic Processes

(i) Thermal processes

Some thermal processes use the energy in various resources, such as natural gas, coal, or biomass, to release hydrogen, which is part of their molecular structure. In other processes, heat, in combination with closed chemical cycles, produces hydrogen from feedstocks such as water - these are known as thermo-chemical processes. Most processes involve a water-gas shift final reaction to form H_2 and CO_2 from any CO product. The various thermal reforming processes are:

- Natural Gas Reforming:
  - Steam methane reforming (see 27.12), 700 - 1000°C
  - Partial oxidation, $2CH_4 + O_2 + 2H_2O \rightarrow 2CO_2 + 6H_2$
- Coal Gasification:
  - $CH_{0.8} + O_2 + H_2O \rightarrow CO + CO_2 + H_2$ + other species
  - $CO + H_2O \rightarrow CO_2 + 2H_2$ + heat
  - $H_2S + ZnO \rightarrow ZnS + H_2O$ for sulphur removal
- Biomass Gasification:
  - $C_6H_{12}O_6 + O_2 + 2H_2O \rightarrow CO + 2CO_2 + 2H_2$
  - $CO + H_2O \rightarrow CO_2 + 2H_2$ + heat

- Renewable Liquid Fuels Reforming:
  - $C_2H_5OH + 3H_2O \rightarrow 2CO_2 + 6H_2$
  - $CO + H_2O \rightarrow CO_2 + 2H_2$ + heat

- High-Temperature Water Splitting, 500°C - 2000°C:
  - $2ZnO$ + heat $\rightarrow 2Zn + O_2$
  - $2Zn + 2H_2O \rightarrow 2ZnO + 2H_2$

(ii) Electrolytic processes

The electrolysis process uses electricity to split water into the diatomic molecules, hydrogen and oxygen.

There are three basic electrolysing methods.

- Polymer Electrolyte Membrane Electrolyser, which operates at 80°C to 100°C
- Alkaline Electrolyser, which operates at 100°C to 150°C
- Solid Oxide Electrolyser, which operates at about 500°C to 800°C

Electrolytic processes use electricity to split water, H_2O into hydrogen H_2 and oxygen O_2, a process that takes place in an electrolyser or an electrolysis cell. The decomposition of water involves two partial reactions that take place at two electrodes. The electrodes are placed in an ion-conducting electrolyte (usually an aqueous alkaline solution with 30% potassium hydroxide KOH). Gaseous hydrogen is produced at the negative electrode (anode) and oxygen at the positive electrode (cathode). The necessary exchange of charge occurs through the flow of OH^- ions in the electrolyte and current (electrons) in the electric circuit. In order to prevent a mixing of the product gases, the two reaction areas are separated by a gas-tight, ion-conducting diaphragm membrane.

About 1 litre of water is required to produce 1 m^3 or 0.09kg hydrogen. Electrolysis requires 367kJ/mol of energy (which is higher than the $\Delta H = 286$kJ/mol that can be derived from H_2) to produce one mole of hydrogen. That is, 1kW of electricity produces 1/267=0.00272 mol/s or 0.00545g/s of H_2.

Anode Reaction:	$2H_2O \rightarrow O_{2(g)} + 4H^+ + 4e^-$	
Cathode Reaction:	$4H^+ + 4e^- \rightarrow 2H_{2(g)}$	0
Overall Cell Reaction:	$2H_2O \rightarrow 2H_{2(g)} + O_{2(g)}$	4x1.23eV

(iii) Photolytic processes

Photolytic processes use light energy to split water into hydrogen and oxygen, with low environmental impact.

- Photobiological Water Splitting
  - Chemical limit:- Glucose + $6H_2O \rightarrow 6CO_2 + 12H_2$
  - Biological limit:- Glucose + $2H_2O \rightarrow 2$Acetate + $2CO_2 + 4H_2$

- Photoelectrochemical Water Splitting
  - Feedstock:- HCl, HBr, Biomass
    - O_2 generation :- $4Br_3^- + 6H_2O \rightarrow 12HBr + 3O_2$
    - H_2 generation:- $6HBr \rightarrow 2Br_3 + 3H_2$

27.10.1 Natural gas reforming

Steam reforming of natural gas, sometimes referred to as steam methane reforming, is the most common method of producing commercial bulk hydrogen as well as the hydrogen used in the industrial synthesis of ammonia. It is also the least expensive method and 48% of the world's hydrogen is produced by steam methane reforming.

The process flow route is shown in figure 27.9 and follows three stages:

stage i Pre-Treatment of the feed

The hydrocarbon feedstock is de-sulphurised (chloride is also removed) using activated carbon filters, pressurised and, depending on the reformer design, either preheated and mixed with process steam or directly injected with the water into the reformer without the need of an external heat exchanger. The water is first softened and demineralised by an ion-exchange water conditioning system.

i. One option is high pressure reforming with integrated heat exchangers and a working pressure of up to 16 bar which reduces the geometric volume of the reformer vessels.

ii. The other option is to operate the reformer at low pressures, 1.5 bar, with an increased conversion ratio and compress the reformate prior to purification.

stage ii Steam reforming and CO-shift conversion

At high temperatures of 700 to 1100°C at 3 to 25 bar, and in the presence of a metal-based catalyst, nickel, steam reacts with methane CH_4, which is the primary component of natural gas, to yield carbon monoxide and hydrogen with minimal carbon dioxide, this synthesized gas is called syngas.

$$CH_4 + H_2O \rightarrow CO + 3H_2 \qquad \text{reformation} \qquad \Delta H = 206 \text{ kJ/mol} \tag{27.8}$$

This reaction is endothermic ($\Delta H > 0$, consumes heat), with the heat required obtained from the combustion of fuel gas and purge/tail gas from the subsequent gas purification stage.

After reforming, the synthesis gas is fed into the CO conversion lower-temperature gas-shift reactor to produce additional hydrogen. The carbon monoxide is reacted with steam over a catalyst to form hydrogen and carbon dioxide, in two stages. The first stage is a high temperature water gas shift at 350°C and then a low temperature shift at 200°C. The reaction is exothermic ($\Delta H < 0$, produces heat) and is summarised by:

$$CO + H_2O \rightarrow CO_2 + H_2 \qquad \text{water-gas shift} \qquad \Delta H = -41 \text{ kJ/mol} \tag{27.9}$$

The chemical reactions that take place are:

$$\begin{aligned} C_nH_m + n\,H_2O &\rightarrow n\,CO + \left(\tfrac{1}{2}m + n\right)H_2 \\ CO + H_2O &\rightarrow CO_2 + H_2 \end{aligned} \tag{27.10}$$

stage iii Gas purification

Hydrogen purification is achieved by means of pressure swing adsorption through four successive vessels filled with selected adsorbents. Purification to remove carbon dioxide and carbon monoxide can achieve hydrogen purities greater than 99.999% by volume and CO impurities of less than 1 vppm (volumetric part per million). The pure hydrogen is compressed, while the gases from recovering the adsorbents, called tail-gas, is fed to the steam reformer burner.

The complete steam reforming process is 70% efficient, with carbon sequestration.

In high-temperature fuel cells (MCFC and SOFC), CO in the fuel stream acts as a fuel. However, it is likely that the water-gas shift reaction is occurring internally and the fuel is actually hydrogen.

$$CO + H_2O \rightarrow CO_2 + H_2 \tag{27.11}$$

Steam reforming can also be used to produce hydrogen from other fuels, such as ethanol, propane, or even petrol.

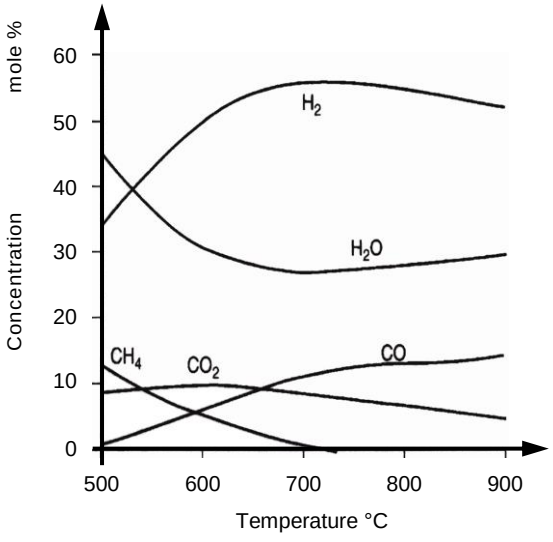

Methane:

$$CH_4 + H_2O\,(+heat) \rightarrow CO + 3H_2$$

Propane:

$$C_3H_8 + 3H_2O\,(+heat) \rightarrow 3CO + 7H_2 \tag{27.12}$$

Ethanol:

$$C_2H_5OH + H_2O\,(+heat) \rightarrow 2CO + 4H_2$$

Petrol, using iso-octane and toluene which are only two of compounds in petrol:

$$\begin{aligned} C_8H_{18} + 8H_2O\,(+heat) &\rightarrow 8CO + 17H_2 \\ C_7H_8 + 7H_2O\,(+heat) &\rightarrow 7CO + 11H_2 \end{aligned} \tag{27.13}$$

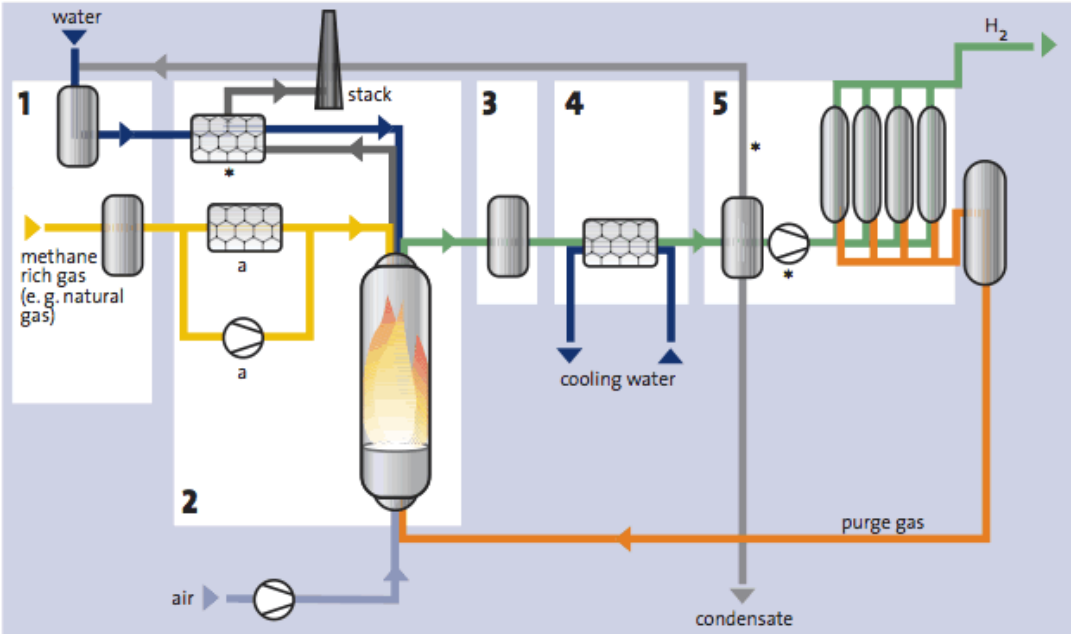

Figure 27.9. *Flow chart of a steam reformer:*
1 Feed Pre-Treatment *2 Reforming and Steam Generation*
3 High Temperature Conversion *4 Heat Exchanger Unit*
5 Purification Unit, depending on reformer design 'a' either heat exchanger for low pressure reformer or compression to 1 bar for high pressure reformer.

27.11 Hydrogen storage and generation from hydrides

Hydrogen can be stored at pressures up to 30MPa (300atm), but the energy density is low. Storage of liquid hydrogen at 22K requires a lot of energy and the energy density is still low. The viable storage possibilities are metal hydrides, glass micro-spheres and carbon nano-fibres.

Table 27.5a Hydrogen storage

Storage media	Metal hydride density g.cm $^{-3}$ at 20°C	H_2 storage by weight	H_2 storage capacity g/cc	Heat of desorption ΔH kJ.mol / H_2
$LaNi_5$	8.3	1.4%	0.11	-8.9
FeTi	6.2	1.75%	0.11	-28.0
Mg_2Ni	4.1		0.15	
Mg	1.74	7.6%	0.13	-74
MgNi eutectic	2.54		0.15	
liquid H_2	0.07		0.07	

Metal hydrides
Metal hydrides offer a safe, constant pressure way to store and subsequently retrieve pure hydrogen. Sodium borohydride is a white solid at room temperature, stable in dry air and decomposing only at temperatures above 400°C. Dry sodium borohydride (or alternatively $LiAlH_4$) use the following metal hydride retrieval reaction:

$$NaBH_{4(aq)} + H_2O_{(l)} \xrightarrow{cat} 4H_{2(g)} + NaBO_{4(aq)} + heat$$

When hydrogen fuel is needed, a sodium borohydride solution is pumped at a controlled rate over a catalyst within the reactor, producing pure hydrogen and sodium borate, a non-toxic compound found in detergents. Hydrogen gas is generated proportionally to the rate at which the borohydride solution is pumped into the reactor. Hydrogen gas is then separated from the liquid metaborate by-product. The hydrogen is humidified because the heat of reaction converts some liquid water to vapour. The by-product can be recycling after removal from the system. Both products and reactants are indefinitely reusable and stable to air. The system has a high effective hydrogen pressure of about 7,000 psi.
Since the highly flammable hydrogen gas is generated in a miniature reactor immediately before use, it is a safe way of storing hydrogen compared to compressed or liquefied hydrogen. $NaBH_4$'s stability in air

also makes it a much safer choice than its pyrophoric reversible metal hydride counterpart. A disadvantage of the method is its high cost since sodium borohydride is not a common chemical reagent. Only 4% of the heavy high pressure tank mass is hydrogen.
A complex hydride system based on lithium amide has been developed based on the following reversible displacive reaction taking place at 285°C and 1 atm:

$$Li_2NH + H_2 \rightarrow LiNH_2 + LiH$$

In this reaction, 6.5 wt. % hydrogen can be reversibly stored with potential for 10 wt.%. The temperature of this reaction can be lowered to 220°C with magnesium substitution, although at higher pressures.

Alloy hydrides
AB_5 and AB_2 type alloys have advantages in hydrogen storage capabilities and operation parameters.
AB_5 alloys combine a hydride forming metal A, usually a rare earth metal (La, Ce, Nd, Pr, Y or their mixture known as Misch metal), with a non-hydride forming element B – nickel. The nickel can be doped with other metals, such as Co, Sn or Aℓ, to improve material stability or to adjust the equilibrium hydrogen pressure and temperature required for hydrogen discharge.
AB_2 alloys, also know as Laves phases, represent a group of alloys containing titanium, zirconium or hafnium at the A-site and a transition metal(s) at a B-site (Mn, Ni, Cr, V and others). Although reversible hydrogen storage capabilities are similar to AB_5 alloys, AB_2 alloys can store additional hydrogen at high pressures and have higher discharge rate capacity when used as battery negative electrodes.
General properties of metal hydride hydrogen storage are:

- Storage capacities up to 3.6 wt.%;
- Reversible;
- Stable in air; and
- Operate at room temperature and 1 to 10 atmospheres.

Table 27.5b Hydrogen storage in alloys

Storage media	Chemical composition	Hydrogen storage capacity wt.% @ 25°C	Equilibrium pressure plateau bar @ 25°C
Lanthanum-nickel alloy	$LaNi_5$	1.5 - 1.6	≈2
Lanthanum-nickel-cobalt alloy	$LaNi_4Co_{0.5}$	1.4 - 1.5	≈0.5
Mischmetal-Nickel alloy	$MnNi_5Mn$ La: 20-27%; Ce: 48-56%; Pr: 4-7%; Nd: 12-20%	1.5 - 1.6	≈10
Titanium-Manganese Alloy	$Ti_{0.98}Zr_{0.02}V_{0.43}Fe_{0.09}Cr_{0.05}Mn_{1.5}$	1.6 - 1.7	≈10

Glass micro-spheres can be encouraged to absorb H_2 gas at higher temperature, then retain it at lower temperatures before releasing it when the temperature is raised. A technology yet to be proven. Storage is safe, is reusable, and un-contaminable, with large H_2 per unit volume. The technology is complicated, expensive, and delicate.

Carbon nano-fibres provide a large surface for H_2 to bind to and increase the amount of H_2 that can be stored for a given tank pressure. Reported capable of absorbing 67% times their own mass of hydrogen and inert storage is safe. The technology is unproven and there are long-term carcinogenic safety concerns with nano-fibres. Carbon nano-fibres are expensive.

Table 27.6: Fuel cell emission properties

Engine Type	Water Vapour	Carbon Dioxide	Carbon Monoxide	Nitrous gases	Hydro-Carbons
	H_2O	CO_2	CO	NO_x	C_xH_y
	kg/km	kg/km	kg/km	kg/km	kg/km
Gasoline Combustion	0.111	0.241	0.013	0.87×10^{-3}	1.75×10^{-3}
Fuel Cell operating on Hydrogen from Gasoline	0.091	0.199	-	-	-
Fuel Cell operating on Hydrogen from Methane	0.071	0.043	0.01×10^{-3}	1.6×10^{-6}	2.1×10^{-6}
Fuel Cell operating on Renewable Hydrogen	0.071	0.0	0.0	0.0	0.0

27.12 Fuel cell emissions

Fuel cells running on hydrogen derived from a renewable source emit only water vapour. The following Table 27.6 shows a comparison of the water vapour plus carbon and nitrogen based emissions from fuel cells, running on a variety of fuels, as compared to the internal combustion engine in the first data row.

27.13 Fuel cell electrical characteristics

A typical fuel cell produces a voltage from 0.6V to 0.7V at full rated load. Voltage decreases as current (and temperature) increases, as shown in figure 27.10, due to numerous factors:

- *Activation loss*, which is the potential difference above the equilibrium value required to produce a current flow.
- *Ohmic losses*, which are voltage drops due to resistance of the cell components and interconnects.
- *Mass transport loss*, which is the depletion of reactants at catalyst sites under high loads, especially at the cathode, causing rapid loss of voltage.
- *Mixed potential reactions* at the electrodes due to parasitic reactions that lower the equilibrium potential. This can be due to fuel impurities, cathode H_2O_2 intermediaries, or anode fuel crossover through the electrolyte.
- *Activation over-potential* at the cathode due to sluggish oxygen reduction kinetics, compared to faster anode reaction rate, which are most pronounced at low current densities.

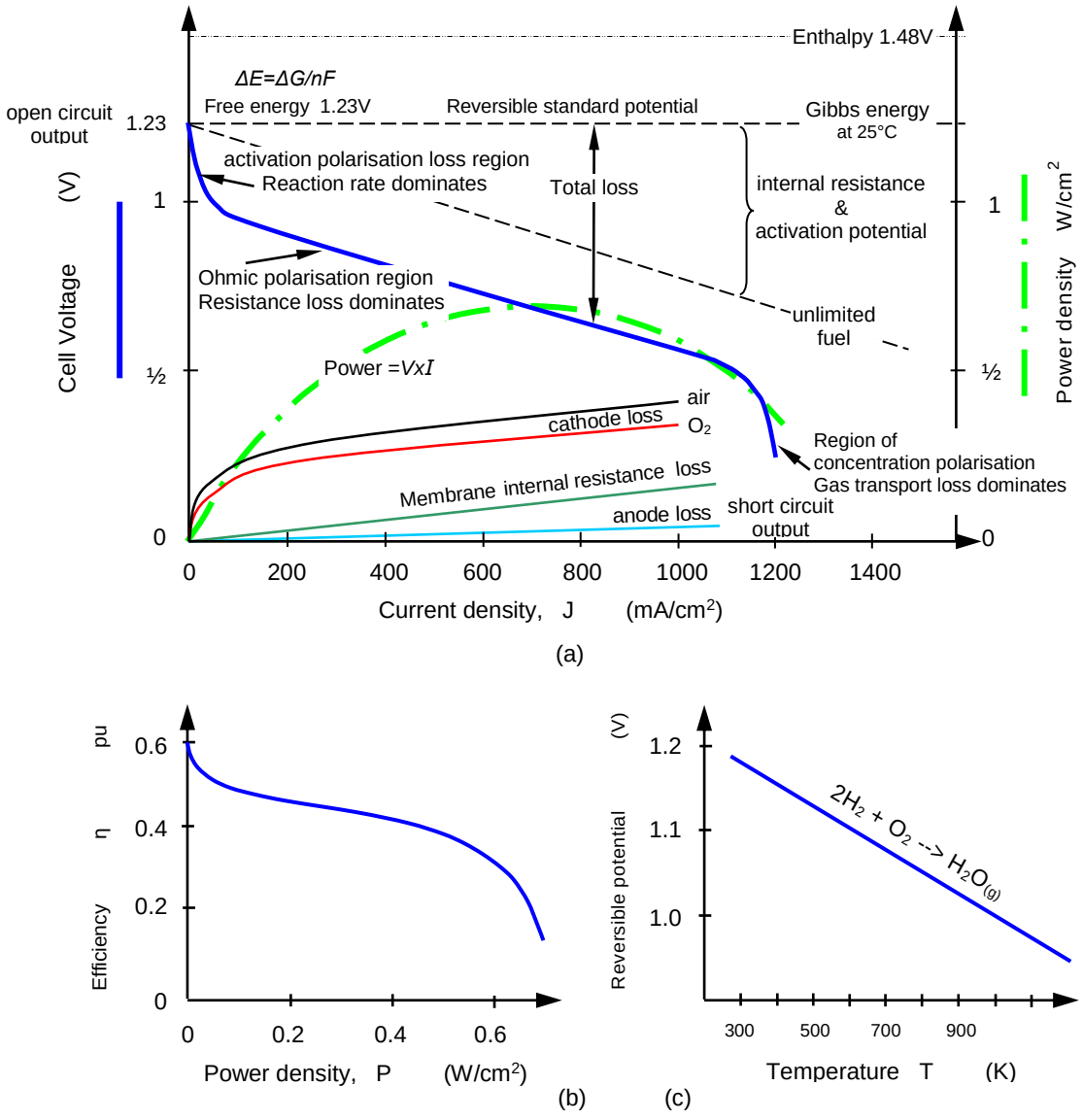

Figure 27.10. *Graphs of a hydrogen/air fuel cell: (a) voltage versus current density, (b) efficiency versus current density; and (c) open circuit voltage versus temperature.*

Energy conversion of a fuel cell can be summarized by the following equation:

Chemical energy of fuel = electrical energy + Heat energy

A single, ideal H_2/air fuel cell should provide 1.16V at zero current, that is, open-circuit, 80°C and 1 atmosphere gas pressure. A measure of energy conversion efficiency for a fuel cell is the ratio of the actual cell voltage to the theoretical maximum voltage for the H_2/air reaction. Thus a fuel cell operating at 0.7V is generating about 60% of the maximum useful energy available from the fuel as electric power. The remaining energy, 40%, is heat. The characteristic performance curve in figure 27.10 for a fuel cell represents the DC voltage delivered at the cell terminals as a function of the current density, that is, total current divided by the membrane area, being drawn from the fuel cell by the load in the external circuit. Note that the efficiency increases as the loading decreases, unlike the internal combustion engine.
The steady-state power, $P = I \times V$, expressed in watts, delivered by a cell is the product of the current I drawn and the terminal voltage V at the current I. Power is also the rate at which energy W is made available, $P = W / t$, or conversely, energy $W = P \times t = V \times I \times t = V \times Q$, expressed in units of joules, or watt-hours, is the continuous power available over a time period t.

- Specific power is the ratio of the power produced by a cell to the mass of the cell, and
- Power density is the ratio of the power produced by a cell to the volume of the cell.

High specific power and power density are important for transportation applications, to minimize the weight and volume of the fuel cell as well as to minimize cost.

27.14 Thermodynamics

Prediction of the maximum possible voltage from a fuel cell process involves evaluation of energy differences between the initial state of the reactants in the process, $H_2 + ½0_2$, and the final state, H_20. Such evaluation relies on state thermodynamic functions in a chemical process, primarily the Gibbs free energy. The maximum cell voltage, at electrical output open-circuit, or emf, ΔE, for the hydrogen/air fuel cell reaction ($H_2 + ½0 \rightarrow H_20$) at a specific temperature and pressure is given by the relationship, in electrical terms:

$$\Delta E = -\frac{\Delta G}{n \times q_e \times N_o} = -\frac{\Delta G}{n \times F} = \frac{W}{n \times F} = \frac{W}{Q} \qquad \text{(V)} \qquad (27.14)$$

where ΔG is the Gibbs free energy change for the reaction or energy available for electrical work, W,
n is the number of moles of electrons involved in the reaction per mole of reactant, H_2, and
F is Faraday's constant, 96,487 C/mol (J/V) (26.8015Ah/kg-equiv), the charge transferred per mole of electrons. ($F = q_e x N_o = 1.60 \times 10^{-19} \text{x} 6.02 \times 10^{23} = 96{,}487$ C/mol)

Faraday's constant is Avogadro's number $N_o = 6.02 \times 10^{23}$ multiplied by the charge of one electron, $q_e = 1.60 \times 10^{-19}$. The product $n \times F$ or charge Q is the amount of electricity produced. At one atmosphere of pressure, the Gibbs net free energy change ΔG in the fuel cell process (per mole of H_2), available for net useful work, is calculated from the reaction temperature T, and from changes in the reaction enthalpy, ΔH, and entropy, ΔS.

$$\Delta G = -n \times F \times \Delta E = \Delta H - T \times \Delta S \qquad \text{(J)} \qquad (27.15)$$

where T is the absolute temperature, K
ΔS is the entropy change for the reaction, ($\Delta S < 0$ for a fuel cell reaction), J/K
ΔH is the enthalpy or energy (change) released by the reaction, J.

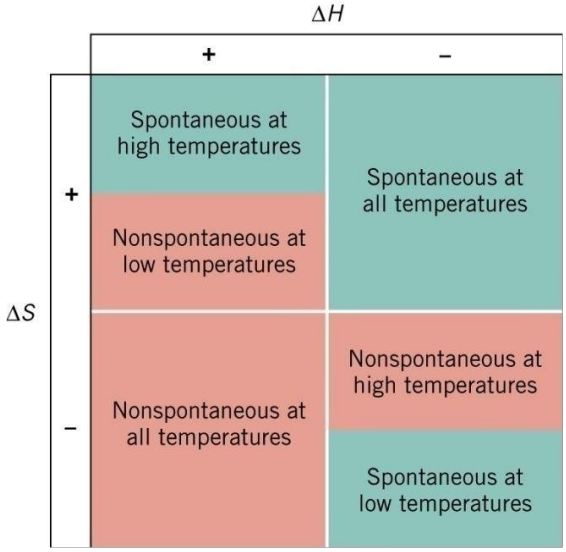

Figure 27.11. *Summary of the effects of the sign of the enthalpy and entropy change on the spontaneity of a process.*

The product $T \times \Delta S$ is the heat associated with the electrochemical processes occurring, leaving $\Delta H - T\Delta S$ available for the externally diverted production of electrical energy. A change will be spontaneous when the enthalpy term (ΔH) and the entropy term ($T\Delta S$) combine to give a negative value of ΔG (when free energy decreases) and a positive emf ΔE, as illustrated in figure 27.11. At equilibrium $T\Delta S = \Delta H$.

Combining equations (27.14) and (27.15), the maximum cell voltage is therefore

$$\Delta E = - \frac{\Delta H \; - \; T \times \Delta S}{n \times F} \qquad \text{(V)} \tag{27.16}$$

When the source is loaded, the total cell internal heat released (losses) q is

$$q = T \times \Delta S + I\left(E_{o/c} - E_I\right) \qquad \text{(W)} \tag{27.17}$$

where $E_{o/c}$ is the cell open circuit voltage ($I = 0$), that is ΔE from equation (27.16) and
E_I is the terminal voltage at load current I.

The term $I \times (E_{o/c} - E_I)$ is the power dissipated in the fuel cell effective internal resistance, or Thevenin resistance.

The various enthalpies and entropies are characterised at 25°C (NTP) and the symbols are annotated with a zero superscript. Operation at temperatures other than NTP and reaction quotient N involves the use of Nernst equation (R is the gas constant, 8.314 J/K mol).

$$E = E_o - \frac{RT}{nF} \ell n N \tag{27.18}$$

The overall cell efficiency comprises three components, namely the Gibbs efficiency η_G, the voltage efficiency, η_V, and the utilisation efficiency is the fraction of the input fuel used, η_u. That is

$$\eta = \eta_G \eta_V \eta_u = - \frac{nF}{\Delta H} E_I = - \frac{Q}{\Delta H} E_I = - \frac{I \times E_I}{\Delta H \times t} \tag{27.19}$$

where the Gibbs thermodynamic efficiency is $\eta_G = \Delta G / \Delta H = 1 - T\Delta S / \Delta H = \Delta E I t / \Delta H$
the voltage efficiency is $\eta_V = E_I / E_{o/c}$ where E_I is the output voltage at current I.

Example 27.1: ***Formation of water vapour***

Based on the table below, is the following reaction spontaneous at 250°C?

$H_{2(g)} + ½O_{2(g)} \rightarrow H_2O_{(g)}$

Compound	Enthalpy ΔH_f^0	Entropy ΔS^0
	kJ/mol	J/mol.K
H_2 (g)	0.0	130.6
O_2 (g)	0.0	205.0
H_2O (g)	-241.8	188.7
H_2O (ℓ) 1Atm & 298K	-285.14	69.91

Solution

First ΔH and ΔS are calculated for the reaction, then the value of ΔG, to see if it is less than zero.
Look up the thermodynamic data.
From the thermodynamic data in the table, ΔH and ΔS are both calculated.
The standard enthalpy of formation of any element is zero, thus using Hess' law, for 1 mole of product

$\Delta H° = \Delta H°_{f(products)} - \Delta H°_{f(reactants)} = -285.8$ kJ/mol $- 0 = -285.8$ kJ/mol.

for a liquid

$$\begin{aligned} \Delta H° \; &= \; \Delta H^o_{f(products)} \; - \; \Delta H^o_{f(reactants)} \\ &= \Delta H^o_{H_2O} - \left(1 \times \Delta H^o_{H_2} \; + \; ½ \times \Delta H^o_{O_2}\right) \\ &= \; -241.8\text{kJ/mol} \; - \; \left(1 \times 0 \; + \; ½ \times 0\right) \\ &= -241.8\text{kJ / mol} \end{aligned}$$

The entropy is

$$\begin{aligned} \Delta S° \; &= \; \Delta S^o_{f(products)} \; - \; \Delta S^o_{f(reactants)} \\ &= \Delta S^o_{H_2O} - \left(1 \times \Delta S^o_{H_2} \; + \; ½ \times \Delta S^o_{O_2}\right) \\ &= \; -188.7\text{J/mol.K} \; - \; \left(1 \times 130.6 \; + \; ½ \times 205.0\right) \\ &= -44.3\text{J / mol} \end{aligned}$$

Combining ΔH and ΔS to give ΔG

$$\begin{aligned}\Delta G &= \Delta H - T \times \Delta S \\ &= -241.8\text{kJ/mol} - 298\text{K} \times (-0.0443\ \text{kJ/mol.K}) \\ &= -241.8\text{kJ/mol} - 13.20\text{kJ/mol} \\ &= -228.5\text{kJ/mol}\end{aligned}$$

The gas reaction is spontaneous, since $\Delta G < 0$.
The chemical reaction can do 228.5kJ/mol of work and produces 13.2kJ/mol of heat to the environment.

♣

Example 27.2: ***Derivation of ideal fuel cell voltage***

The reaction $\frac{1}{2}O_{2(g)} + H_{2(g)} \rightarrow H_2O_{(\ell)}$ is used in fuel cells to produce an electrical current. The reaction can also be carried out by direct combustion.

Thermodynamic data, from table 27.9:
molar entropies $\Delta S°$ in J/mol.K: $H_2O_{(\ell)}$ 70.0; $O_{2(g)}$ 205.0; $H_{2(g)}$ 130.6;
molar enthalpies $\Delta H°_f$ in kJ/mol: $H_2O_{(\ell)}$ -285.8 (note, liquid H_2O).
Use this information (and table 27.9 if necessary) to find

i. The amount of heat released when the reaction takes place by direct combustion;
ii The amount of heat released by the fuel cell under the same conditions;
iii The amount of electrical work the same reaction can perform when carried out in a fuel cell at 298K under reversible conditions;
iv. The cell voltage at an operating temperature of 80°C;
v. The fuel cell has an active area of 100cm^2 and generates 0.6A/cm^2. Estimate the cell efficiency and heat generated, if the cell voltage is 0.7V at this current density; and
vi. If the water is formed as a gas, calculate the open circuit voltage and the cell thermodynamic efficiency for $H_2O_{(g)}$ $\Delta H°_f$ = -241.8 kJ/mol and $\Delta S°$ =188.7 J/mol.K.

Solution

In this reaction, 1.5 moles of gas (½ mole of O_2, 16g and 1 mole of H_2, 2g) are consumed to be replaced by 18 mL of water (1 mole of H_2O weighs 18g).

First, find $\Delta H°$ and $\Delta S°$ for the process at 298K (see example 27.1).

i. The standard enthalpy of formation of any element is zero, thus using Hess' law
$\Delta H° = \Delta H°_{f(\text{products})} - \Delta H°_{f(\text{reactants})}$ = -285.8 kJ/mol - 0 = -285.8 kJ/mol.
That is, when hydrogen and oxygen combine directly, the heat released is -285.6kJ/mol

Similarly, $\Delta S° = S°_{f(\text{products})} - S°_{f(\text{reactants})}$ = (70.0) - (½×205.0 + 130.6) = -163.2 J/mol.K

ii. The heat released in the fuel cell reaction is the difference between the enthalpy change (the total energy available) and the reversible work that was expended:

$$\begin{aligned}T \times \Delta S &= (298\text{ K}) \times (\text{-}163.2\text{ J/K}) \\ &= \text{-}\ 48{,}600\text{ J} = \text{-}\ 48.6\text{ kJ}\end{aligned}$$

iii. The Gibbs free energy change in the fuel cell process (per mole of H_2) gives the maximum electrical work the fuel cell can perform and is calculated from equation (27.15):

$$\begin{aligned}W = \Delta G = \Delta H &- T \times \Delta S \\ &= \text{-}\ 285{,}800\text{ J - (298 K)} \times (\text{-}163.2\text{ J/K}) \\ &= \text{-}\ 237{,}200\text{J}\end{aligned}$$

iv. From equation (27.14), for the hydrogen/air fuel cell at 1 atmosphere pressure and 25°C (298K), the cell voltage is 1.23V:

$$\Delta E = -\frac{\Delta G}{nF}$$

$$= -\frac{\text{-}237{,}200\text{ J}}{2 \text{ x } 96{,}487\text{ J/V}} = 1.23\text{ V}$$

As temperature rises from room temperature to that of an operating fuel cell, 80°C or 353 K, the enthalpy values of ΔH and ΔS change slightly, but T changes by 55°C. Thus the absolute value of ΔG decreases. As an estimation, assume no change in the values of ΔH and ΔS.

$$\Delta G = \Delta H - T \times \Delta S$$
$$= -285{,}800 \text{ J/mol} - (353 \text{ K})(-163.2 \text{ J/mol K}) = -228{,}200 \text{ J/mol}$$

Thus, the maximum cell voltage decreases (for the standard case of 1 atm), from 1.23 V at 25°C to 1.18V at 80°C:

$$\Delta E = -\frac{\Delta G}{nF}$$
$$= -\frac{-228{,}200 \text{ J}}{2 \text{ x } 96{,}487 \text{ J/V}} = 1.18\text{V}$$

An additional correction for air, instead of pure oxygen, and using humidified air and hydrogen, instead of dry gases, further reduces the maximum voltage obtainable from the hydrogen/air fuel cell to 1.16V at 80°C and 1 atmosphere pressure.

v. The cell current is

$$I_{cell} = J(\text{A/cm}^2) \times Area(\text{cm}^2)$$
$$= 0.6\text{A/cm}^2 \times 100\text{cm}^2 = 60\text{A}$$

The excess heat generated per fuel cell can be estimated as follows

$$P_{heat} = P_{total} - P_{electrical}$$
$$= V_{ideal} I_{cell} - V_{cell} I_{cell}$$
$$= 1.16\text{V} \times 60\text{A} - 0.7\text{V} \times 60\text{A}$$
$$= 69.6\text{W} - 42.0\text{W}$$
$$= 27.6\text{W or } 27.6\text{J/s}$$

The cell produces 69.6W of which 27.6W are internal losses with 42W delivered to the electrical load. Alternatively, the cell loses 27.6 J every second.
The effective internal resistance is

$$R = \frac{V_{ideal} - V_{cell}}{I_{cell}}$$
$$= \frac{1.16\text{V} - 0.7\text{V}}{60\text{A}} = 7.7\text{m}\Omega$$

Assuming 100% of the hydrogen reacts, for equation (27.19) the cell efficiency at 60A is

$$\eta = -\frac{nF}{\Delta H} E_I$$
$$= -\frac{2 \text{ x } 96{,}487 \text{ J/V}}{-285{,}800 \text{ J}} 1.09\text{V} = 73.6\%$$

vi. The entropy can be calculated as in part i. $\Delta S = [188.7] - [130.6 + ½ \text{ x } 205] = -44.4$ J/mol.K.

$$\Delta E = -\frac{\Delta H - T \times \Delta S}{nF}$$
$$= -\frac{-241{,}800 \text{ J} - (298 \text{ K}) \times (-44.4 \text{ J/K})}{2 \text{ x } 96{,}487 \text{ J/V}}$$
$$= -\frac{\Delta G}{nF} = -\frac{-228{,}600 \text{ J}}{2 \text{ x } 96{,}487 \text{ J/V}} = 1.185\text{V}$$

The Gibbs thermodynamic efficiency is given by

$$\eta_G = \frac{\Delta G}{\Delta H} = \frac{228{,}600 \text{ J}}{241{,}800 \text{ J}} = 94.5\%$$

which is higher than the liquid case, which from part iii is 237,200J / 285,800J = 83%.

♣

Example 27.1 along with figure 27.10c, illustrate how fuel cell open-circuit voltage ΔE (and efficiency, $\Delta G / \Delta H$) decreases with increased operating temperature. Table 27.7 shows the standard potentials for the various types of fuel cells, when functioning at their normal operating temperature which is well in excess of NTP conditions, when 1.23V is predicted if only water and heat are products. The table also shows the Carnot efficiency ($\eta_{carnot} = 1 - T/298\text{K}$) for pure hydrogen and oxygen forming water at an ambient of 25°C. This efficiency shows that the fuel cell potential efficiency (SOFC) is higher than conventional combustion energy conversion, for temperatures below 870°C.

Table 27.7: Ideal standard potential for different fuel cell types at 1 atm (1 bar) pressure

Fuel type	Cell type	Ideal $H_2 + O_2$ cell	PEMFC	AFC	PAFC	MCFC	SOFC
temperature	°C	25	80	150	200	650	800 / 1000
H_2	V	1.230	1.183	1.155	1.143	1.021	0.98 / 0.919
ΔG	kJ/mol	-237.2	-228.2	-222.7	-220.4	-196.6	-188.6 / -177.4
η Efficiency	%	83	80	78	77	69	66 / 62
η_{carnot} = 1 - T/298K	%	0	15	29	37	68	72 / 77
CH_4	V	N/A	N/A	N/A	N/A	1.036	1.034 / 1.032

Example 27.3: ***Carbon fuel cell***

A fuel cell has the following reactions:

Anode: $C + 2O^{2-} \rightarrow CO_2 + 4e^-$

Cathode: $4e^- + O_2 \rightarrow 2O^{2-}$

At STP, the changes of enthalpy and of free energy, per mole of CO_2, are:

ΔH = -393.5 kJ/mol

ΔG = -394.5 kJ/mol

i. What is the overall reaction?
ii. What is the ideal emf?
iii. What is the difference in entropy between reactants and products?

Assume that the internal resistance of the cell is 1mΩ. Otherwise, the cell behaves as an ideal voltage source. If the cell is to deliver 1 MWh of electricity to the load in minimum possible time:

iv. What is the load resistance under such conditions?
v. How much carbon is needed?

Solution

i. The overall reaction is

$$C + O_2 \rightarrow CO_2 \qquad \Delta H = -393.5 \text{ kJ/mol}$$

ii. Since for each mole of product CO_2, 4 moles of electrons pass trough the load ($n_e = 4$), the open-circuit voltage is

$$V_{OC} = \frac{\Delta G}{n_e q N_o}$$

$$= \frac{394.4\text{kJ/mol}}{4 \times 1.6 \times 10^{-19} \times 6.02 \times 10^{23}} = 1.024\text{V}$$

iii. Assume that the cell operates isothermally at 298 K (reactants and products at the same temperature). Then

$$\Delta G = \Delta H - T\Delta S$$

$$\Delta S = \frac{\Delta H - \Delta S}{T}$$

$$= \frac{-393.44\text{kJ/mol} - 394.5\text{kJ/mol}}{298\text{K}} = 3\text{J/mol.K}$$

Notice that in this reaction, owing to the free energy change being (in absolute value) larger than the enthalpy change, there is an increase in entropy. If the cell is to operate reversibly, that is, with no entropy change, then it has to absorb heat - it will have to operate endothermically.

iv. Maximum power transfer occurs when the load resistance is equal to the internal resistance, $R_L = R = 1\text{m}\Omega$.

v. To transfer 1 MWh (3.6×10^9 J) in minimum time, maximum power is when $R_L = R = 1\text{m}\Omega$, and the current is

$$I_L = \frac{V_L}{R + R_L} = \frac{1.024\text{V}}{2\text{m}\Omega} = 512\text{A}$$

The load voltage is

$$V_L = I_L R_L = 512\text{A} \times 1\text{m}\Omega = 0.512\text{V}$$

The power in the load is

$$P_L = V_L I_L = 0.512\text{V} \times 512\text{A} = 262.1\text{W} \ (\text{or J/s})$$

The time necessary to deliver 3.6×10^9 J at the rate of 262.1 J/s is

$$t = \frac{\text{energy}}{\text{power}} = \frac{3.6 \times 10^9\text{J}}{262.1\text{W}} = 13.7 \times 10^6\text{s}$$

The energy that the fuel cell must deliver is $2 \times 3.6 \times 10^9$ J $= 7.2 \times 10^9$ J because the internal loss is equal to the power in the load.
If 1 mole of carbon delivers 394.5 kJ of electricity, then to deliver 7.2×10^9 J, the number of moles of carbon must be

$$N = \frac{7.2 \times 10^9\text{J}}{394.5\text{kJ}} = 18.25 \text{ kmoles}$$

♣

27.15 Fuel cell features

Having considered the structure and operating mechanisms and characteristics, the following fuel cell features can be summarised.

Advantages

- Fuel cell power is a clean alternative to the internal combustion engine, fuelled with only hydrogen and producing no pollutants other than water. Direct energy conversion.
- Simple fuelling requiring only hydrogen fuel, taking the required oxygen from the air.
- Fuel flexibility in high operating temperature cells.
- No recharging is necessary, low maintenance.
- A perpetual efficient, primary cell.
- So long as fuel is provided, the cells can provide continuous power.
- Maximum efficiency at low power levels; opposite to the internal combustion engine.
- Operate with high efficiency >60%; internal combustion engine is typically about 30%.
- High energy density.
- Silent operation and safe, with no moving parts, vibration free.
- Portable, modular construction.

Shortcomings

- The environmentally friendly credentials of fuel cells overlook the processes needed to generate and distribute the necessary hydrogen fuel. Fuel cells merely shift the pollution from the fuel cell to the reforming location.
- 98% of hydrogen is produced from fossil fuel sources.
- No infrastructure exists to provide and distribute the necessary hydrogen fuel.
- Electrolyte freeze-up at low temperatures.
- Electrodes and catalysts are prone to contamination and are expensive.
- Because of the exotic materials and complex design, the system is expensive.
- Not yet proven commercially viable in common usage, compared to the alternatives.
- Best as primary source.
- Limited availability.
- Low durability.
- Low power density per unit volume, not volume efficient due to associated ancillaries.
- Alternatively hydrogen can be generated in situ, as required, from hydrocarbon fuels such as ethanol, methanol, petrol or compressed natural gas from the reforming process. Reforming generates carbon dioxide as a waste product. It is also expensive with a chemical plant in situ, but this does simplify the fuel supply infrastructure problem, however the fuel could just as readily be used in an internal combustion engine.
- Despite safety precautions, there is a perception that hydrogen fuel is unsafe.
- The low cell voltage, 0.6V to 0.7V, means that many series connected cells are needed.

- Pulse demands shorten lifetime.
- The process is not reversible within the fuel cell and as with the primary cell, it cannot accept or store regenerative energy. The reactants must flow continuously.
- Fuel cells have a low dynamic range and slow transient response which causes an unacceptable lag in responding to instant power demands. At low powers levels, a power boost from a battery or supercapacitor would improve transient performance.
- Most designs operate at high temperatures so as to achieve reasonable operating efficiencies. To generate the same efficiencies at lower temperatures requires large quantities of expensive platinum catalysts.
- Complex to operate.

27.16 Fuel cell challenges

The shortcomings of the fuel cell represent the possible challenges of this energy source.

27.16.1 Chemical technology challenges

Fuel cell material development is mainly concern with electrolytic membrane materials. Many of the following challenges are orientate towards EV application using the PEM fuel cell.

- Durability: More durable PEMFC membranes are needed that can operate at temperatures greater than 100°C and still function at sub-zero ambient temperatures. A 100°C temperature target is required in order for a fuel cell to have a higher tolerance to impurities in fuel. Also, water by-product at over 100ºC has better co-generation possibilities. Because of frequent start and stop, it is important for the membrane to remain stable under cycling conditions. Membranes tend to degrade with cycling, particularly as operating temperatures rise.
- Hydration: PEMFC membranes must be hydrated in order to transfer hydrogen protons. At around 80°C, hydration is lost without a high-pressure hydration system. Membranes are needed for sub-zero temperature operation, low humidity environments, and high operating temperatures.
- The SOFC durability: Solid oxide systems have issues with material corrosion. Seal integrity is also a major concern. The cost goal for SOFC's is less restrictive than for PEMFC systems, but material costs are high. SOFC durability suffers with the cell temperature repeatedly heat cycled with start-up and shut down sequences.
- Aromatic-based membranes: An alternative to current perfluorosulphonic acid membranes are aromatic-based membranes like benzene, pyridine or indole. These membranes are more stable at higher temperatures, but still require hydration. They swell when they lose hydration, which reduces fuel cell efficiency.

27.16.2 System technology challenges

Cost and durability are the major challenges to widespread fuel cell commercialization. However, hurdles vary according to the application in which the technology is employed. Size, weight, and thermal and water management are barriers to the commercialization of fuel cell technology. In transportation applications, fuel cell technologies face more stringent cost and durability hurdles. In stationary power applications, where cogeneration of heat and power is desired, use of PEM fuel cells would benefit from raised operating temperatures to increase efficiency performance. The key challenges include:

- Cost: The fuel cell power system is more expensive than conventional technologies.
- Durability and Reliability: The durability of fuel cell systems has not been established. For transportation applications, fuel cell power systems are required to achieve the same level of durability and reliability of current energy sources in terms of lifespan time, performance, and ambient operating temperature.
- System Size: The size and weight of fuel cell systems must be reduced to the levels of other technologies. This reduction applies to the fuel cell stack and the ancillary components and major subsystems (for example, fuel processor, compressor/expander, and sensors) making up the balance of power system.
- Improved Heat Recovery Systems: The low operating temperature of PEM fuel cells limits the amount and type of CHP applications. Technologies need to be developed that will allow higher operating temperatures and/or more effective heat recovery systems and improved system designs to enable CHP efficiencies exceeding 80%.
- Infrastructure: unfamiliar technology to power industry, with no infrastructure in place.

27.17 Fuel cell summary

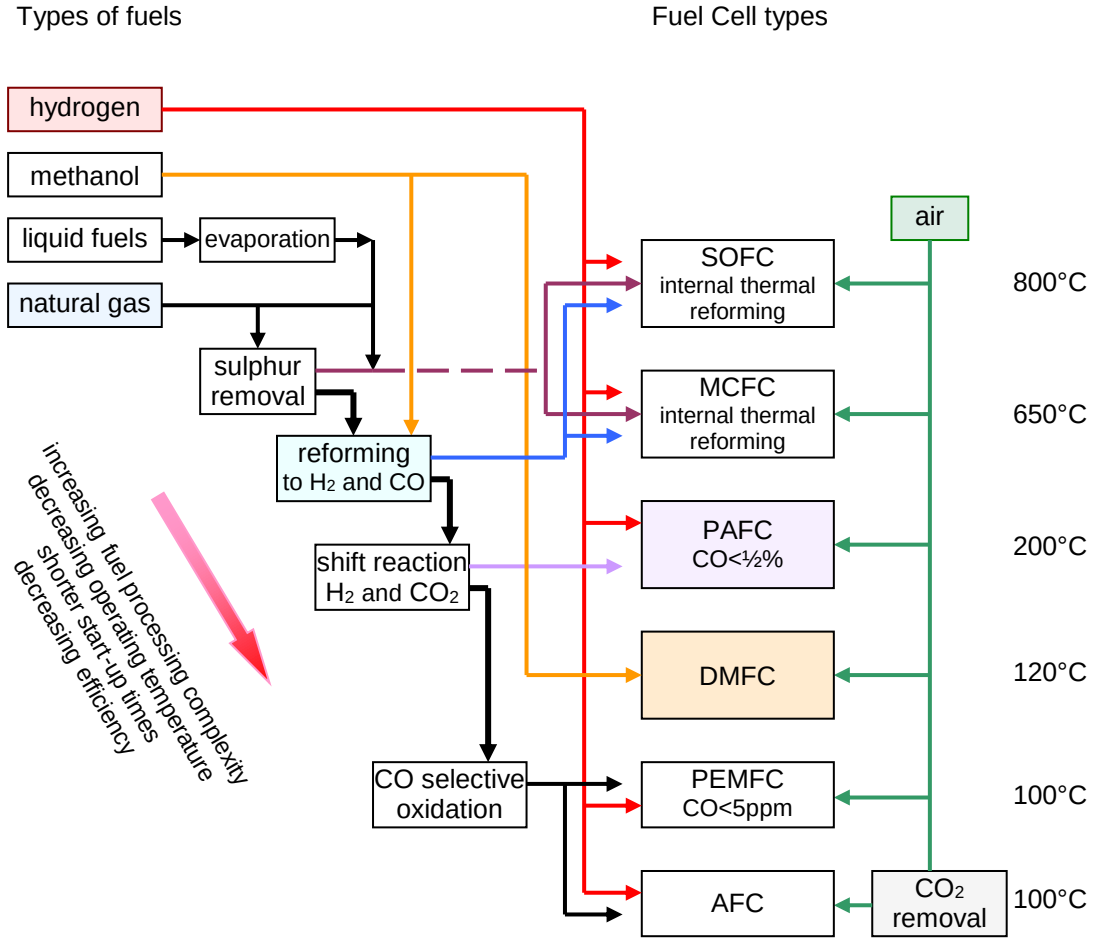

Figure 27.12. *Fuel cells operating temperatures and applicable fuels.*

The following table lists the key manufacturers by fuel cell type:

Table 27.8: Fuel cell stack manufacturers

PEM	Ballard, Plugpower, H-Power, UTC, Nuvera, Siemens, h2-interpower
AFC	Astris, UTC, Zetek
DMFC	Ballard, Manhattan Scientific, Medis, MTI Micro FuelCells, Smartfuelcell
PAFC	UTC
MCFC	Fuel Cell Energy (FCE), MTU
SOFC	Sulzer Hexis, Siemens Westinghouse, Global Thermolectric

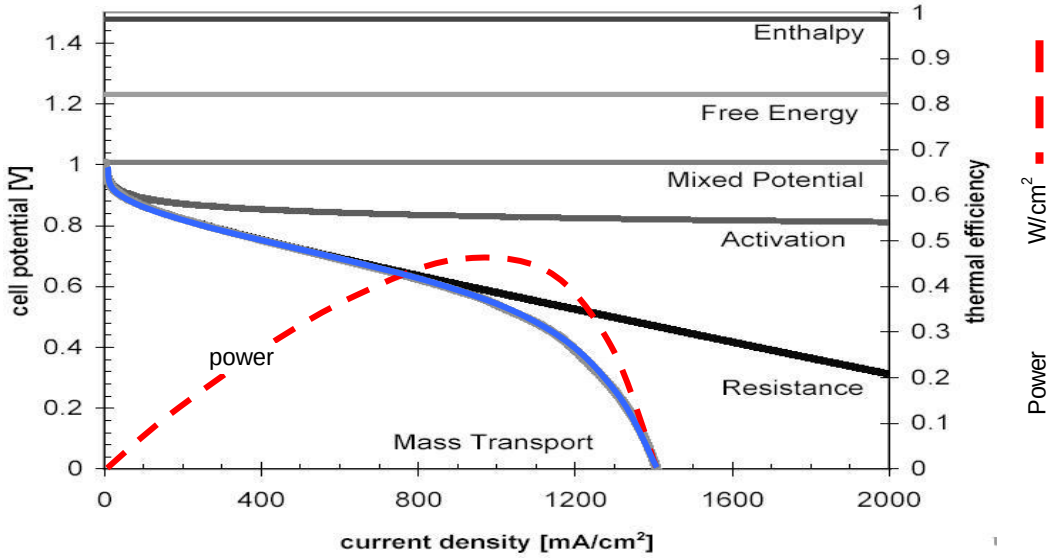

Table 27.9: Thermodynamic data for common fuel cell reactions at 1 atm pressure and 298K

Species		*Molecular weight*	ΔH_{298K}	ΔG_{298K}	ΔS_{298K}	*Freezing point*	*Boiling point*	*Enthalpy @ 25°C*	*Heat of vaporisation*	*Liquid density*
		g	kJ/mol	kJ/mol	J/mol.K	°C	°C	kJ/mol	kJ/kg	kg/l
H_2	(gas)	2.02	0	0	130.6	-259.2	-252.77	241.8	445.6	77
0_2	(gas)		0	0	205.0					
H_20	(gas)		-241.8	-228.6	188.7					
H_20	(liquid)		-285.9	-237.2	70.0					
H_20_2	(liquid)		-187.6	-120.2	109.5					
CH_4	(gas)	16.04	-74.9	-50.8	186.1	-182.5	-161.5	802.5	510	425
C	(graphite)		0	0	5.7					
C_2H_6	(gas)		-84.7	32.9	229.5		-42.1			
C_3H_8	(gas)	44.1	-103.8	-23.5	269.9					
CH_3OH	(gas)	32.04	-201.2	-161.9	237.7	-97.8	64.7	638.5	1100	792
CH_3OH	(liquid)	32.04	-238.6	-166.2	126.8	-97.8	64.7	638.5	1100	792
C_2H_5OH	(liquid)	46.07	-277.7	-174.8	160.7	-117.3	78.5	1275.9	855	789
$C_6H_{12}O_6$	(glucose)		-126.8	-91.0	212					
C_8H_{18}		114.2				-56.8	125.7	5512.0	368.1	702
NH_3	(gas)	17.03	-46.1	-16.45	192.5	-77.7	-33.4	316.3	1371	674
CO	(gas)		-110.5	-137.2	197.5					
CO_2	(gas)		-393.5	-394.4	213.7					
KOH	(solid)		-425.8	-380.2	79.3					
NO	(gas)		377.8	362.3	881.6					
NO_2	(gas)		138.9	213.4	1003.7					

Table 27.10: Comparison of Fuel Cell Technologies

Ion & Fuel Cell Type	Common Electrolyte	anode cathode	Operating T °C Electo-catalyst	Density/power efficiency	Applications	Features	Shortcomings
H^+ Polymer Electrolyte Membrane (PEM)	Hydrated Solid organic polymer poly-perfluoro-sulphonic acid or Polymer membrane (ionomer) Poly-benzimidazole fibre	Carbon or metal	H_2 40 - 100°C platinum (0.2-1.8 mg/cm^2) (Nafion) 50–120°C (PBI) 125–220°C	4 - 7 kW/m^3 <1kW–500kW Cell: 50–70% 53–58% (transportation) 25–35% (stationary)	•Backup power •Portable power •Small distributed generation •Transportation •1A/cm^2 @ 0.7V	•Carbon or metal electrodes •Solid electrolyte reduces corrosion and electrolyte management problems •Low temperature •Fast start-up, second/min •Solid long-life construction •non-volatile electrolyte	•Expensive platinum catalyst •CO poisoning, <50 ppm •High sensitivity to fuel impurities •Low temperature waste heat not suitable for Cogeneration •External fuel processor •slow O_2 kinetics
OH^- Alkaline (AFC)	Aqueous (50%) alkaline solution of KOH potassium hydroxide soaked in an asbestos matrix	Anode Ni (transition) Cathode Lithiated NiO	H_2 65 - 160°C Ni, Ag, MetalO_2, noble metals	1-3 kW/m^3 1kW– 100kW Cell: 60 - 70% System: 62%	•Military •Space •1A/cm^2 @ 0.7V	•non- Platinum •Platinum alternatives •Metal electrodes •Cathode reaction faster in alkaline electrolyte, higher performance	•Expensive removal of CO_2 from fuel and air streams required (CO_2 degrades the electrolyte) •Caustic medium, but low cost •External fuel processor, large size •No cogen heat
H^+ Direct methanol (DMFC)	Polymer membrane (ionomer) 200µm Similar to PEM	Carbon or metal 100µm stable	Methanol CH_3OH 50–120°C Pt Pt/Ru reduces anode poisoning	2.5 kW/m^3@½V 100 kW–1 MW Cell: 30–45% System: 25%	•Portable power •Transportation •0.4A/cm^2 @ 0.7V & 60°C	•no reformer needed •Compact design •Fuel flexibility •Fast start-up, seconds/min •Liquid fuel	•×10 platinum of PEMF •Low efficiency, increases with temperature, poor cogen •External fuel processor •Low practical voltage, 0.6V
H^+ Phosphoric Acid (PAFC)	Immobilized molten liquid 100% phosphoric acid H_3PO_4 soaked in a SiC matrix	PTFE bonded Pt/ Graphite	H_2 150 - 205°C Pt or platinum alloys	1 - 2 kW/m^3 50kW –11MW (250kW/module) Cell: 55% System: 40% Co-Gen: 90%	•Distributed generation •0.8V/cell, 0.4A/cm^2@205°C	•High efficiency with Cogen •electrolyte rejects CO_2 •Increased tolerance to impurities in hydrogen, up to 1.5% CO	•Expensive platinum catalyst •Low current and power •Corrosive electrolyte •Slow start-up, hours •External fuel processor, only H_2 •large size and weight
CO_3^{2-} Molten Carbonate (MCFC)	Molten liquid lithium, sodium (62%-38%), and/or potassium carbonates $NaHCO_3$ (60%-40%) soaked in Li$A\ell O_2$ matrix	Anode Ni-Cr Cathode NiO-MgO	H_2 , CH_4 550 - 700°C Porous, electrode anode Ni cathode NiO	1 - 3 kW/m^3 1kW – 10MW (250kW/module) Cell: 55% System: 47% Co-Gen: 80%	•Electric utility •Large distributed generation •0.15A/cm^2 @ 0.8V & 600°C	•High efficiency with co-gen •Fuel flexibility CO/CH_4 etc. •Use a variety of catalysts •Internal fuel processor	•High temperature speeds corrosion & breakdown of cell components •Complex electrolyte management •Slow start-up, hours •Durability, limited life, S intolerant
O^{2-} Solid Oxide (SOFC)	Solid oxide Ceramic 40µm thick (Perovskites) Solid zirconium dioxide ZrO_2 stabilised with Yttria Y_2O_3 (>750°C)	Anode Ni-ZrO_2 Cermet (perovskite) Cathode $LaMnO_3$+ Sr	H_2 , CH_4, CO 650 - 1000°C Cermet catalyst is electrode	1 - 7 kW/m^3 5kW – 3MW 40–45% Co-Gen: 80%	•Auxiliary power •Electric utility •Large distributed generation •1A/cm^2 @ 0.7V	•Electrode is catalyst •High efficiency with Cogen •Fuel flexibility, S insensitive •Variety of catalysts •Solid electrolyte reduces electrolyte problems •solid state - flexible shape •0.7V/cell, 4kA/m^2 @ 990°C	•High temperature enhances corrosion and breakdown of cell components •Expensive materials •Start-up: planar type -hours tubular - minutes •High conductivity ceramic electrolyte brittleness with thermal cycling

27.18 Photovoltaic cells: converting photons to electrons

Photovoltaic, PV, as the word from the Greek implies, phos means light and voltaic is after Alessandro Volta, now taken to mean electricity, is the conversion of sunlight directly into electricity.
The photoelectric effect is the physical atomic level process by which a photovoltaic (PV) cell converts sunlight photon energy directly into electricity. When light shines on a PV cell (also called a solar cell), it may be reflected, absorbed or transmitted. Only the absorbed light photons may generate electricity.
A photon with short enough wavelength and sufficient energy can cause an electron in a photovoltaic material to break free of the atom that holds it. If a nearby electric field is provided, released electrons are swept toward a metallic contact, from where they emerge as an electric current.

27.19 Silicon structural physics

Single-crystal silicon is used extensively in PV cells.
The silicon atom has 14 electrons, arranged in three orbital shells. The inner two shells, those closest to the nucleus, are full. The outer shell, however, is only half full/empty, having only four electrons. A tetravalent silicon atom will attempt to fill its outer shell with eight electrons. To do this, it will covalently share electrons with four of its neighbouring silicon atoms, therein forming part of a regular lattice.
Pure silicon is a poor conductor of electricity as the covalently bonded electrons are not free to move, being tied in the crystalline structure. Atoms of elements such as boron or phosphorus used as doping agents in silicon, alter the electron conductivity.
If a silicon atom in the lattice is substituted by a group V atom, a phosphorus atom for instance, one of its five valence electrons is not involved in the tetravalent bonds; as a result of thermal agitation, it soon moves to the conduction band, thus becoming free to move randomly through the crystal, leaving behind a hole, bound to the doping atom. This is electron conduction, and the semiconductor is designated an *n-type* doped semiconductor. An *n-type* semiconductor has an abundance of electrons, which have a negative electrical charge.
If a silicon atom is substituted by an atom from group III, boron for instance, which has three valence electrons, one electron is missing from a possible tetravalent bonding state. If all bonds are to be maintained, an electron may move to fill this gap. A hole thus arises elsewhere, contributing to conduction, and the semiconductor is termed a *p-type* doped semiconductor. A *p-type* semiconductor has an abundance of 'holes', which have a positive electrical charge.
Although both *p*-type and *n*-type materials are electrically neutral, *n*-type silicon has excess electrons and p-type silicon has excess holes. Homogeneously melding of the two materials creates a *p-n* junction at their metallurgical interface. The excess electrons move from the *n*-type side to the *p*-type side. The result is a build-up of positive charge along the *n*-type side of the interface and a build-up of negative charge along the *p*-type side, thereby inducing an electric field across the two neutral charge regions, which form a space charge or charge depletion layer straddling the *p-n* junction charge boundary.
The silicon diode is electrically neutral at the junction, where the electric field separates and maintains the two sides at balance. The electric field acts as a diode in which electrons can only move in one direction. Placing metallic contacts on the n and p regions forms a diode.

Silicon PV cell physics
PV cells are in fact large area semiconductor p-n diodes and single-crystal silicon type PV cells are the most widely used. When light, in the form of photons, illuminates the junction region, its energy may liberate electron-hole pairs.
Photons having an energy equal to, or higher than, the width of the band gap, yield their energy to the electrons, each photon causing an electron to move from the *valence band* to the *conduction band*, leaving behind a hole. The movement of electrons effectively means holes appear to move around the material, thus giving rise to an electron-hole pair.
The bandgap, E_G, is the energy difference between the conduction band and valence band.
The relationship between frequency *f*, incident photon energy, and resultant electrical energy is given by:

$$W_{photon} = hf = \frac{hc}{\lambda} = \frac{p}{\lambda} = qE_G = W_{electrical} \qquad (\text{J}) \qquad (27.20)$$

where: *h* is Planck constant, 6.626×10^{-34} Ws^2 (J.s) or 4.14×10^{-15} eVs
f is frequency of the photon, Hz
p is momentum, h/λ
q is the electron charge,1.602×10^{-19}, C
The relationship between speed *c*, 2.998×10^{8}m/s, frequency *f*, and wavelength λ, in m, is

$$c = f\lambda \qquad (\text{m/s}) \qquad (27.21)$$

If the free-state electron state occurs near the junction built-in electric field, or if a free electron and free hole appear in its field of influence, the field forces the electron to the n-side and a hole appears on the p-side. This causes further disruption of electrical neutrality, and if an external current path exists, electrons flow through the external path back to their original junction side, the p-side, to recombine with

holes that the electric field has maintained there, the electrons doing work along the way. The electron flow is the current, and the cell's electric field creates a voltage, thus power is produced.
Visible light is only part of the electromagnetic spectrum, as illustrated in figures 27.14 and 27.22. Electromagnetic radiation is not monochromatic - it is made up of a range of different wavelengths, and therefore energy levels. Photon energy increases with increased frequency, as shown by equation (27.20). Sunlight can be separated into different wavelengths, as in a rainbow.
The photon energy of light varies according to the different wavelengths of the light. The entire spectrum of sunlight, from infrared to ultraviolet, covers a range of about ½eV to about 2.9eV. The radiation spectrum has a peak at 0.8eV. Red light has energy of about 1.7eV, and blue light has energy of about 2.7eV. Most PV cells cannot use about 55% of the energy of sunlight, because this energy is either below the bandgap of the photoelectric material or carries excess energy.
The single p-n junction, generates only one electron-hole pair for each absorbed photon, and wastes as heat any incoming photon energy in excess of the semiconductor band gap. Each photon can produce only one electron-hole pair. The basic conversion process is shown in figure 27.13.
Different PV materials have different energy band gaps. Photons with energy equal to the band gap energy are absorbed to create free electrons. Photons with less energy than the band gap energy are re-emitted and pass through the material as if it were transparent and do not produce any electrical current or heat. Still other photons have too much energy. Only a certain amount of energy, the band gap energy, measured in electron volts (eV) and defined by the cell semiconductor material (about 1.12 eV or a wavelength of 1.11μm for crystalline silicon), is required to knock an electron loose. If a photon has more energy than the required amount, then the extra energy is lost as heat in the PV cell. These two effects alone account for the loss of around 70 percent of the radiation energy incident on a cell.
The band gap also determines the voltage of the electric field, and if this voltage is too low, then the extra current gained (by being able to absorbing more photons), is offset by having a small voltage, since power is voltage times current. The optimal band gap, balancing these two effects, is around 1.4 eV for a cell made from a single semiconducting material.
The most energy that a single junction cell can absorb is around 25 percent, with 15 percent or less being more likely.

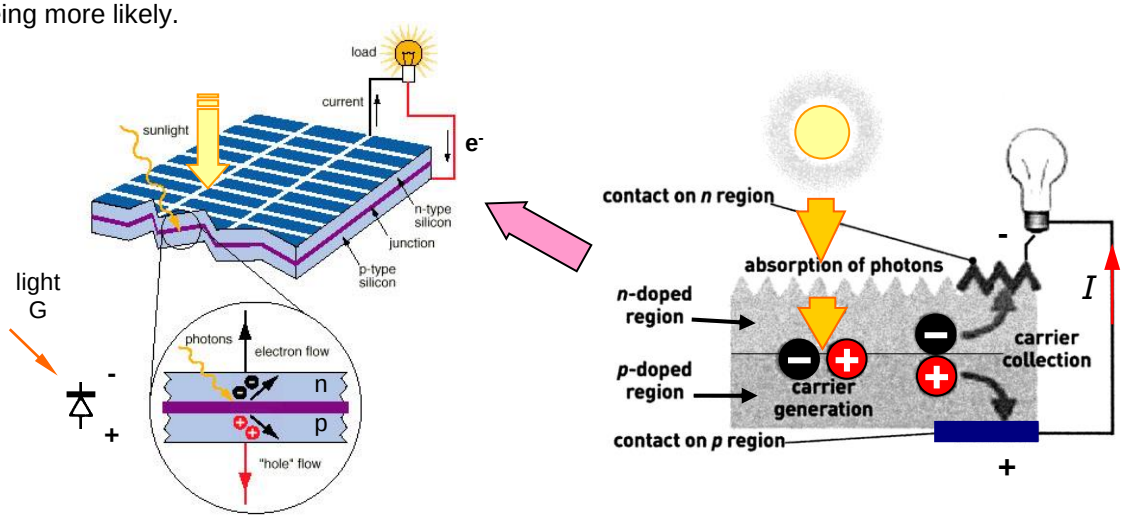

Figure 27.13. *PV cell structure and electrical connection.*

Example 27.4: ***Photons to create hole-electron pairs in silicon***

Assuming silicon has a band gap of 1.12eV at 300K and 1eV = 1.6×10^{-19}J.
What maximum wavelength can a photon have to create hole–electron pairs in silicon?
What is the associated minimum frequency?

Solution

One photon can excite only one electron, any energy above the 1.12eV needed is dissipated as waste heat in the cell.
From equation (27.20) the wavelength must be less than

$$\lambda \le \frac{hc}{E}$$
$$= \frac{6.626\times10^{-34}\ \text{J}\cdot\text{s}\ \times\ 3\times10^{8}\ \text{m/s}}{1.12\ \text{eV}\ \times\ 1.6\times10^{-19}\text{J/eV}}$$
$$= 1.11\times10^{-6}\ \text{m} = 1.11\ \mu\text{m}$$

and from equation (27.21) the frequency must be at least

$$f \geq \frac{c}{\lambda}$$

$$= \frac{3\times10^{8}\ \text{m/s}}{1.11\times10^{-6}\ \text{m}} = 2.7\times10^{14}\ \text{Hz}$$

♣

27.20 Semiconductor materials and structures

Single-crystal silicon is not the only material used in PV cells, as indicated in figure 27.15. Polycrystalline silicon is used in an attempt to reduce manufacturing costs, although the resulting cells are not as efficient as with single crystal silicon. Amorphous silicon, which has no crystalline structure, is also used, again in an attempt to reduce costs. Other materials used include gallium arsenide, copper indium diselenide, and cadmium telluride. Since different materials have different band gaps, they are responsive to different frequencies, or photons of different energies, as given by equation (27.20).
Efficiency is improved by cascading two or more p-n junction layers of materials with different band gaps. The higher band-gap p-n material is on the surface, absorbing high-energy photons while allowing lower-energy photons to be absorbed by the lower band-gap material beneath. This technique results in much higher efficiencies. These so-called *multi-junction cells* have more than one electric field in series.

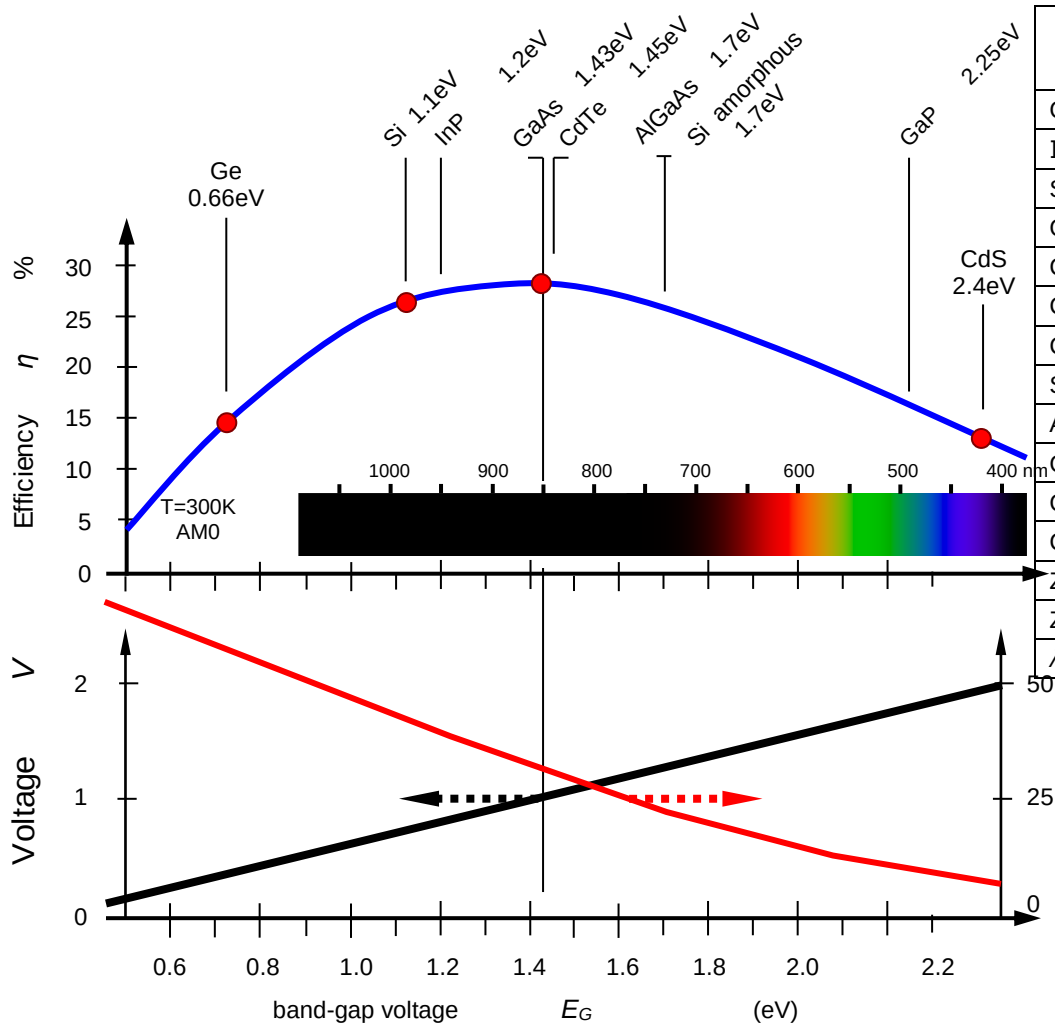

material	band-gap eV @ 300K
Ge	0.66
In	0.7
Si $\lambda \leq 1.11\mu m$	1.11
GaAs $\lambda \leq 0.87\mu m$	1.43
CdSe	1.74
CdTe $\lambda \leq 0.83\mu m$	1.44
$CuInSe_2$	1.0
Si amorphous	1.7
AℓGaAs	1.7
GaInP	1.8
GaP	2.25
CdS	2.4
ZnO	3.2
ZnS	3.6
λ nm	$1241/E_G$

Figure 27.14. *Calculated single solar cell efficiency for different band-gap semiconductors.*

Silicon is not the only material that will respond to sunlight by generating electron-hole pairs of charge carriers. Any two dissimilar semiconductor materials will form a junction and an electric field at their interface. There are many design choices to be made in making a PV device, both in material properties and device designs. The most important design parameters to consider are:

- The material's electronic properties, especially its degree of crystallinity
- The amount of light that can be absorbed in a given thickness of material; its absorptivity
- The range of wavelengths in the sun's spectrum that can be absorbed and used; the band-gap
- The expected cost, due to the amount and type of material used and the complexity of the manufacturing process.

Single-crystal silicon has a high degree of crystallinity, which makes a high sunlight-to-electricity conversion efficiency relatively easy to attain. Its absorptivity is relatively low, however, which is why older silicon cell designs required about 300μm of semiconductor material thickness to absorb all the sunlight possible, and newer silicon cell designs still require about 100μm of material. Silicon's band gap of 1.1eV is not ideal. Single junction PV cells with the highest theoretical efficiencies employ materials with band gaps of 1.4 to 1.5eV, as shown in figure 27.14, although sunlight goes up to 4eV.

PV cells can therefore be made from a wide range of semiconductor materials. The following sections discuss the various PV cell possibilities and semi-conducting material combinations:

- Silicon, Si - including
  - single-crystalline Si,
  - multicrystalline Si, and
  - amorphous Si
- Polycrystalline thin films - including copper indium diselenide (CIS), cadmium telluride (CdTe), and thin-film silicon
- Single-crystalline thin films - including high-efficiency gallium arsenide (GaAs)
- Nanocrystalline PV cells

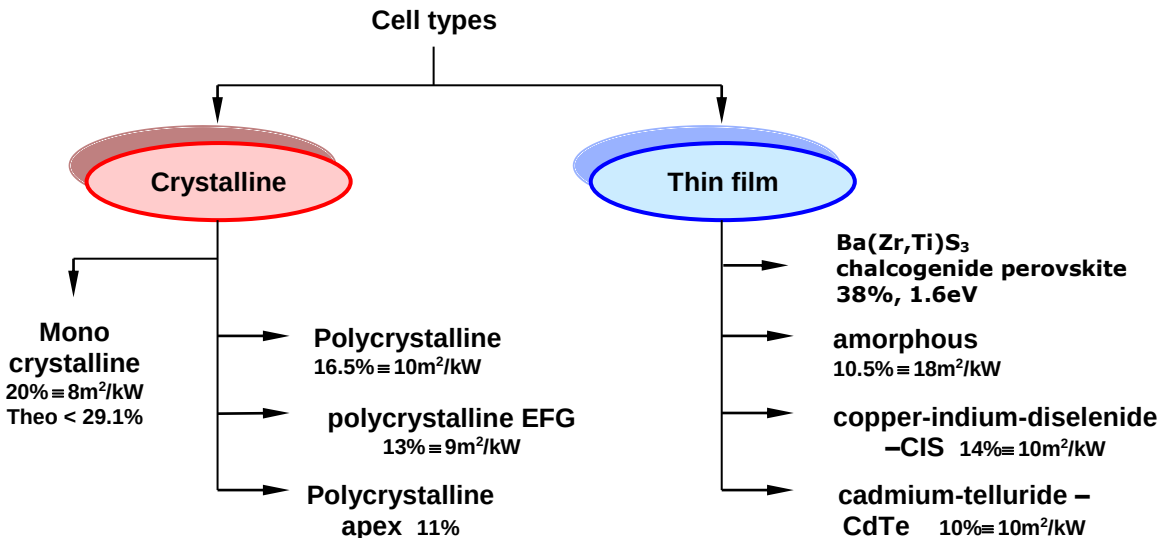

Figure 27.15. *Photovoltaic cell types and efficiencies, hence required per unit surface area.*

27.20.1 Silicon

Three types of silicon crystalline structures are introduced and considered in chapter 1.5, namely mono (single), poly (multi), and amorphous silicons.

i. Single-crystalline silicon

Mono-crystalline or single-crystalline PV cells and modules are made with the following process and production steps.

1. Casting

The raw material for making solar cells is monocrystalline silicon.
Silicon feedstock is melted in a crucible to form either monocrystalline or multicrystalline silicon, depending on the production process used.
During the melting process, a small quantity of boron is mixed to make the silicon p-type, giving it a positive electrical characteristic. It is made into ingots or bricks, which are cut to a more appropriate shape. After shaping, the silicon ingot, sawn with diamond saw into thin silicon wafers, is the foundation for PV cell production. Wafers of 1mm thickness, sawn with 100μm precision, are placed between two plane-parallel metal plates, which rotate into opposite directions. The procedure enables wafer thickness adjustment to 1μm precision.

2. Etching and texturing

The wafers are cleaned with industrial soaps and then etched a few micrometres to remove saw damage and crystalline-structure irregularities. Monocrystalline wafers are further etched in a hot solution of sodium hydroxide and isopropanol to form surface square-based pyramids, called texture. Texturization reduces the reflection of sunlight but is not particularly effective in the case of multicrystalline wafers, whence other texturing methods are used to enhance light capture.

3. Diffusion and edge isolation

Wafers that have been pre-doped with boron during the casting process are then given a negative n-type surface characteristic by diffusion with a phosphorus gaseous source at high temperature, 800°C, which creates the n-p junction. An oxide layer rich with phosphorus is formed on top of the wafers due to oxygen subsequently introduced into the reaction.

Phosphorus diffuses not only into the desired wafer surface but also into the sides and the opposite surface, to some extent. This gives an edge shunt path between the cell front and rear. Removal of the shunt path at the wafer edge, called edge junction isolation or passivation, is performed by coin stacking the cells to form a cube and exposing the edges to an oxygen etch in a plasma etching chamber. The next phase removes the oxide layers from on top of the wafer by wet chemical etching.

4. Anti-reflection coating

Pure silicon is a shiny grey material and can act as a mirror, reflecting more than 30% of the incident light. Photons that are reflected are not used by the cell. To improve the conversion efficiency of a PV cell, the amount of light reflected is minimised so that the semiconductor material can capture as much light as possible to use in liberating electrons. Thus an anti-reflective coating is applied to the top of the cell. A single layer reduces surface reflection to about 10%, and a second layer, termed a double-layer antireflection coating, lowers reflection to less than 4%.

Two techniques are commonly used to reduce incident light reflection.

- The first technique is to coat the top surface with a thin layer of silicon monoxide Si0 or titanium dioxide $Ti0_2$. The material used for coating is
  - heated until its molecules boil-off and travel to the silicon and condense, called plasma enhanced chemical vapour deposition. This process not only deposits an antireflective layer but also improves the electronic properties of the silicon by injecting hydrogen, or
  - the material undergoes sputtering. In this process, a high voltage knocks molecules off the material and deposits them onto the silicon at the opposite electrode, or
  - the silicon itself is allowed to react with oxygen or nitrogen gases to form silicon dioxide $Si0_2$ or silicon nitride Si_3N_4.
- A second technique is to texture the top surface, as performed at stage 2 and shown in figure 27.13. Chemical etching creates a pattern of cones and pyramids, which capture light rays that might otherwise be reflected away from the cell. Reflected light is redirected into the cell, where it can be absorbed. Light with an 80% probability of being absorbed by a flat surface has a 96% chance of being absorbed by a textured surface.

Commercial PV cell manufacturers tend to use silicon nitride as the anti-reflective coating.

5. Metallization and electrical contact placement

The cells are now capable of generating electricity. The front and the rear surfaces need to have contacts added, usually in the form of electrically conductive metal strips. Two metallisation techniques are common:

i. The back contact of a cell (away from the sun) is usually coated in a layer of aluminium or molybdenum metal. The front contact is a narrow grid of fingers so as not to block sunlight into the cell. Metals such as palladium/silver, nickel, or copper are vacuum-evaporated, or sintered, through a photoresist, silk-screened, or merely deposited on the exposed portion of cells that have been partially covered with wax. In each case, the part of the cell on which a contact is not desired is protected, while the remainder of the cell is exposed to the metallization.
ii. Alternatively, silver, with 1% aluminium, is a used metal for contact formation owing to its solderability. Silver in the form of a paste is screen printed onto the front and the rear. In addition, aluminium paste is applied to the rear to achieve the back surface field which improves solar cell performance. These metal pastes are subsequently heated above their alloying temperature to form a good ohmic contact.

The fingers of the grid must be wide enough to conduct with low resistance, but narrow enough to block a minimal of incoming light, about 3% to 5% of the surface area.

After the contacts are in place, thin separating strips, normally tin-coated copper, are placed between cells.

6. Encapsulating the cell and solar modules

Since each solar cell produces about half a volt when exposed to light, each PV module is made by connecting cells (usually 36) in series and parallel to achieve useful levels of voltage and current.
The PV module consists of the silicon semiconductor surrounded by protective material in a metal frame. The protection is an encapsulant of transparent silicon rubber or butyryl plastic bonded, which are then embedded in silicon rubber or ethylene vinyl acetate. The encapsulated PV cells are then placed into an aluminium frame where a polyester film such as Mylar or Tedlar makes up the backing sheet. A front glass cover is found on terrestrial arrays; a lightweight plastic cover on satellite arrays. Silicone is used as the cement to hold the structure together. The basic constructional arrangement is shown in figure 27.16.

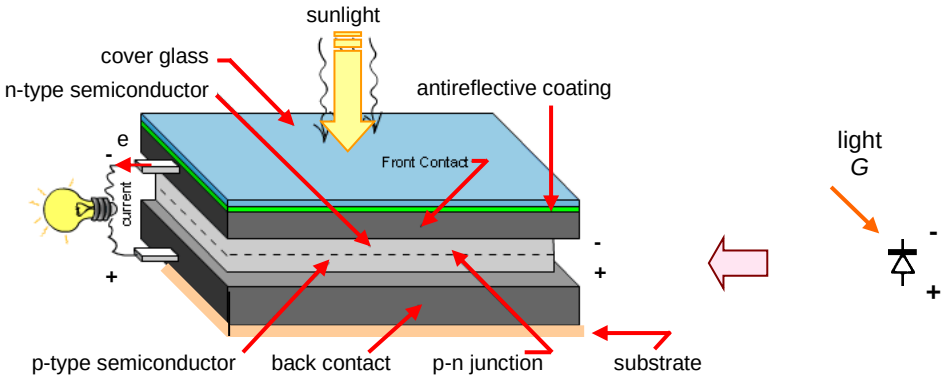

Figure 27.16. *Basic structure of a generic silicon p-n junction PV cell.*

ii. Multicrystalline silicon

Pure poly-crystalline silicon is extracted from tri-chlorine-silane. Furnaces are heated by electric current, which flows through silicon electrodes. The 2m long electrodes measure 8mm in diameter and the current flowing through the electrodes can reach up to 6kA. The furnace walls are cooled to prevent the formation of any unwanted reactions due to gas side products. The procedure results in pure poly-crystalline silicon which is used as a raw material for PV cell production. Poly-crystalline silicon can be formed from silicon by heating it up to 1500°C and then cooling it down to 1412°C, which is just above solidification of the material. The cooling produces an ingot of poly-crystalline silicon of dimensions 40x40x30cm, in which the silicon structure has non-uniform and irregular grain boundaries.

Free electrons and holes are much more likely to recombine at grain boundaries than within a single crystal. This recombination at the grain boundaries looks like an internal electrical resistance, hindering current flow, resulting in a loss of cell voltage. Thus the net effect of grain boundaries is to reduce the power output of a PV cell. Multicrystalline silicon cells therefore do not yield as high efficiencies as single-crystal silicon cells.

iii. Amorphous silicon

Amorphous silicon PV cells are produced with similar technological procedures as integrated circuits. Hence these cells are also known as thin-film PV cells, thence thin-film modules. Amorphous PV cell production can succinctly be described as follows:

- Glass substrate is thoroughly cleaned.
- Lower contact layer is deposited.
- The surface is then structured - divided into bands.
- The amorphous silicon layer is applied in a vacuum, under a high frequency electric field.
- The surface is re-banded.
- Upper metal electrodes are deposited.

Amorphous non-crystalline silicon, like common glass, is a material in which the atoms are not arranged in any particular order. They do not form crystalline structures, and contain large numbers of structural and bonding defects.
Amorphous silicon absorbs PV radiation 40 times more efficiently than single-crystal silicon, so a 1μm thick film can absorb 90% of the usable incident light energy. For this reasons, amorphous silicon can reduce the cost of photovoltaics. Other economic advantages are that it can be produced at lower temperatures and can be deposited on low-cost substrates such as plastic, glass, and metal. This makes amorphous silicon ideal for building PV integration.
There is a short-range structure order in the sense that most silicon atoms tend to bond with four other silicon atoms at distances and angles nearly the same as in a crystal. But this uniformity does not translate any distance, resulting in deviations that disrupt the long-range order. This lack of order results

in a high degree of defects such as dangling bonds, where atoms are missing a neighbour to which they can bond. These defects provide places for electrons and holes to recombine. Ordinarily, such materials are unacceptable for electronic devices because the defects limit the flow of current, in much the same way that grain boundaries interfere with the flow of current in polycrystalline material. But if amorphous silicon is deposited in such a way that it contains 5% to 10% hydrogen, then the hydrogen atoms combine chemically with some of the dangling bonds. This removes the dangling bonds and enhances the freedom of movement, or mobility, of electrons and holes in amorphous silicon (see chapter 1.5).

Because of amorphous silicon's unique properties, PV cells are designed to have an ultra-thin (0.008µm) *p*-type top layer, a thicker (0.5 to 1µm) intrinsic central layer, and a thin (0.02µm) *n*-type bottom layer. This design is called a *p-i-n* structure, because of the three layers, as shown in figure 27.17. The top layer is made so thin and relatively transparent that most light passes through it, to generate free electrons in the intrinsic layer. The *p* and *n* layers produced by doping the amorphous silicon create an electric field across the entire intrinsic region, thus inducing electron movement in the *i-layer*. Since the charge carriers are generated in the intrinsic layer, the poor charge mobility in the doped *p*+ and *n*+ layers is less important.
Amorphous silicon has a band-gap energy of about 1.7eV, which is greater than crystalline silicon's band-gap energy of 1.1eV. A PV cell's output voltage is directly related to its band gap magnitude, so PV cells made of amorphous silicon have higher output voltages than cells made of crystalline silicon. The higher output voltage compensates for the fact that lower-energy photons (with energies below 1.7eV) are not absorbed by amorphous silicon.

Cell construction
Typically, the construction of a hydrogenated amorphous silicon *p-i-n* cell is shown in figure 27.17, and begins with the deposition of a *p*+ layer onto a textured transparent conducting tin-oxide film - the top electrode. This is followed by the intrinsic *i*-layer, and a thin *n*+ layer. The cell is then given a reflective, conductive coating on the bottom, usually of aluminium or silver. A textured transparent conducting oxide substrate and the reflector helps trap the maximum possible amount of light in the PV cell.
After amorphous silicon modules are first exposed to light, their conversion efficiency decreases by 10% to 20%. This problem is eliminated by low temperature annealing. Self-annealing occurs in devices operated at about 50°C to 80°C.

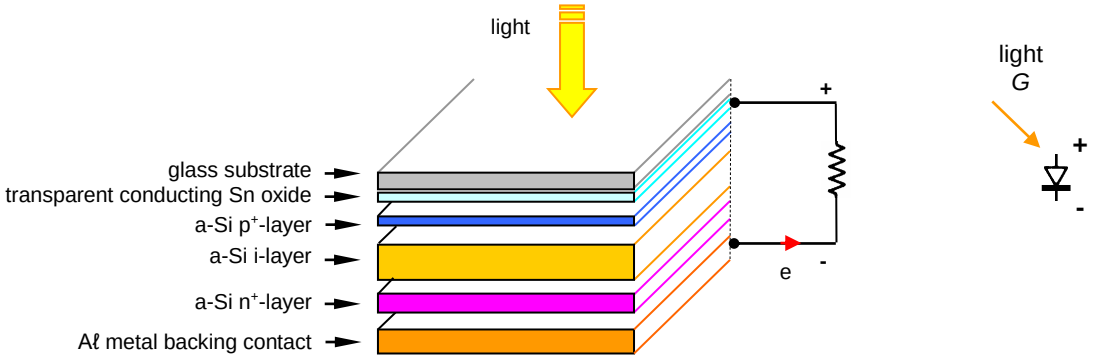

Figure 27.17. *A typical amorphous silicon p-i-n cell, with an intrinsic layer (i-layer) between a p-layer and an n-layer.*

Glow-discharge deposition is the method used to make the most efficient amorphous silicon PV cells. A stream of silane (SiH_4) and hydrogen gas is passed between a pair of electrodes whose polarity is reversed at high frequency. This voltage reversal induces an oscillation of energetic electrons between the electrodes. The electrons collide with the silane, breaking it down into SiH_3 and hydrogen. Since SiH_3 is chemically a radical, hence unstable, it adheres to a substrate on one of the electrodes to gain stability. Hydrogen is then released from the substrate, leaving a film of amorphous silicon with about 10% hydrogen. Doping is accomplished by adding diborane (B_2H_6) or phosphine (PH_3) gas to the silane.

Other PV cells
Among less frequently used PV cell types are cells produced by the EFG (Edge defined Film fed Growth) method and Apex PV cells from silicon, cadmium telluride PV cells and copper-indium selenide (CIS) PV cells. EFG monocrystalline PV cells are produced directly from silicon melt eliminating wafer sawing, which results in lower production costs and material saving for there is no waste due to sawing. Using the EFG procedure, a silicon ribbon tubular shaped with eight flat sides is drawn from silicon melt. The tube length extends several metres. The tube flat sides are laser sawn into separate PV cells. Most PV cells are square shaped, about 100x100mm.
The module power is greater with a smaller surface than crystal modules with truncated sides. The window surface contact strips are of copper.

Apex cells are poly-crystalline. Cadmium telluride and copper-indium selenide (CIS) cells are rarely used.

27.20.2 Polycrystalline thin-films

The *thin-film* term comes from the method used to deposit the film, not from the thinness of the film: thin-film cells are deposited in thin, consecutive layers of atoms, molecules, or ions. They have many advantages over 'thick-film' counterparts. For example,

- they use much less material - the cell's active volume is usually only 1 to 10µm thick, whereas thick films are typically 100 to 300µm thick.
- thin-film cells can be manufactured in a large-area process, which can be an automated, continuous production process.
- they can be deposited on flexible substrate materials, such as flexible plastics, metal, and glass.

Unlike most single-crystal cells, the typical thin-film cell does not use a metal grid for the window-surface electrical contact. Instead, a thin layer of a transparent conducting oxide is used. Suitable oxides, such as tin oxide, indium tin oxide, and zinc oxide, are transparent and electrically conductive. They collect the current effectively from the top of the cell, and losses due to lateral resistance are minimal. A separate antireflection coating may be used on the top surface, or the transparent conducting oxide may also serve this function.
This thin-film flexibility offers potential for building applications.

Thin-film deposition
Several different deposition techniques can be used, and are less expensive than the ingot-growth techniques required for crystalline silicon. Deposition techniques can be broadly classified (of typically hydrogenated amorphous silicon) into physical vapour deposition, chemical vapour deposition, electrochemical deposition, or a combination. Individual 'cells' are formed by vertical laser scribing. Production is faster, cheaper, uses less energy, and is applicable to mass production. Like amorphous silicon, the layers can be deposited on various low-cost substrates (or 'superstrates') such as glass, stainless steel or plastic, in virtually any shape.
In addition, the deposition processes can be scaled up, which means that the same technique used to make a 5cm x 5cm cell can be used to make a 60cm x 160cm PV single-cell module. Thin-film devices can be made as a single monolithic unit with layer upon layer being deposited sequentially on the same substrate, including deposition of an antireflection coating and the transparent conducting oxide.

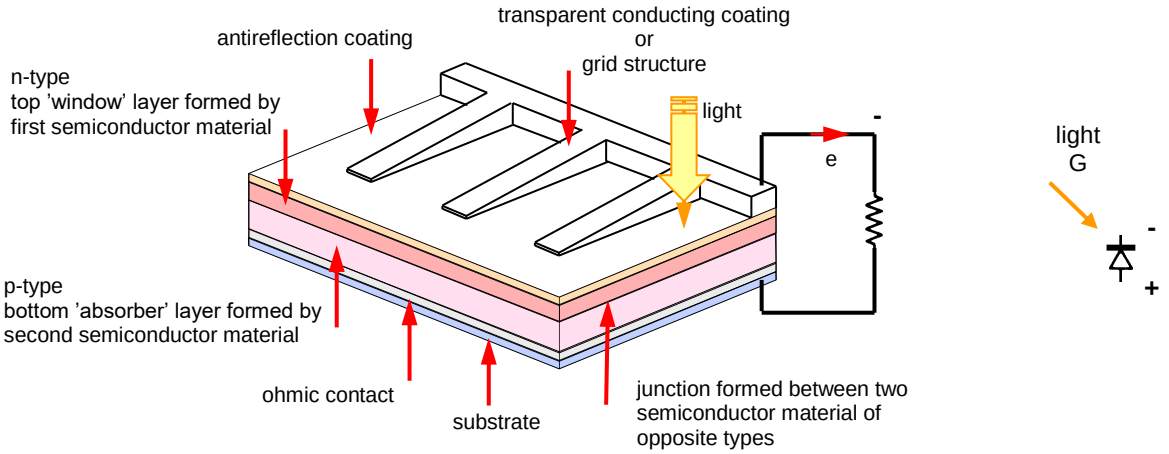

Figure 27.18. *A polycrystalline thin-film cell showing an n-type window and p-type absorber layer.*

Thin-film cell structure
Polycrystalline thin-film cells are made of many tiny crystalline grains of semiconductor materials. An electric field is created at the interface between two different semiconductor materials. This interface is called a *hetero-junction* (*hetero* because the junction is formed from two different semiconductor materials, as opposed to the *homo-junction,* meaning formed by two doped layers of the same material).
The typical polycrystalline thin film, as shown in figure 27.18, has a thin (less than 0.1µm) *n*-type layer on top called the 'window' layer. Its role is to absorb light energy from only the high-energy end of the spectrum. It is thin enough and has a wide enough bandgap (2.8eV or more) to let all the available light through the interface (*hetero-junction*) to the *p*-type absorbing layer. The absorbing layer under the

window is typically only 1 to 2μm thick and has a high absorptivity (ability to absorb photons) for high current and a suitable band gap to provide an adequate voltage.
An ohmic contact is often used to provide a good electrical connection to the substrate. But the top contact uses the thin transparent conducting oxide layer.

Three types of polycrystalline thin-film PV cells are:

- Copper indium diselenide (CIS)
- Cadmium telluride (CdTe)
- Thin-film silicon

i. Copper Indium Diselenide (CIS)

Copper indium diselenide ($CuInSe_2$ or 'CIS') has a high absorptivity, which means that 99% of the light shining on CIS will be absorbed in the first micrometre of the material. It is stable, with no degradation due to environmental exposure. Cells made from CIS are usually heterojunction structures - structures in which the junction is formed between semiconductors having different bandgaps. The most common material for the window layer is cadmium sulphide (CdS), although zinc is can be added to improve transparency. Adding small amounts of gallium to the lower absorbing CIS layer boosts its bandgap from a normal 1.0eV, which improves the voltage and therefore the efficiency of the cell. This variation is called a copper indium gallium diselenide or 'CIGS' PV cell.
CIS is an efficient, about 17%, but complex thin film material that is difficult to manufacture, a process that involves the toxic gas hydrogen selenide, as indicated in figure 27.19.

CIS element combinations		
$(I)(III)(VI)_2$		
Group I	Group III	Group VI
Cu	Aℓ	S
Ag	Ga	Se
Au	In	Te

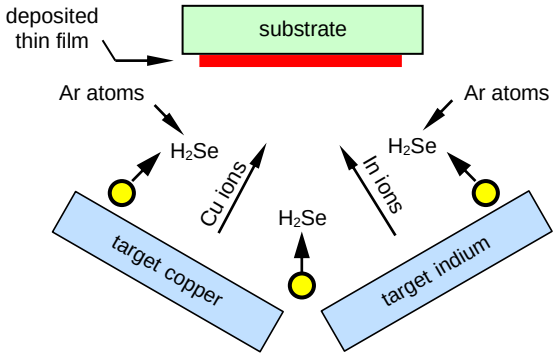

Figure 27.19. *Typical evaporated formation of a CIS PV cell.*

The CIS cell layers are formed by several different processes. The CIS layer consists of three different elements, specifically copper, indium, and selenium. Preparation methods for the CIS layer include:

- *Evaporation*. Small amounts of each of the elements are electrically heated to a point where the atoms vaporize. They then condense on a cooled substrate to form a CIS layer.
- *Sputtering*. High-energy ions bombard the surface, driving off atoms of the target material. These then condense on a substrate to form a thin layer.
- *Pyrolysis*. Copper indium diselenide is deposited on a substrate by spray pyrolysis. Solutions of the salts of the necessary elements are sprayed onto a hot substrate. They react under elevated temperatures to form the required CIS layer, while the solvent evaporates.
- *Electrodeposition*. The CIS layers are deposited in the same way precious metals are plated. Passing electricity through a solution containing ions of the required elements causes them to be deposited out of solution onto an electrode, which acts as the substrate.

CIS layers can be made using any one of these methods to deposit only the copper and the indium. This is followed by a treatment with hydrogen selenide gas, called selenization, to add the selenium.

ii. Cadmium Telluride (CdTe)

Cadmium telluride is a polycrystalline thin-film material produced by deposition or sputtering. A disadvantage is that poisonous production materials are used. PV cells efficiency is up to 10%.

With a near ideal bandgap of 1.44eV, CdTe also has a high light absorptivity. Although CdTe is most often used in PV devices without being alloyed, it is easily alloyed with zinc, mercury, and a few other elements to vary its properties. Like CIS, films of CdTe can be manufactured using low-cost techniques.

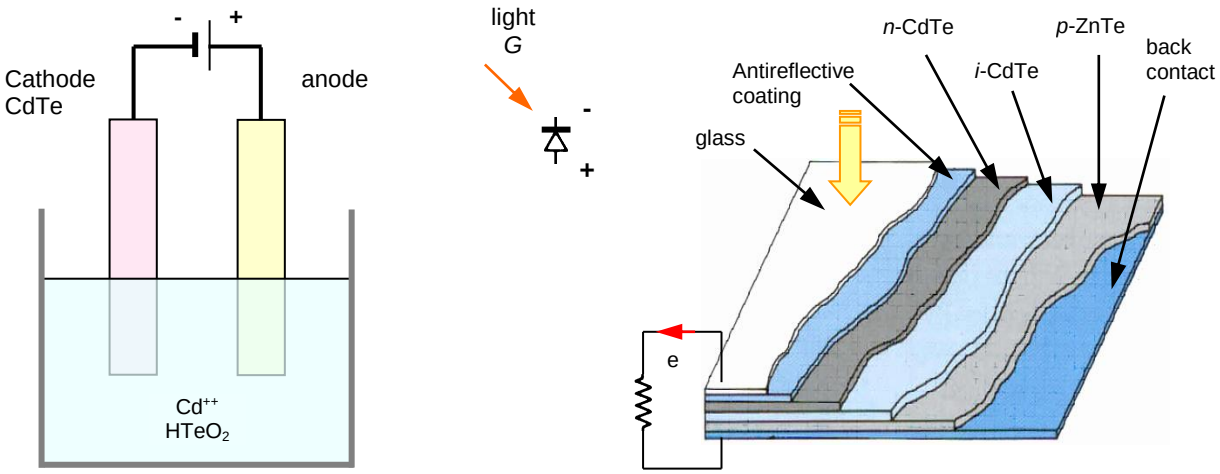

Figure 27.20. *A CdTe PV cell:*
(a) formation by electrolysing deposition and (b) the basic layer structure.

Also like CIS, the best CdTe cells employ a heterojunction interface, with cadmium sulphide (CdS) acting as the thin window layer. Tin oxide is used as a transparent conducting oxide and antireflection coating. The p-type CdTe films are highly resistive electrically, which leads to significant internal resistance losses. The back electrical contact tends to suffer rust-like deterioration. This high resistivity problem is circumvented by the CdTe layer being intrinsic (that is, neither p-type nor n-type, but undoped), and a layer of p-type zinc telluride (ZnTe) is added between the CdTe and the back electrical contact. Although the n-type CdS and the p-type ZnTe are separated, as shown in figure 27.20b, they still form an electrical field that extends through the intrinsic CdTe. A wide variety of CdTe production methods are possible, including closed-space sublimation, electro-deposition (figure 27.20a), and chemical vapour deposition. Such cells designs show no degradation after 3,000 hours of service.
CdTe contacts are more stable if properly protected from water vapour and oxygen by hermetically sealing. Cadmium is an accumulative toxic heavy metal.

iii. Thin-film silicon
The term ‘thin-film silicon’ typically refers to silicon-based PV devices other than amorphous silicon cells and single-crystalline silicon cells, where the silicon layer is thicker than 200µm. These thin films have a high light absorptivity and require cell thicknesses of only a few micrometers. Nanocrystalline silicon and small-grained polycrystalline silicon - considered thin-film silicon - can replace amorphous silicon alloys as the bottom cell in multi-junction devices. As with other thin films, advantages include material savings, monolithic device design, use of inexpensive substrates, and manufacturing processes that are low temperature and possible over large areas.

27.20.3 Single-crystalline thin film

Single-crystal thin-film GaAs
To be cost-effective, gallium arsenide GaAs high-efficiency cells are best suited for concentrator systems. GaAs offers high light absorptivity and high energy conversion efficiency, up to 25%, and up to 28% with concentrated solar radiation.
Gallium arsenide (GaAs) is a compound semiconductor: a mixture of two elements, gallium and arsenic. Gallium is a by-product of the smelting of metals, notably aluminium and zinc, and is rarer than gold. Arsenic is not rare, but is poisonous.
GaAs is suitable for use in multi-junction and high-efficiency PV cells, for several reasons:

- The GaAs bandgap is 1.43 eV, ideal for single-junction PV cells.
- GaAs has a high absorptivity and requires a cell only a few microns thick to absorb sunlight. Crystalline silicon requires a layer of at least 100µm.
- Unlike silicon cells, GaAs cells are relatively insensitive to heat. Cell temperatures can often be high in concentrator applications.
- Alloys made from GaAs and aluminium, phosphorus, antimony, or indium have characteristics that are complementary to those of gallium arsenide, allowing cell design flexibility.
- GaAs is resistant to radiation and along with its high efficiency, GaAs is desirable for space applications.

A GaAs base cell can have several layers of different compositions; allowing precise control of the generation and collection of electrons and holes.

In silicon cells, the *p*-*n* junction is formed by treating the top of a *p*-type silicon wafer with an *n*-type dopant. This diffusion process does not work with gallium arsenide. Instead, all the active parts of a GaAs PV cell are made by growing sequences of thin, single-crystal layers on a single-crystal substrate. As each layer is grown, it is doped in different ways to form the *p*-*n* junction and to control other aspects of cell performance. This control facilitates cell efficiencies closer to theoretical levels. Common GaAs cell structures use a thin window layer of aluminium gallium arsenide. The thin layer results in the charge carriers being created close to the electric field across the junction.

The GaAs layers are grown via one of two techniques:

- In molecular beam epitaxy, a heated substrate wafer is exposed to gas-phase atoms of gallium and arsenic that condense on the wafer growing a thin GaAs film, or
- In metal-organic chemical vapour deposition, a heated substrate is exposed to gas-phase organic molecules containing gallium and arsenic, which react under the high temperatures, freeing gallium and arsenic atoms to adhere to the substrate.

In each case, single-crystal GaAs layers grow epitaxially with the new atoms deposited on the substrate continuing the same crystal lattice structure as the substrate, resulting in a high degree of crystallinity and in high cell efficiency.

GaAs design challenges

GaAs cells use a costly single-crystal GaAs substrate. GaAs cells are normally used in concentrator systems, each concentrator cell measuring about ¼cm^2 in area. In this configuration, the cost is sufficiently low to make GaAs cells competitive, assuming that module efficiencies are better than 25% and that the PV ancillary system is cost-effective.

Cheaper substrates result by growing GaAs cells on a removable, reusable GaAs substrate or making GaAs thin films, similar to those made of copper indium diselenide and cadmium telluride.

Growing quality GaAs crystals for PV cells requires a substrate with a crystal structure matching that of gallium arsenide and with similar thermal expansion properties. Silicon and germanium substrates can be used which are cheaper and more durable than gallium arsenide. But the slight mismatch in crystal structures between Si or Ge and GaAs causes imperfections in the GaAs crystal growth. So a buffer layer of gallium arsenide is deposited between the silicon and the active GaAs cell. The buffer layer progressively rectifies the imperfection effects in the new crystal growth structure. Another method is to treat cells with hydrogen, as with semi-crystalline silicon, which lessens the effects of imperfections and dangling bonds, but does not address the thermal mismatch aspect.

Table 27.11: PV cell general characteristics

Characteristics of photovoltaic cells					
structure	material	Electronic material properties	absorptivity	band gap	cost
single junction	single crystal silicon	high	low	medium	high
	polysilicon silicon	medium	low	medium	medium
	amorphous silicon	low	high	medium	low
	single crystal thin film	high	high	high	high
	polycrystalline thin film	medium	high	medium-high	low
multi-junction	silicon	low-high	high	high	low-high

27.20.4 Nanocrystalline

These structures use thin-film light absorbing materials but are deposited as an extremely thin absorber on a supporting matrix of conductive polymer or mesoporous metal oxide, resulting in a high surface area with increased internal reflections, hence increased light absorption.

PV cells based on a silicon substrate with a nanocrystal coating are called quantum dots (electron confined nanoparticles), and increase the efficiency and reduce the cost of silicon photovoltaic cells. Quantum dots of lead selenide PbSe can produce as many as seven excitons from one high energy photon of sunlight (7×1.11eV = 7.8 times the bandgap energy). Conventional photovoltaic cells produce one exciton per high-energy photon, with high kinetic energy carriers losing their energy as heat. This multiple excitation does not result in a 7-fold increase in output, but boosts the maximum theoretical efficiency to over 40%. Quantum dot photovoltaics are cheap to manufacture, as they are made using simple chemical reactions.

Table 27.12: PV cell general properties

	Efficiency	Durability	Comments
Monocrystalline	13% - 15%	> 30 years	• Highest efficiency = least surface area. • Expensive due to complicated manufacturing process. • Highest achieved efficiency is 23%. • Generate approximately 35mA/cm^2 at a voltage of 550mV at full illumination.
Polycrystalline	10% - 13%	> 25 years	• Most commonly used type of cell as it offers good efficiency at reasonable cost.
Thin Film / Amorphous	5% - 7%	> 20 years	• Low efficiency hence requires large surface area. • Made from flexible material. • Better in diffused light than mono and polycrystalline. • Current density of up to 15mA/cm^2, and the cell open-circuit voltage of 0.8V, is more that a crystalline cell. • Spectral response reaches maximum at the wavelengths of blue light therefore, ideal with fluorescent light sources.

The properties and features of the different PV technologies are summarised in tables 27.11 and 27.12.

27.21 PV cell structures

Most PV devices use a single junction to create an electric field. In a single-junction PV cell, only photons with energy equal to or greater than the band gap of the cell material can elevate an electron into the conduction band. In other words, the photovoltaic response of single junction cells is limited to the portion of the sun's spectrum with energy above the band gap of the absorbing material. Lower-energy photons are not used.
One way around this limitation is to use two or more cells, with more than one band gap and more than one junction, to generate a series cell voltage. These structures are referred to as multi-junction cells. Multi-junction cells can achieve a higher total conversion efficiency because they can convert more of the energy spectrum of light to electricity.
The actual structural design of a photovoltaic cell depends on the limitations of the material used in the PV cell. There are four basic device designs commonly used with the semiconducting materials.

- Homojunction
- Heterojunction
- *p-i-n/n-i-p*
- Multi-junction

27.21.1 Homojunction device

A single semiconductor material, crystalline silicon, is altered so that one side is *p*-type, dominated by positive holes, and the other side is n-type, dominated by negative electrons. The *p-n* junction is located so that the maximum amount of light is absorbed near it. The free electrons and holes generated by the light in the silicon diffuse to the *p-n* junction, then separate to produce an external current.
In the homojunction design, several cell aspects are varied to increase the conversion efficiency:

- Depth of the *p-n* junction below the cell's surface
- Amount and distribution of dopant atoms on either side of the *p-n* junction
- Crystallinity and purity of the silicon

Numerous homojunction Si cell examples have been presented in previous sections of this chapter.

27.21.2 Heterojunction device

An example of this type of device structure is a CIS cell (figure 27.19), where the junction is formed by contacting two different semiconductors, CdS and $CuInSe_2$. This structure is often used for thin-film cells, which absorb light much better than silicon. The top and bottom layers in a heterojunction device have different functions. The top layer, or *window* layer, is a material with a high bandgap selected for its light transparency. The window allows almost all the incident light to reach the bottom layer, which is a material with a low bandgap that readily absorbs light. This light then generates free electrons and holes near the junction, which separates the electrons and holes before they can recombine.
A high band-gap window layer reduces the cell's series resistance. The window material can be made highly conductive, and the thickness can be increased without reducing the transmittance of light. Light-generated electrons can therefore readily flow laterally in the window layer to the electrical contact.

27.21.3 p-i-n and n-i-p devices

Typically, amorphous silicon thin-film cells use a *p-i-n* structure, whereas CdTe cells use an *n-i-p* structure. A three-layer sandwich is created, with a middle intrinsic (*i*-type or undoped) layer between *n*-type and *p*-type layers. This geometry sets up an electric field between the p and n type regions that breaches the middle intrinsic resistive region. Light generates free electrons and holes in the intrinsic region, which are then separated by the electric field.

In the *p-i-n* amorphous silicon cell shown in figure 27.17, the top layer is *p*-type amorphous silicon, the middle layer is intrinsic silicon, and the bottom layer is *n*-type amorphous silicon. Amorphous silicon has many atomic-level electrical defects when it is highly conductive. Little current flows due to diffusion. However, in a *p-i-n* cell, current flows because the free electrons and holes are generated within the influence of an electric field, rather than having to move toward the field. Carrier lifetimes are long in the intrinsic layer.

In a CdTe cell shown in figure 27.20, the device structure is similar to the amorphous silicon *i* cell, except the order of layers is inverted. Specifically, in a typical CdTe cell, the top layer is *p*-type cadmium sulphide (CdS), the middle layer is intrinsic CdTe, and the bottom layer is *n*-type zinc telluride (ZnTe).

27.21.4 Multi-junction devices

A multi-junction structure can achieve a higher total conversion efficiency by capturing a larger portion of the solar spectrum. In the typical multi-junction cell shown in figure 27.21, individual cells with different bandgaps are stacked in descending bandgap order beneath one-another. The sunlight falls first on the material having the widest bandgap E_{G1}. Photons not absorbed in the first cell are transmitted to the second cell E_{G2}, which then absorbs the higher-energy portion of the remaining solar radiation while remaining transparent to the lower-energy photons. These selective absorption processes continue through to the final cell, which has the narrowest bandgap E_{G3}.

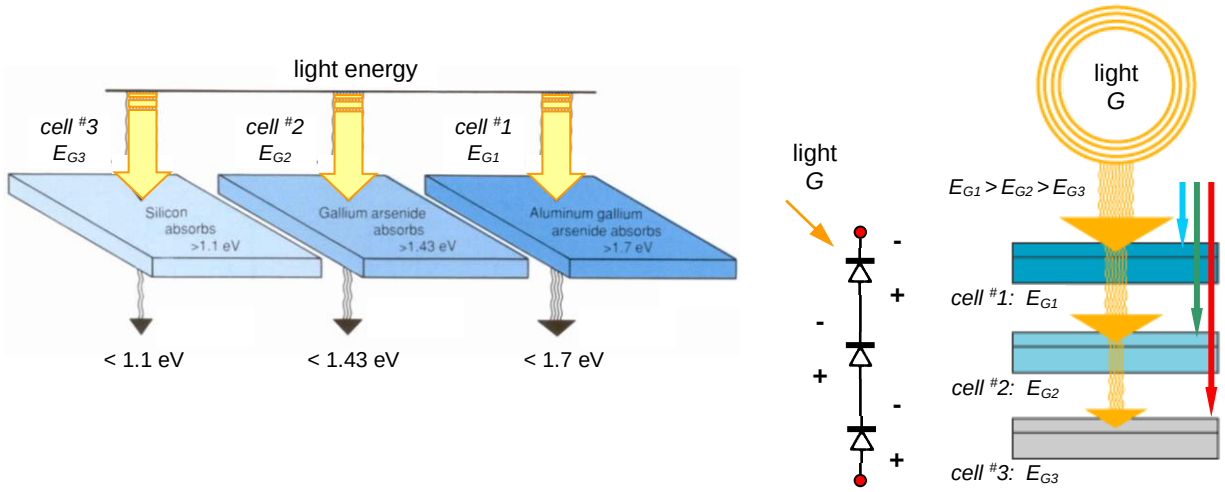

Figure 27.21. *A typical multi-junction PV cell showing three progressively decreasing band gap cells.*

A multi-junction cell can be made in two different ways.

- In the mechanical stack approach, two individual PV cells are made independently, one with a high bandgap and one with a lower bandgap. Then the two cells are mechanically stacked, the one with the higher bandgap on top of the other.
- In the monolithic approach, one complete PV cell is made first, and then the layers for the second cell are grown or deposited directly on the first cell.

i. The multi-junction device in figure 27.22 has a top cell of gallium indium phosphide, then a *tunnel junction* to allow the flow of electrons between the cells through a thin insulating layer, and a bottom cell of gallium arsenide.

ii. Another monolithic cell, a device that uses indium phosphide for the top cell and indium gallium arsenide for the bottom cell (InP/InGaAs), reaches 31.8% efficiency under 50 suns concentration. There are several aspects about this device.

- Traditionally, for highest efficiency in a two-junction device, the top cell should have a high band gap of approximately 1.9eV while the bottom cell should have a band gap of about 1.4eV. For this device, the band gap of the top cell is 1.35eV and that of the bottom cell is about 0.75eV.
- The cell is ideally suited for space applications because the resistance of indium phosphide to radiation is 50% better than that of silicon and 15% better than that of gallium arsenide, which are the two materials used for PV power in space. This means

that arrays using InP/InGaAs cells are lighter, cheaper, more reliable, have longer lifetime, and are more powerful.

- The band gap of indium gallium arsenide can be altered by varying the ratio of the constituent materials. This offers possibilities for spectrally tuning the cell.

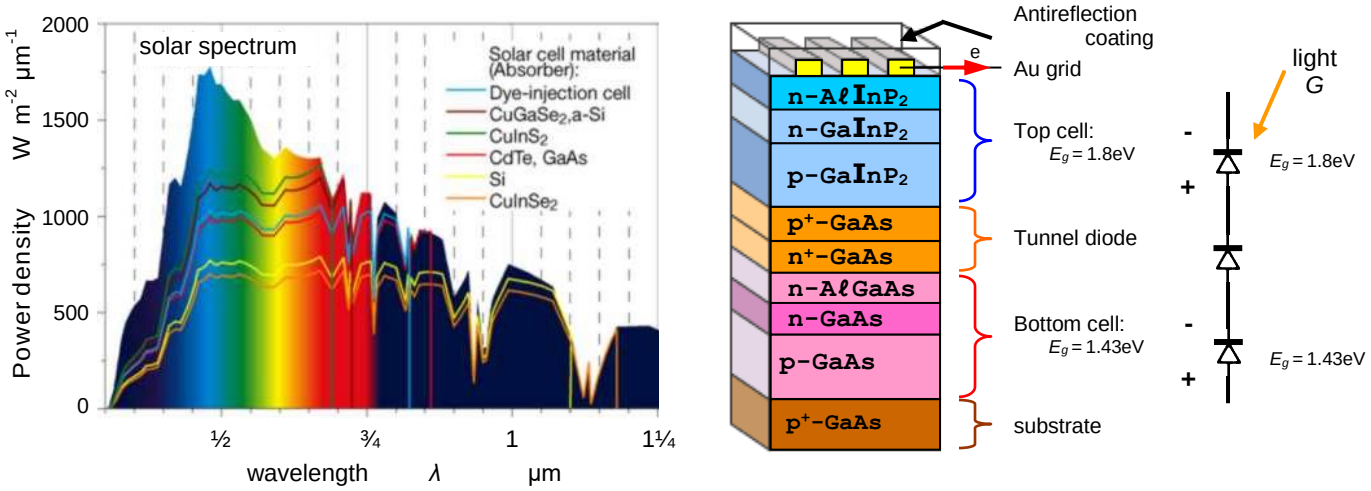

Figure 27.22. *A monolithic multi-junction PV cell based on GaAs and GaInP.*

High efficiency multi-junction cells focus on gallium arsenide as one, or all, of the component cells which gives efficiencies of more than 35% under concentrated sunlight. Other multi-junction cells include the use of amorphous silicon and copper indium diselenide. A further combination is the 39% efficient monolithically grown GaInP/GaAs/Ge triple-junction solar cell.

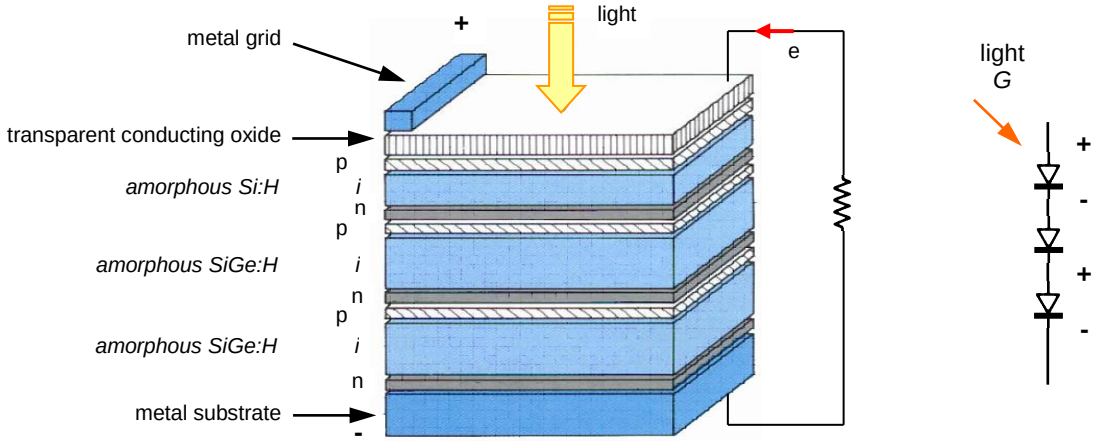

Figure 27.23. *An amorphous silicon multi-junction p-i-n type PV cell.*

i. Amorphous silicon multi-junctions

Amorphous silicon cells, include silicon carbon alloyed *p-i-n* cells, *n-i-p* cells, and stacked cells. Multi-junction devices not only achieve higher efficiencies than single-junction cells, but they also experience less light induced degradation. Because the intrinsic layers are so thin, the electric field sweeps charge carriers from these layers with minimal recombination.

Multi-junction devices use two, or three, individual amorphous silicon cells stacked as shown in figure 27.23. To capture a broader portion of the sun's spectrum, the cells are made of materials with different band gaps. Amorphous silicon alloys with carbon, germanium, nitrogen, and tin can be used to vary the band gap and material properties to improve multi-junction devices.

Since the depositions needed to make thin-film multi-junction devices do not use much energy, such devices are potentially inexpensive to fabricate. Making a multi-layered cell is similar to making one cell; just adding one thin-film after another.

ii. Copper Indium Diselenide multi-junction

Copper indium diselenide cells have a band gap of 1.0eV and are used as a single junction cell or with a higher band-gap material in a multi-junction device. Amorphous silicon, with a band gap of about 1.7eV, on top of CIS is an example of a multi-junction cell, as shown in figure 27.24.

Copper indium diselenide, a versatile material, is used as a bottom cell in conjunction with top cells of materials such as CdTe and GaAs, which have band gaps of approximately 1.43 and 1.44eV.

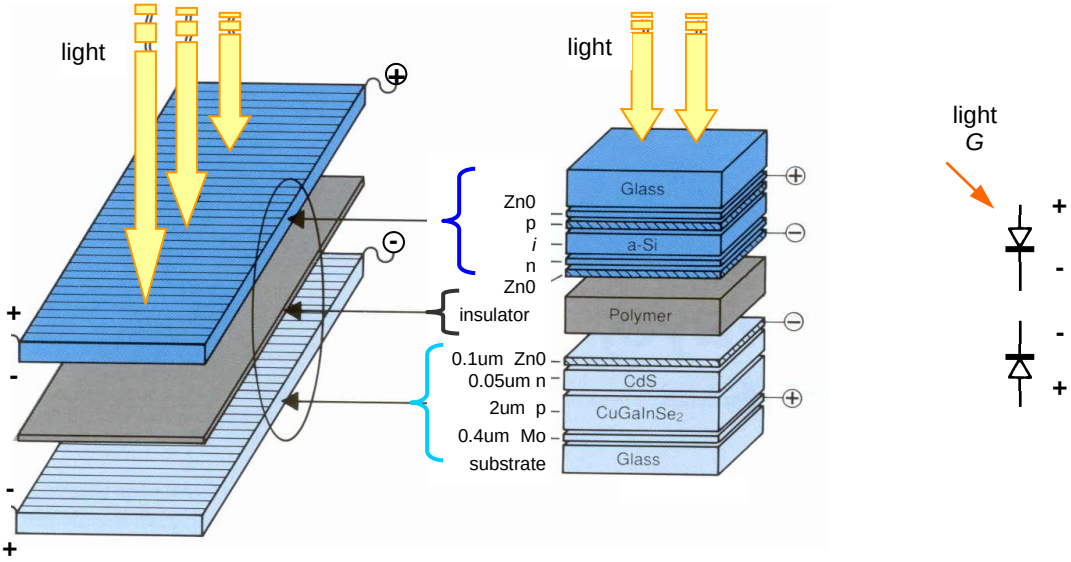

Figure 27.24. *A CID multi-junction PV cell.*

27.22 Equivalent circuit of a PV cell

To understand the electronic behaviour of a PV cell, it is useful to create a circuit model which is electrically equivalent, and is based on discrete electrical components whose behaviour is well known. An ideal single PV cell may be modelled by a current source, but its non-ideal, non-linear behaviour is due to the inherent shunting diode. Shunt resistance and series resistance components are also added to the model.

27.22.1 Ideal PV cell model

During darkness the PV cell is not active and behaves as a diode, that is, a *p-n* junction diode, not producing current.

The simplest PV cell model consists of diode and current source parallel connected as shown in figure 27.25a. The current source current I_{ph} is directly proportional to the solar radiation G (with incident optical power P_{in}). The diode (modelled by the Shockley diode equation) represents the *pn* junction of a PV cell. The equations of an ideal PV cell, which represents the ideal PV cell model, are:

$$I_D(V) = I_o\left\{e^{\frac{qV}{\gamma kT}} - 1\right\} = I_o\left\{e^{\frac{V}{\gamma V_{th}}} - 1\right\} \tag{27.22}$$

$$I_{ph} = \eta_g \times G \times A_c = \frac{q}{h \times v} P_{in} \tag{27.23}$$

where G is the ambient irradiance – intensity of incoming light, W/m^2,
η_g is the generation efficiency – response factor, and
A_c is the cell effective or active area, m^2.

The net output current I is the difference between the photocurrent I_{ph} and the normal diode current I_D

$$I(V) = I_{ph} - I_D = I_{ph} - I_o\left\{e^{\frac{V}{\gamma V_{th}}} - 1\right\} \tag{27.24}$$

where V is the diode voltage (V)
I_{ph} is the photo-current from the current source (proportional to the incident light intensity), A
I_o is the diode dark saturation current or reverse saturation current, A (approximately 10^{-8}/m^2)
k is Boltzmann's constant, 1.38 x 10^{-23}J/K,
h is Planck's constant, 6.626x10^{-34} J.s
q is the charge on an electron, 1.6 x 10^{-19} J/V, C or As,
v is the photon frequency, Hz, and
T is the working temperature of the cell in degrees Kelvin, K.

$$V_{th} = \frac{kT}{q} \tag{27.25}$$

where V_{th} - thermal voltage, V_{th} = 25.7mV at 25°C,
γ - diode non-ideal factor = 1 to 2 (γ = 1 for ideal diode)

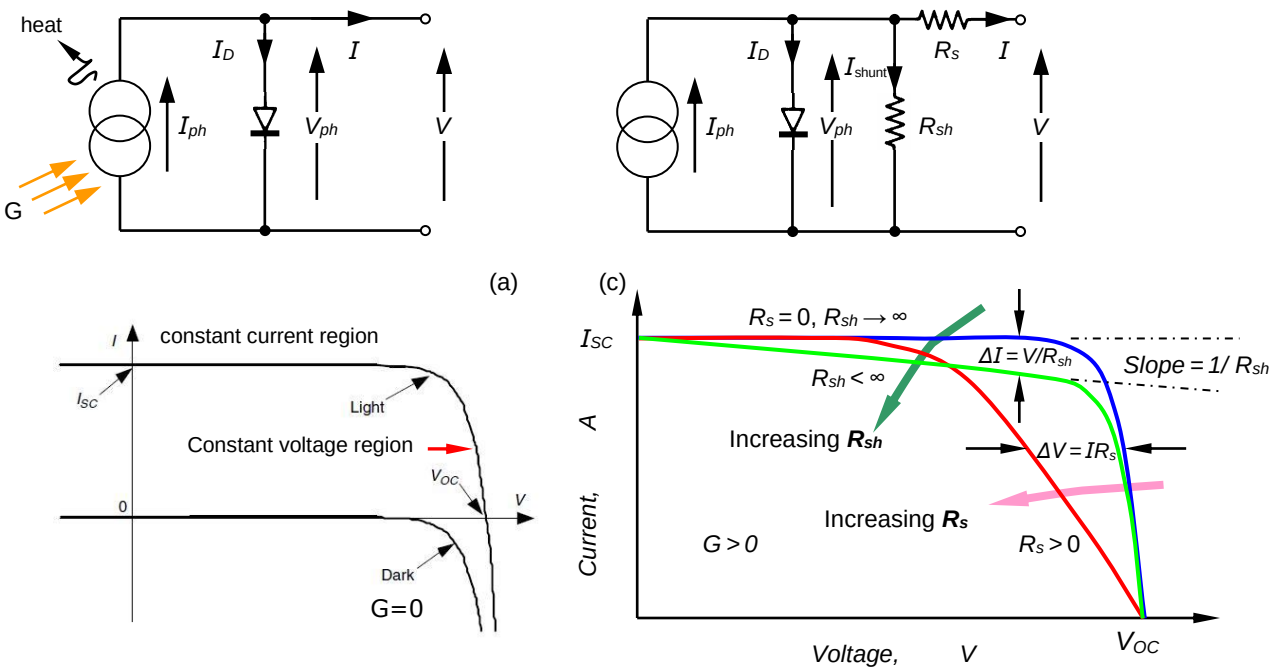

Figure 27.25. *PV cell electrical circuit model:(a) basic model and (b) its I-V characteristics, and (c) extended model incorporating series and shunt resistances.*

Both I_o and I_{ph} are strongly dependant on temperature.

$$I_o(T) = I_{SC}(T_1)\left(\frac{T}{T_1}\right)^{\frac{3}{\eta}}\left(\frac{e^{\frac{-qE_G}{\gamma k}\left(\frac{1}{T}-\frac{1}{T_1}\right)}}{e^{\frac{V_{OC,T_1}}{\gamma V_{th,T1}}}-1}\right) \tag{27.26}$$

$$I_{ph}(T) = G\,\frac{I_{SC,nom,T_1}}{G_{nom}}\left\{1+\frac{I_{SC,T_2}-I_{SC,T_1}}{T_2-T_1}(T-T_1)\right\} \tag{27.27}$$

G_{nom} = 1kW/m^2, termed 1 sun,
E_G is the band gap voltage, eV,
V_{OC} is the open circuit output voltage, which has a temperature coefficient of 2.3mV/°C for silicon, and
I_{SC} is the short circuit output current, the largest output current, when $V = I_D = 0$ in equation (27.24), whence $I_{SC} = I_{ph}$.

The cell open circuit voltage V_{OC} (the cell voltage at night, $G = 0$) is when the output current is zero, $I = 0$, such that the model diode current I_D equals to photo generated current I_{ph}. That is, equating equation (27.24) to zero

$$I(V) = I_{ph} - I_o\left\{e^{\frac{V}{\gamma V_{th}}}-1\right\} = 0 \tag{27.28}$$

gives

$$V_{oc} = \gamma V_{th}\,\ell n\left(\frac{I_{ph}}{I_o}+1\right) \tag{27.29}$$

27.22.2 Practical PV cell model

The equivalent circuit of a practical PV cell is a constant current source in parallel with an ideal diode and a shunt resistor R_{sh}, plus that all in series with a series resistor R_s.
The equations which describes the relationship between the output current and output voltage characteristics, I-V, of the PV cell are

$$I(V) = I_{ph} - I_D - I_{shunt} = I_L - I_o\left\{e^{\frac{V-IR_s}{\gamma V_{th}}}-1\right\} - \frac{V-IR_s}{R_{sh}} \tag{27.30}$$

27.22.3 Maximum-power point

A PV cell may operate over a wide range of output voltages V and currents I. The product of I and V is the power output of the cell P, and the solution of the equation that maximizes that product yields the voltage V_{mpp} and current I_{mpp} at the maximum power point P_m, as shown in equation (27.31). By increasing the load resistance on an irradiated cell, continuously from zero (a short circuit) to a very high value (an open circuit) the maximum-power point can be determine, the point that maximizes $V \times I$, that is, the load for which the cell can deliver maximum electrical power at that level of irradiation. The output power is zero in both the short circuit and open circuit extremes.

$$P_m = V_{mpp} \times I_{mpp} \tag{27.31}$$

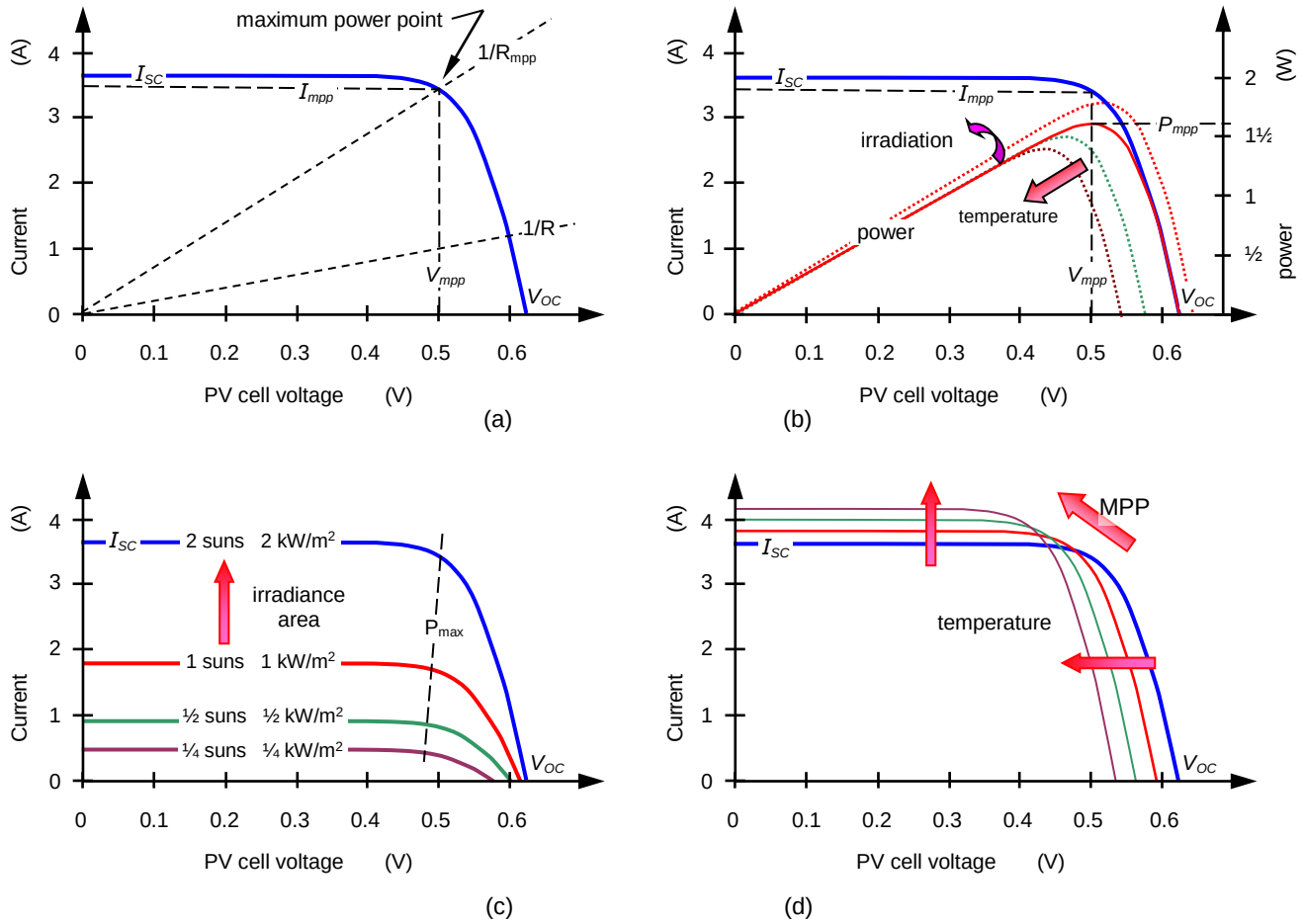

Figure 27.26. *A typical PV cell characteristics: (a) voltage-current I-V curve; (b) I-V and power characteristics; (c) effects of increased incident irradiance and cell area; and (d) effects of increased temperature on I-V characteristics.*

A high quality, monocrystalline silicon PV cell, at 25°C cell temperature, may produce an open circuit output voltage of V_{OC} = 0.60V. The cell temperature in full sunlight, even with a 25°C ambient air temperature, will probably be close to 45°C, reducing the open circuit voltage to 0.55 Volts per cell, as indicated in figure 27.26d. The voltage drops modestly, with this type of cell, until the short circuit current I_{SC} is approached. Maximum power (with a 45°C cell temperature) is typically produced with 75% to 85% of the open circuit voltage (0.43V in this case) and 80% to 90% of the short circuit current. This output can be up to 70% of the V_{OC} x I_{SC} product. The power output of the cell is almost directly proportional to the intensity of the sunlight. For example, if the intensity of the sunlight is halved the power will also be halved, as shown in figure 27.26c. The short circuit current I_{SC} from a cell is nearly proportional to the illumination, while the open circuit voltage V_{OC} may drop only 10% with a 80% drop in illumination. Lower quality cells have a more rapid drop in voltage with increasing current and may produce only ½V_{OC} at ½ I_{SC}. The usable power output could thus drop from 70% of the V_{OC} x I_{sc} product to 50% or even as little as 25%.

[Typical temperature coefficients: V_{OC}=-2 x10^{-3}/°C, V_{mpp}=-2.5 x10^{-3}/°C, I_{sc}=0.6x10^{-3}/°C, I_{mpp}=0.4x10^{-3}/°C]

From equation (27.24), the maximum power point is: when $\frac{dP}{dV} = 0$, $\left(1 + \frac{V_{mpp}}{V_{th}}\right) e^{\frac{qV_{mmp}}{kT}} = 1 + \frac{I_{ph}}{I_o}$

27.23 Photovoltaic cell efficiency factors

Energy conversion efficiency

PV cell energy conversion efficiency η, is the percentage of power converted (from absorbed light to electrical energy) and collected, when a PV cell is connected to an electrical circuit. This efficiency is calculated using the ratio of the maximum power point, P_m, divided by the input light irradiance (G, in W/m²) under standard test conditions (STC) and the surface area of the PV cell, A_c in m².

$$\eta = \frac{P_m}{G \times A_c} = \frac{V_{mpp} \times I_{mpp}}{G \times A_c} = \frac{FF \times V_{OC} I_{SC}}{G \times A_c} \tag{27.32}$$

STC specifies a temperature of 25°C, an irradiance of 1000W/m², and a 0 m/s wind speed with an air mass 1.5 (AM = 1/cosθ, where angle θ is relative to the zenith, the vertical,) spectrum. These correspond to the irradiance and spectrum of sunlight incident on a clear day upon a sun-facing 37° - tilted surface with the sun at an angle of 41.81° above the horizon.
The losses of a PV cell are divided into:

- reflectance losses,
- thermodynamic efficiency,
- recombination losses, and
- resistive electrical loss.

The overall efficiency is related to the product of each of these individual losses, but these losses are not directly measurable. Other measurable parameters are used instead to specify efficiency:

- Thermodynamic Efficiency,
- Quantum Efficiency,
- V_{oc} ratio, and
- Fill Factor, *FF*.

Reflectance losses are a portion of the Quantum Efficiency. Recombination losses make up a portion of the Quantum Efficiency, V_{oc} ratio, and Fill Factor. Resistive losses are predominantly categorized under Fill Factor, but also make up minor portions of the Quantum Efficiency and V_{oc} ratio.

Thermodynamic efficiency limit

PV cell efficiency is limited because it operates as a quantum energy conversion device. Photons with energy below the band gap of the absorber material cannot generate an electron-hole pair, and as such the photon energy is not converted to useful output. When a photon of greater energy than the band gap is absorbed, the excess energy above the band gap is converted to heat as the excess kinetic energy is released as the electron slows to equilibrium velocity. This loss is termed the *Thermodynamic Efficiency Limit*.

Quantum efficiency

An elevated electron-hole pair may travel to the surface of the PV cell and contribute to the current produced by the cell; such a carrier is said to be collected. Alternatively, the electron may give up its energy and once again become bound to an atom within the PV cell without reaching the surface; this is called recombination, and carriers that recombine do not contribute to the production of electrical current.
Quantum efficiency refers to the percentage of photons that are converted to electric current (that is, collected carriers) when the cell is operated under short circuit conditions. External quantum efficiency is the fraction of incident photons that are converted into electrical current, while internal quantum efficiency is the fraction of absorbed photons that are converted into electrical current. Mathematically, internal quantum efficiency is related to external quantum efficiency by the reflectance of the PV cell; given a perfect anti-reflection coating, they are the same.

V_{OC} ratio

Due to electron recombination, the open circuit voltage V_{oc} of the cell will be below the band gap voltage of the cell semiconductor. Since the energy of the photons must be at or above the band gap to generate a carrier pair, a cell voltage below the band gap voltage represents a loss. This loss is represented by

$$V_{OC}\ ratio = \frac{V_{OC}}{E_G} \tag{27.33}$$

Fill factor

Another term in the overall efficiency behaviour of a PV cell is the fill factor, *FF*, which is the ratio of the maximum power divided by the product of the open circuit voltage V_{oc} and the short circuit current I_{sc}:

$$FF = \frac{P_m}{V_{OC} I_{SC}} = \frac{I_{mpp} V_{mpp}}{V_{OC} I_{SC}} = \frac{\eta A_c G}{V_{OC} I_{SC}} \tag{27.34}$$

The cell fill-factor can be expressed as a function of the open circuit voltage by:

$$FF \approx \frac{\frac{V_{OC}}{\gamma V_{th}} - \ell n\left(\frac{V_{OC}}{\gamma V_{th}} + 0.72\right)}{\frac{V_{OC}}{\gamma V_{th}} + 1} \tag{27.35}$$

Concentrators

A concentrator is a PV cell designed to operate under illumination greater than 1 sun. The incident sunlight is focused or guided by optical elements such that a high intensity light beam shines on a small area PV cell. Concentrators have several potential advantages, including a higher efficiency potential than a one-sun PV cell and the possibility of lower cost. The short-circuit current from a PV cell depends linearly on light intensity, such that a device operating under 10 suns would have 10 times the short-circuit current as the same device under one sun operation. However, this effect does not provide an efficiency increase, since the incident power also increases linearly with concentration. Instead, the efficiency benefits arise from the logarithmic dependence of the open-circuit voltage on short circuit. Therefore, under concentration, V_{OC} increases logarithmically with light intensity, specifically:

$$V_{OC}^{X} = \gamma V_{TH}\,\ell n\left(\frac{X \times I_{SC}}{I_o}\right) = \gamma V_{TH}\left[\ell n\left(\frac{I_{SC}}{I_o}\right) + \ell nX\right] = V_{OC} + \gamma V_{TH}\,\ell nX \tag{27.36}$$

where X is the concentration of sunlight.

From equation (27.36), a doubling of the light intensity (X=2) causes an 18 mV rise in V_{OC}.

The cost of a concentrating PV system may be lower than a corresponding flat-plate PV system since only a small area of PV cells is needed.

The efficiency benefits of concentration may be reduced by increased losses in the series resistance as the short-circuit current increases and also by the increased operational temperature of the PV cell. As losses due to short-circuit current depend on the current squared, power loss due to series resistance increases as the square of the concentration.

Example 27.5: ***Solar cell characteristics***

A 1cm^2 silicon solar cell has a saturation current I_o of 10^{-12}A and is illuminated with sunlight yielding a short-circuit photocurrent I_{SC} of 25mA. Calculate the solar cell efficiency and fill factor, assuming a power density of 1kW/m^2.

Solution

The maximum power is generated when:

$$\frac{dP}{dV} = \frac{d}{dV}\left(V\left[I_{ph} - I_o\left(e^{\frac{V}{V_{th}}} - 1\right)\right]\right) = 0 = I_{ph} - I_o\left(e^{\frac{V_{mpp}}{V_{th}}} - 1\right) - V_{mpp} I_o \frac{1}{V_{th}} e^{\frac{V_{mpp}}{V_{th}}}$$

where the voltage, V_{mpp}, is the voltage corresponding to the maximum power point. This voltage is obtained by solving the following transcendental equation, with V_{th} = 25.7mV and I_{ph} =25mA (since the short circuit current equals the photocurrent, $I_{SC} = I_{ph}$ at V_{SC}) at 25°C:

$$V_{mpp} = V_{th}\,\ell n\frac{1 + \frac{I_{ph}}{I_o}}{1 + \frac{V_{mpp}}{V_{th}}} = 0.0257\text{V} \times \ell n\frac{1 + \frac{25 \times 10^{-3}\text{A}}{10^{-12}\text{A}}}{1 + \frac{V_{mpp}}{0.0257\text{V}}}$$

Iteration gives V_{mpp} =0.536V. The corresponding maximum power point current I_{mpp} is 0.0239A.

The efficiency, assuming the irradiance power G of the sun is 1kW/m^2, equals:

$$\eta = \frac{V_{mpp} I_{mpp}}{P_{in}} = \frac{0.536\text{V} \times 0.0239\text{A}}{1 \times 10^{-4}\text{m}^2 \times 1\text{kW/m}^2} = 12.8\%$$

The open circuit voltage is calculated from (27.29) which gives

$$V_{OC} = V_{th} \ln\left(\frac{I_{ph}}{I_o} + 1\right)$$

$$= 0.0257\text{V} \times \ln\left(\frac{25\text{mA}}{10^{-12}} + 1\right) = 0.615\text{V}$$

The fill factor is:

$$\textit{fill factor} = FF = \frac{V_{mpp} I_{mpp}}{V_{OC} I_{SC}} = \frac{0.536\text{V} \times 0.0239\text{A}}{0.615\text{V} \times 0.025\text{A}} = 83.3\%$$

♣

Example 27.6: ***PV cell and module characteristics***

A 100cm^2 PV cell has I-V characteristics as shown in figure 27.25 parts a and b, at 25°C, achieved using a concentrator which gives 2kW/m^2 on each cell.
The PV cell is characterised by $V_{OC} = 0.625\text{V}$ $V_{mpp} = 0.50\text{V}$
$I_{SC} = 3.7\text{A}$ $I_{mpp} = 3.5\text{A}$

With diode properties $\gamma = 1.5$ and $V_{th} = 25.7\text{mV}$ at 25°C.
Use this information (and figures 27.26 and 27.28, if necessary) to find

i. The maximum cell power and optimal load resistance for delivering this power;
ii The fill factor *FF*;
iii The V_{OC} efficiency ratio, if the band gap of the silicon cell is 1.11eV at 25°C;
iv. The open-circuit voltage and short-circuit current values if a module uses 36 of such cells series connection, with three cells parallel connected at each voltage level; and
v. The module maximum power output and optimal load resistance for the given conditions.

Solution

i. The maximum cell power P_m is given by equation (27.31), that is

$$P_m = V_{mpp} \times I_{mpp}$$
$$= 0.5\text{V} \times 3.5\text{A} = 1.75\text{W}$$

ii. The efficiency fill factor *FF* is

$$FF = \frac{P_m}{V_{OC} I_{SC}}$$
$$= \frac{1.75\text{W}}{0.625\text{V} \times 3.7\text{A}} = 75.7\%$$

Alternatively, using equation (27.35)

$$FF \approx \frac{\frac{V_{OC}}{\gamma V_{th}} - \ell\text{n}\left(\frac{V_{OC}}{\gamma V_{th}} + 0.72\right)}{\frac{V_{OC}}{\gamma V_{th}} + 1} = \frac{16.21 - \ell\text{n}(16.21 + 0.72)}{16.21 + 1} = 77\%$$

iii. The V_{OC} efficiency ratio is

$$V_{OC}\ ratio = \frac{V_{OC}}{E_G} = \frac{0.625\text{V}}{1.11\text{eV}} = 56.3\%$$

iv. With 36 series connected cells the open circuit output voltage is

$$V_{M,OC} = n \times V_{OC}$$
$$= 36 \times 0.625\text{V} = 22.5\text{V}$$

The short circuit output current for three parallel connected cells at each voltage level is

$$I_{M,sc} = k \times I_{SC}$$
$$= 3 \times 3.7\text{A} = 11.1\text{A}$$

v. The module maximum power P_M is

$$P_M = n \times k \times P_m$$
$$= 36 \times 3 \times 1.75\text{W} = 189\text{W}$$

where the output voltage is 36×0.50V=18V and the output current is 3×3.5A=10.5A (18V×10.5A=189W)

♣

27.23.1 Impact of temperature and insolation on I-V characteristics

PV I–V curves show that the characteristics shift as insolation and cell temperature change. Figure 27.27a shows a 120W multicrystal-silicon module. As insolation drops, short-circuit current drops in direct proportion. Halving insolation, for example, halves I_{SC}. Decreasing insolation also reduces V_{OC}, logarithmically resulting in relatively modest changes in V_{OC}.
As cell temperature increases, the open-circuit voltage decreases substantially while the short-circuit current increases slightly. Photovoltaics perform better on cold, clear days. For crystalline silicon cells,

V_{OC} drops by about 0.37% for each degree Celsius increase in temperature and I_{SC} increases by approximately 0.05%. The net result when cells heat up is the MPP slides slightly upward and toward the left with a decrease in maximum power available of about 0.5%/°C.
Cells vary in temperature not only because ambient temperatures change, but also because insolation on the cells changes. Since only a small fraction of the insolation is converted to electricity, most of the incident energy is absorbed and converted to heat.
The nominal operating cell temperature NOCT is cell temperature in a module when the ambient is 20°C, solar irradiation is 0.8kW/m^2, and wind-speed is 1m/s. The following expression is used to account for other ambient conditions:

$$T_{cell} = T_{amb} + (NOCT - 20°C) \times \frac{S}{0.8} \tag{27.37}$$

where T_{cell} is cell temperature (°C), T_{amb} is ambient temperature, and S is solar insolation (kW/m^2).

27.13:Typical and maximum module and cell conversion efficiencies at Standard Test Conditions

Type	Typical module efficiency	Maximum recorded module efficiency	Maximum recorded laboratory efficiency
	%	%	%
Single crystalline silicon	12-15	22.7	24.7
Multi-crystalline silicon	11-14	15.3	19.8
Amorphous silicon	5-7	-	12.7
Cadmium telluride, CdTe	-	10.5	16.0
$CuInGaSe_2$, CIGS	-	12.1	18.2

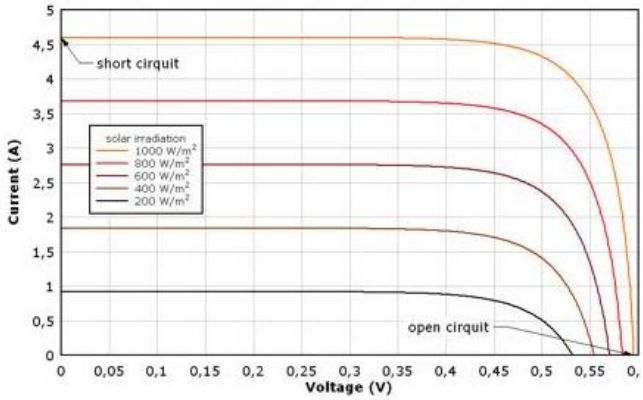

Solar cell I-V characteristics for different irradiation values

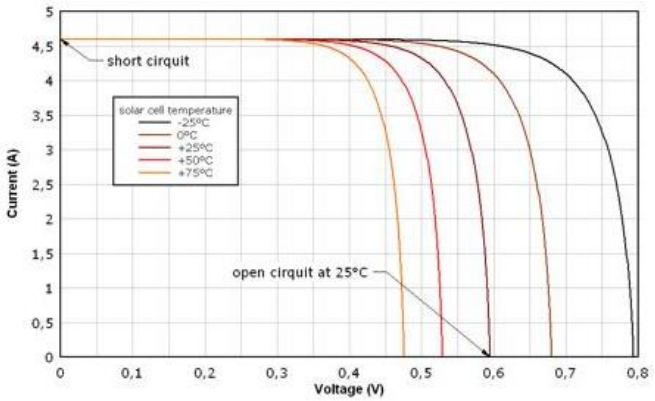

Solar cell I-V characteristics temperature dependency

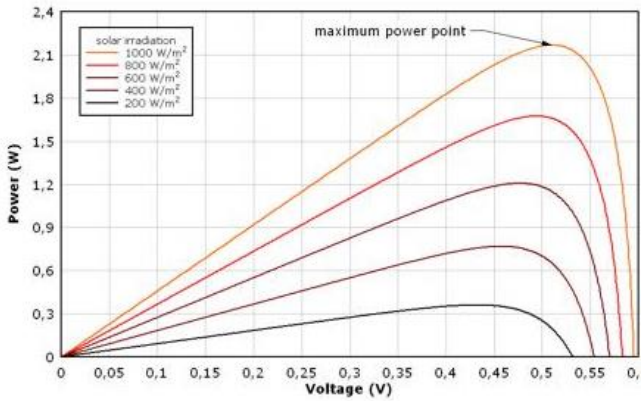

Solar cell power characteristics for different irradiation values

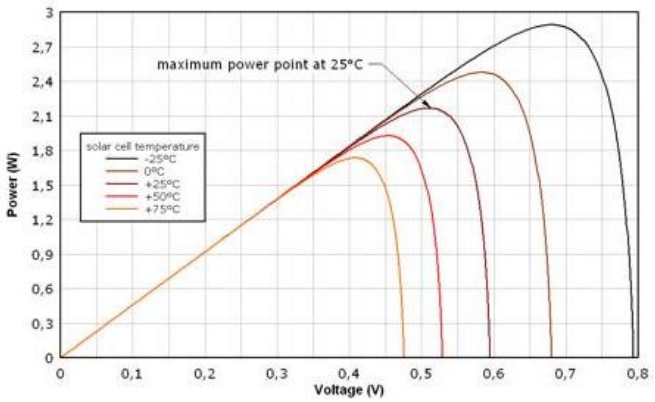

Solar cell power characteristics temperature dependency

(a)

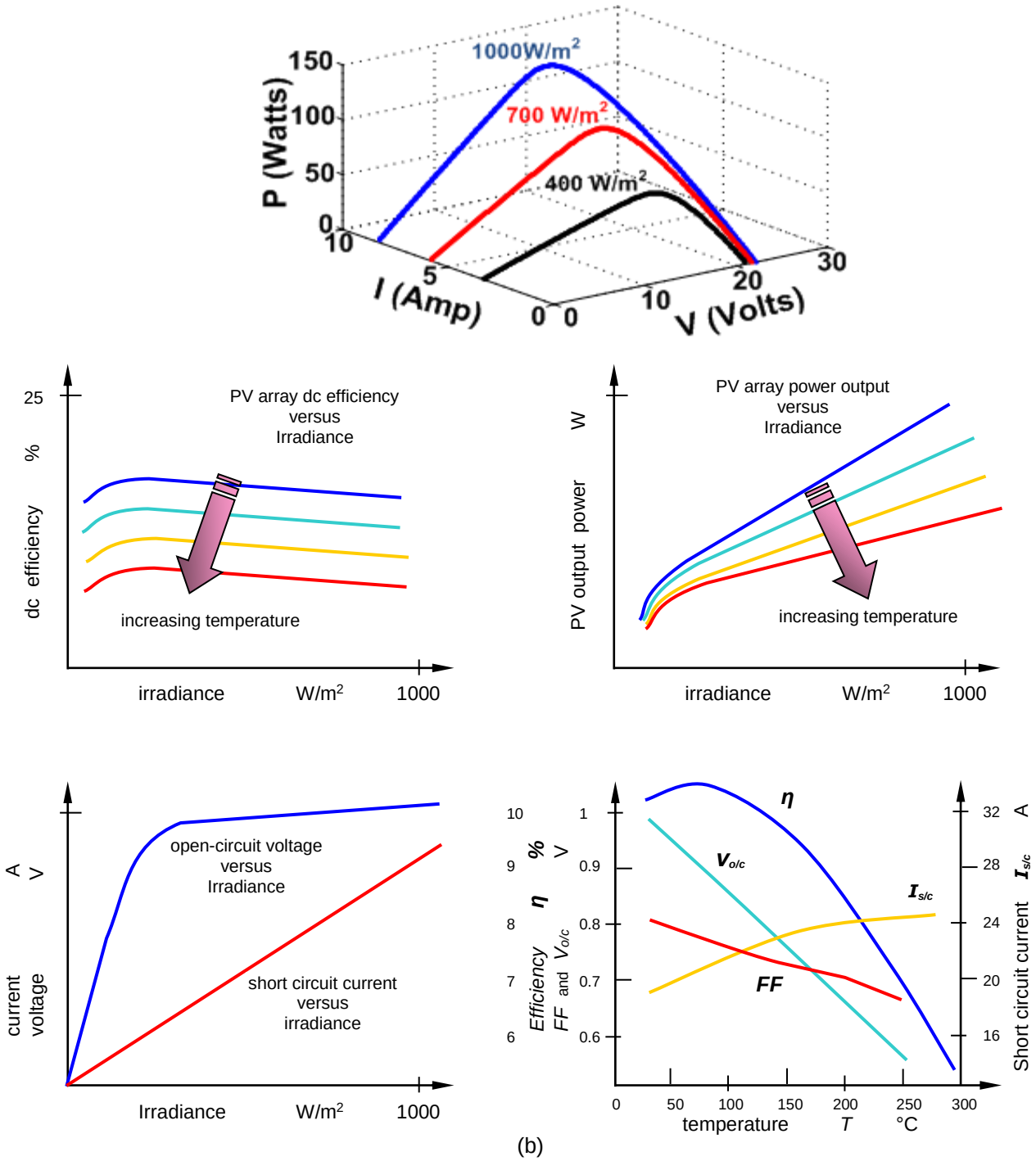

(b)

Figure 27.27. *I-V characteristics of a typical PV module under various cell temperatures and irradiance levels.*
(a) *at 1kW/m², 1.5AM, 25°C: 36 cells, η=12.9%, 120W, 16.9V (21.5V o/c). 7.1A (7.5A s/c) and (b) other typical cell and array characteristics.*

Example 27.7: ***PV module temperature characteristics***

Estimate cell temperature, open-circuit voltage, and maximum power output for the 120W module in figure 27.27 under conditions of 1-sun insolation and 30°C ambient temperature. The module has a NOCT of 47°C.

Solution

Using equation (27.37) with S = 1 kW/m², the cell temperature is estimated to be

$$T_{cell} = T_{amb} + (NOCT - 20°C) \times \frac{S}{0.8}$$

$$= 30°C + (47°C - 20°C) \times \frac{1}{0.8} = 63.75°C$$

From the caption in figure 27.27, for this module at the standard temperature of 25°C, V_{OC} = 21.5V.

Since V_{OC} drops by 0.37%/°C, the operating V_{OC} will be

$$V_{OC} = 21.5V\text{x}[1 - 0.0037\text{x}(63.75 - 25)] = 18.4V$$

With maximum power expected to drop about 0.5%/°C, this 120W module at its maximum power point will deliver

$$P_{max} = 120W\text{x}[1 - 0.005\text{x}(63.75 - 25)] = 96.75W$$

which is a 19.4% drop from rated power of 120W.

♣

27.24 Module (or array) series and parallel PV cell connection

Identical PV cells are series and parallel connection to form high-voltage, high-current, modules. For high current applications, modules are connected in parallel. For high voltage applications, modules (and strings) are connected in series.

If all the PV cells in a module have identical electrical characteristics, and all experience the same insolation and temperature, then all the cells will operate at the same current and voltage. In this case, the *I-V* curve of the PV module has the same shape as that of the individual cells, except that the voltage and current are increased.

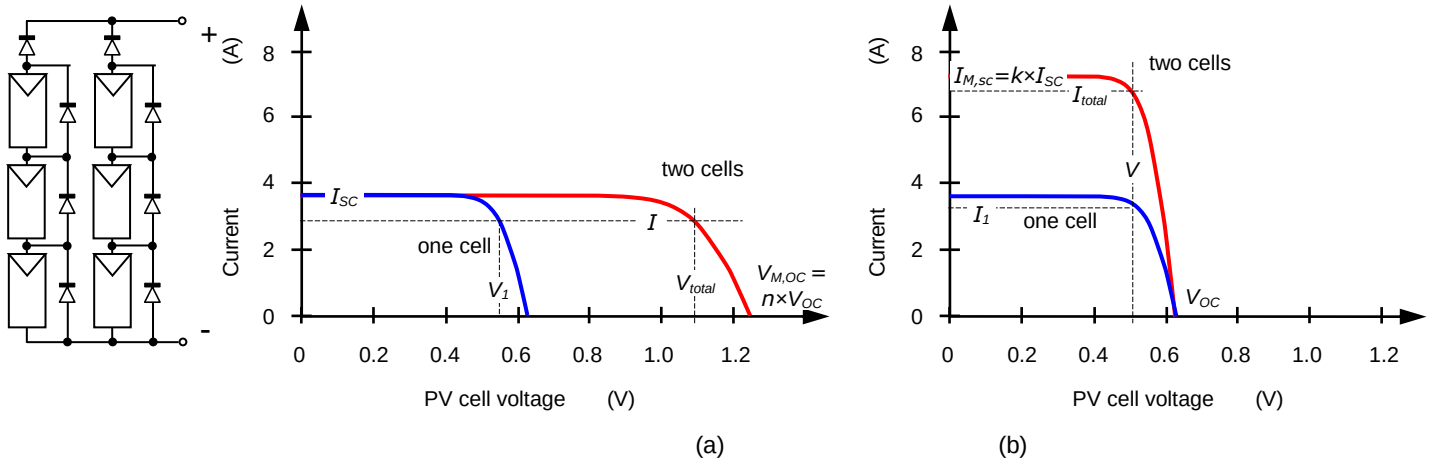

Figure 27.28. *I-V characteristics of identical PV cells connected in (a) series and (b) parallel.*

Series connection of *n* identical cells:

- When series connected, to form a string, voltage adds $V_{total} = V_1 + V_2 + ... + V_n$
- The current remains constant $I_{total} = I_1 = I_2$

With a series connection of voltage sources, the voltage of each source adds incrementally.

For *n* series connected PV cells, each with open circuit voltage V_{OC}, the module open circuit voltage is

$$V_{M,OC} = n \times V_{OC} \tag{27.38}$$

Parallel connection of *k* identical cells:

- When parallel connected, the currents add $I_{total} = I_1 + I_2 + .. + I_k$
- The voltage remains constant $V_{total} = V_1 = V_2 .....$

With the parallel connection of voltage sources, the currents add. The voltage corresponds to that of a single source.

For *k* parallel connected PV cells, each with short circuit current I_{SC}, the module short-circuit current is

$$I_{M,sc} = k \times I_{SC} \tag{27.39}$$

If each cell has a series resistance R_s, the Thevenin equivalent resistance of the module is

$$R_{M,s} = \frac{n}{k} R_s \tag{27.40}$$

The same formula applies to the calculation of the equivalent module shunt resistance:

$$R_{M,sh} = \frac{n}{k} R_{sh} \tag{27.41}$$

The module maximum power P_M deliverable to a resistive load is

$$P_M = n \times k \times P_m \tag{27.42}$$

The module terminal voltage V_M and current I_M characteristic equation can be expressed in terms of each cell or the characteristics of the module, namely

$$I_M(V_M) = I_{M,SC}\left(1 - e^{\frac{V_M - V_{M,OC} + R_{M,s} \times I_M}{n\gamma V_{th}}}\right) \quad (27.43)$$

or, in terms of the individual cell characteristics:

$$I_M(V_M) = k \times I_{SC}\left(1 - e^{\frac{V_M - n \times V_{OC} + \frac{n}{k} R_s \times I_M}{n\gamma V_{th}}}\right) \quad (27.44)$$

In terms of the simple model in figure 27.25a

$$I_M(V_M) = k \times I_{ph} - k \times I_o\left(e^{\frac{V_M}{n\gamma V_{th}}} - 1\right) \quad (27.45)$$

Bypass diodes for shade mitigation

The voltage drop associated with shaded cells can be partially mitigated by adding a *bypass diode* across each cell, as shown in figure 27.28. When a solar cell is in the sun, there is a voltage rise across the cell so the bypass diode is cut off and no current flows through it - as if the diode were absent, as shown in figure 27.29a. When the solar cell is shaded, however, the drop that would occur if the cell conducted any current would turn on the bypass diode, diverting the current flow through that diode. The bypass diode, when it conducts, drops about 0.6V. So, the bypass diode controls the voltage drop across the shaded cell, limiting it to a relatively modest -0.6V instead of the rather large drop that may occur without it. Using the synchronous mosfet rectifier shown in figure 27.29b can further reduce the negative reverse bias.

In real modules, it would be impractical to add bypass diodes across every solar cell, but at least one bypass diode is used around a module to help protect arrays, and sometimes several such diodes around groups of cells within a module. These diodes do not influence shading problems of a single module, but they can be important when a number of modules are connected in series. Just as cells are connected in series to increase module voltage, modules can be connected in series to increase array voltage. Also, just as a single cell can impede the current within a module, a few shaded cells in a single module can restrict the current delivered by the entire string in an array. The benefit demonstrated for a bypass diode on a single cell also applies to a diode applied across a complete module.

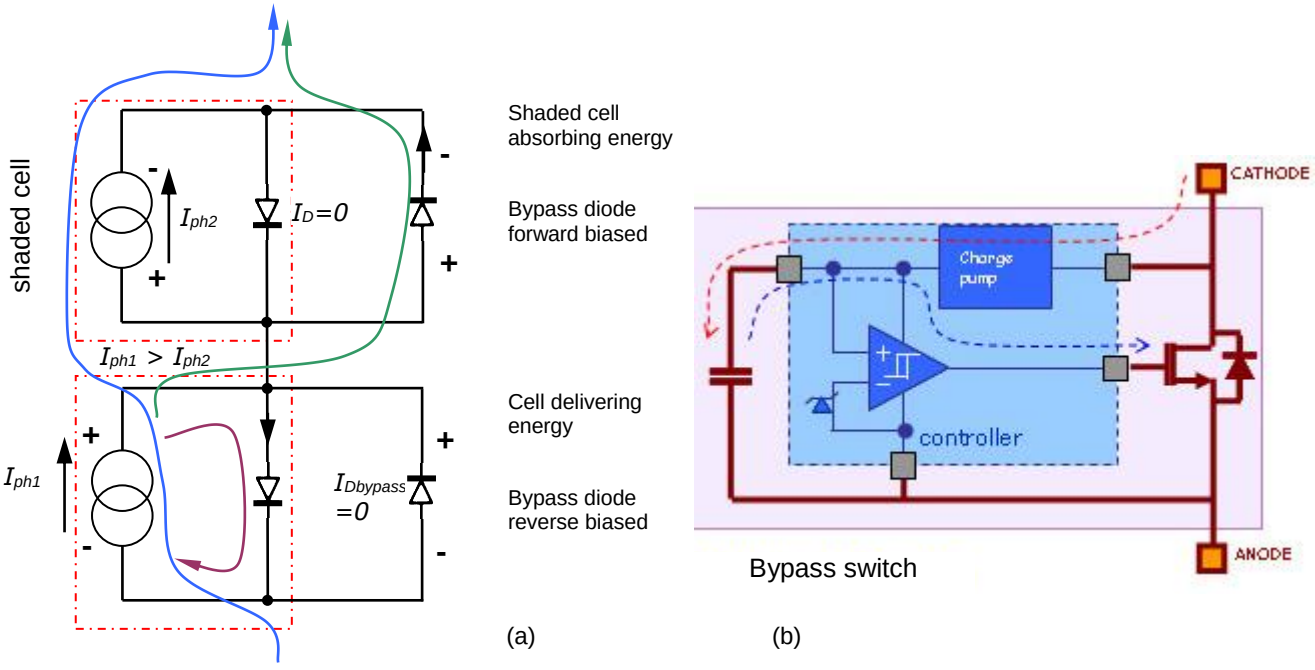

Figure 27.29. *Shaded cell: (a) bypass diode operation and (b) synchronous rectifying bypass mosfet alternative for reduced cell losses.*

Blocking diodes

Bypass diodes help current divert around a shaded or malfunctioning module within a string. This not only improves string performance, but also prevents hot spots from developing in individual shaded cells. When strings of modules are connected in parallel, a similar problem may arise when one of the

strings is not functioning correctly. Instead of supplying current to the array, a malfunctioning or shaded string can draw current from the rest of the array. By placing *blocking diodes* (also called *isolation diodes*) at the top of each string as shown in figure 27.28, the reverse current drawn by a shaded string can be prevented.

27.25 Battery storage

PV cells can only produce electricity during the day, and then only on clear days. To be independent of the grid, energy storage is needed but batteries add cost and maintenance to the PV system. This problem is avoided with connection to the utility grid, buying power when needed and selling when producing more than needed, as shown in figure 27.30. This way, the utility acts as a practically infinite bidirectional storage system. Suitable inverter equipment is needed to ensure that the power sold to the utility is synchronous with the grid, specifically the same sinusoidal waveform and frequency. The utility has to be assured that if there is a power outage, the PV system does not try to feed electricity into lines. This disconnection is called *islanding*.

Batteries need regular maintenance, and replacement after a few years, although the PV modules last for 20 years or more. Batteries in PV systems can also be dangerous because of the voltage level at which the energy is stored and the acidic electrolytes they contain, so the protective environment must be well-ventilated and non-metallic.

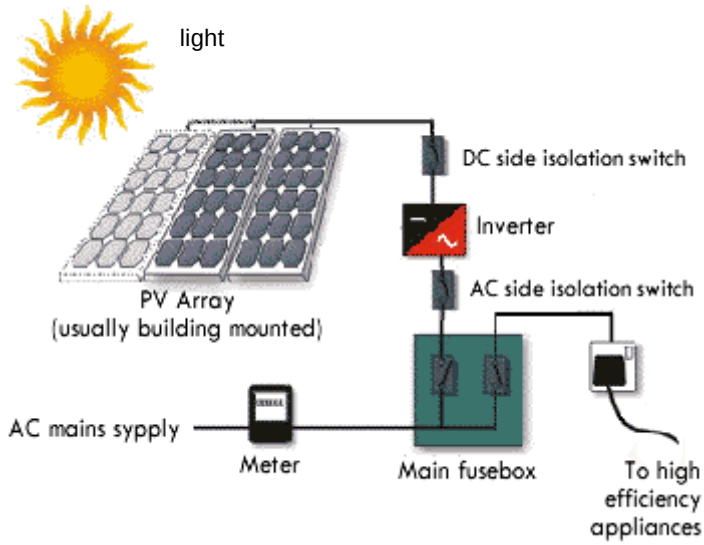

Figure 27.30. *Schematic of a typical residential PV system with battery storage.*

A lead-acid car type battery is a shallow-cycle battery and PV storage requires deep-cycle batteries which can discharge a significant amount of their stored energy while still maintaining long life. PV batteries generally have to discharge a small current for a long period (such as all night), while being charged during the day. The nickel-cadmium battery is the most commonly used deep-cycle battery, which is more expensive than the lead-acid battery, but last longer and can be discharged more completely without harm. Lead-acid batteries cannot be deep-cycled or discharged 100 percent without seriously shortening battery life. Generally, if a PV system uses lead-acid batteries, the system is designed to discharge the batteries by no more than 40 percent or 50 percent.
For long battery life, a charge controller is needed to prevent overcharging and complete discharge.
The other problem besides energy storage is that the electricity generated by PV modules, and extracted from the storage batteries if used, is in dc form while household appliances and the utility grid need ac voltage. Most distributed generation inverters automatically control the system. Some PV modules, called AC modules, have a built-in system inverter, eliminating the need for a large, central inverter, and simplifying wiring and safety issues.
A PV system requires little maintenance (especially if no batteries are used), and can provide electricity cleanly and quietly for 20 years or more.

Weather and temperature
Weather naturally affects the performance of PV modules but not as may be expected. The amount of sunlight is most important in determining the output a PV electric system will produce at a given location, but temperature is also important. PV modules actually generate more power at lower temperatures with other factors being equal. This is because PV cells generate electricity from light, not heat. Like most electronic devices, PV cells operate more efficiently at cooler temperatures. In temperate climates, PV

panels will generate less energy in the winter than in the summer but this is due to the shorter days, lower sun angles and greater cloud cover, not the cooler temperatures.
PV module output is proportional to the sun's intensity, so cloud cover will reduce the system output. Typically, the output of any industrial PV module is reduced to 5% to 20% of its full sun output when operated under cloudy conditions.

During a typical sunny day, a PV array one metre square exposed to the sun at noon will receive approximately 1kW of power. Multi-crystalline cells convert roughly 15% of this irradiation energy into electricity, hence 1m² of cells generates 150W in full sunshine. The warmer the cells become, the higher the losses. At 60ºC the capacity decreases by about 18% to 123W, and at 70ºC output drops by 24% to 114W. As shown in figure 27.26d, this reduced power output is because:

- the voltage decreases, at an increasing rate, with increased temperature
- the current increases minimally with increasing temperature.

This means that the maximum power output of a PV cell decreases with increased temperature, especially under higher irradiation levels.

27.26 The organic photovoltaic cell

Following absorption of photons by the polymer, bound electron-hole pairs (excitons) are generated, subsequently undergoing dissociation, as shown in figure 27.31. Due to inherent limitations in organic materials (exciton lifetime and low charge mobility), only a small fraction of photon-generated electron-hole pairs effectively contribute to the photocurrent. The organic cell facilitates volume distribution of the photogeneration sites, thereby enhancing exciton dissociation. This is achieved by increasing the junction surface area, with an interpenetrating network of the donor-acceptor type, effecting transport of holes to the indium-tin oxide anode, and of electrons to the aluminium metallic cathode. While quantum separation efficiency, for photo-induced charges in systems associating a semiconducting polymer, polythiophene, with a fullerene derivative, is thus close to unity, the objective is to restrict recombination and trapping processes, limiting charge transport and collection at the electrodes, to improve overall device efficiency, this currently still being low, less than 5%. The rise of the pathway is also dependent on the cell aging mechanisms and thin-film technologies, to protect the device against atmospheric oxygen and water vapour ingress.

Organic PV cells
Operation of organic PV cells is mechanistically more complex. First, a molecule of an organic compound absorbs a photon and forms an excited state (exciton). Further, the exciton diffuses to a junction border between n- and p- types of semiconductor where it dissociates to form free charge carriers. Organic p- and n- transporters are also known as donors and acceptors respectively.
If there is no junction border nearby, the exciton may recombine (decay) via photoluminescence, or thermally, back into the ground state of the molecule. This is the main reason, why mono- and bi-layered (the scheme in figure 27.31) organic PV cells are poorly performing devices.

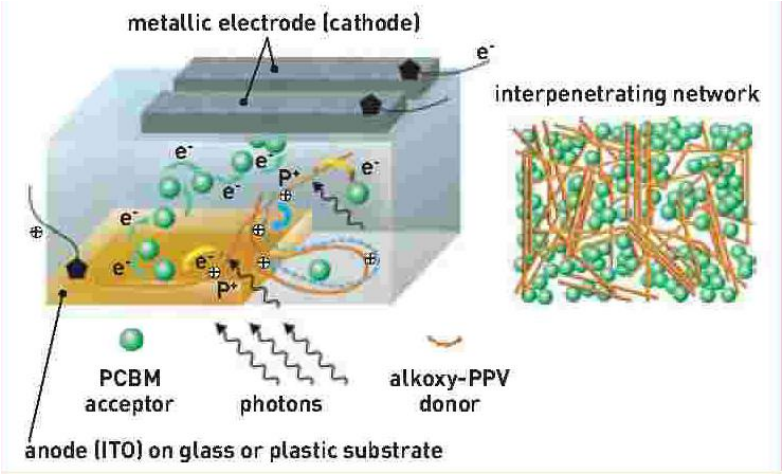

Figure 27.31. *Organic PV cell.*

The bulk heterojunction shown in figure 27.32 is a compact blend of a *p*-type conductor (donor), and *n*-type conductor (acceptor) in the photoactive layer of a device, where the concentration of each component often gradually increases when approaching the corresponding electrode. This magnifies the

p-n junction's total surface and strongly facilitates exciton dissociation. The implication of this concept in practice allows increased power conversion efficiencies of up to 5% for all-organic PV cells.

For the realization of the bulk-heterojunction concept, the organic cells and materials need further development in order to foster commercial application. Advantages of organic PV cells are: lightweight, environmentally friendly, no requirements for rare metals and minerals, no high temperatures and purity demand at the production stage, potentially inexpensive, and virtually unlimited possibilities for further material improvements.

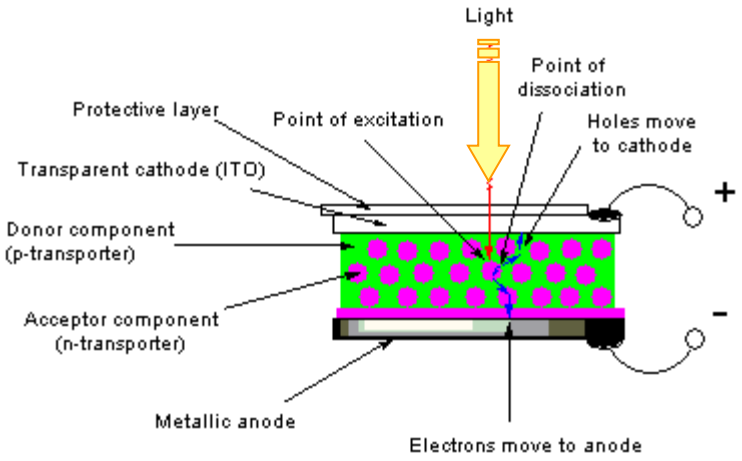

Figure 27.32. *Bulk heterojunction organic solar cell.*

27.27 Summary of PV cell technology

PV advantages

- Infinite source of input energy. The 89 petawatts of sunlight reaching the earth's surface is plentiful - almost 6,000 times more than the 15 terawatts of average power consumed by humans.
- The silicon cells manufactured from one ton of sand produce as much electricity as burning 500,000 tons of coal.
- Solar electric generation has the highest power density (global mean of 170W/m²) among renewable energies.
- Low maintenance and long service lifetime, durable with minimal degradation over 10 years.
- No emissions of $C0_2$, $S0_2$, $N0_2$, radiation.
- Peak output matches daily peak demand.
- Can be installed near point of energy need.
- Grid-connected PV electricity can be used locally thus reducing transmission/distribution losses or used decentralized.
- Grid system integration possible, or independent of the grid thereby avoiding lack any of transmission and distribution infrastructure.
- Quick installation.
- Modular and expandable, for increased power.
- Low operating costs, no fuel, transport and storage costs.
- No moving parts to wear, operate silently with minimal system movement.
- Environmental benign, no waste, no noise, free energy, no fuel transport costs.
- High public acceptance.
- Excellent safety record, with no combustible fuels.
- Suitable for harsh environments.
- Can be portable.
- Suitable for remote locations, including high-temperature, high-altitude environments, with improved performance, where hydrocarbon based systems are derated.

PV disadvantages

- Sunlight is a low intensity energy source, hence limited power density, 2 to 5 kW·h/m².
- Produces dc, which must be converted to ac with at least 2% losses.
- Hi-tech skills to create the technology, but not necessary for installation, operation, and maintenance.

- Some PV materials are toxic, for example the cadmium in cadmium telluride PV cells, therefore requiring careful end of life treatment.
- Energy not available at night or during overcast weather.
- Expensive initial cell costs, plus expensive component replacement costs.
- High installation costs.
- Poor ancillary equipment reliability of grid tie inverters and storage methods, e.g., batteries, although PVs are highly reliable if maintained (cleaned and protected).
- Lack of commercial storage facilities.
- Accelerated sunlight ageing of associated synthetic materials.
- Local weather patterns and sun conditions directly affect the potential of photovoltaic systems. Some locations will not be able to use solar power.

There are two disadvantages often used by environmentalist concerning high-tech PVs:

- Production Pollution:- Fossil fuels are extensively utilized to extract, produce and transport PV panels. These processes also entail corresponding sources of pollution. The life cycle analysis of a PV system is a net positive for the environment because it can offset fossil fuel energy production over its approximately 25-year lifetime.
- High energy cost:- Require much energy to produce. The three types of photovoltaic (PV) materials, which make up the majority of the active PV market: single crystal, polycrystalline, and amorphous silicon PV cells pay for themselves in terms of energy in a few years (1 to 5 years). They thus generate enough energy over their lifetimes to reproduce themselves many times (6 to 31 reproductions) depending on what type of material, balance of system, and the geographic location of the system.

Table 27.14: Summary of PV cell technology (AR:- antireflective coating)

Material	Thickness	Efficiency	Colour	Features
Mono-crystalline Si	300µm	15-18%	Dark blue, black with AR coating, grey without AR coating	Lengthy production procedure - wafer sawing necessary. Highly researched PV cell material. Highest power/area ratio.
Polycrystalline Si	300µm	13-15%	Blue, with AR coating, silver-grey without AR coating	Wafer sawing necessary. Currently the most important production procedure.
Polycrystalline transparent Si	300µm	10%	Blue, with AR coating, silver-grey without AR coating	Lower efficiency than monocrystalline PV cells.
Edge defined Film fed Growth EFG	280µm	14%	Blue, with AR coating	Limited use of this production procedure. Very fast crystal growth, no wafer sawing necessary .
Polycrystalline ribbon Si	300µm	12%	Blue, with AR coating, silver-grey without AR coating	Limited use of this production procedure, no wafer sawing necessary. Decrease in production costs expected.
Apex (polycrystalline Si)	30 to 100µm + ceramic substrate	9.5%	Blue, with AR coating, silver-grey without AR coating	Single source wafer production procedure, no wafer sawing, production in form of band possible. Significant decrease in production costs.
Monocrystalline dendritic web Si	130µm incl contacts	13%	Blue, with AR coating	Limited use of this production procedure, no wafer sawing, production in form of band possible.
Amorphous silicon	0.1µm + 1 to 3mm substrate	5-8%	Red-blue, Black	Lower efficiency, shorter life span. No sawing necessary, production in the form of band.
Cadmium Telluride (CdTe)	8µm + 3mm glass substrate	6-9% (module)	Dark green, Black	Poisonous raw materials. High production costs.
Copper-Indium-Diselenide (CIS)	3µm + 3mm glass substrate	8-10% (module)	Black	Limited indium supply in nature. High production costs.
Hybrid silicon (HIT)	20µm	18%	Dark blue, black	Limited use of this production procedure, higher efficiency, better temperature coefficient, and lower thickness.

Example 27.8: ***PV cell open circuit voltage and short circuit current***

A 100mm by 100mm photocell (with 80% quantum efficiency) is illuminated by monochromatic light of 600 nm wavelength with a power density of 1000 W/m^2. The reverse saturation current I_o is 100 pA. Find

i. the short-circuit current.
ii. assuming zero internal resistance, the open-circuit voltage at 300 K.

Solution

i. The frequency that corresponds to light with 400 nm wavelength is

$$f = c/\lambda = 3\times10^8/600\times10^{-9} = 500\times10^{12} \quad \text{Hz}$$

The corresponding photon energy is

$$W_{ph} = hf = 6.62\times10^{-34}\times500\times10^{12} = 331\times10^{-21} \quad \text{J}$$

The light power density, P, is the product of the photon flux (number of photons per second per m^2) times the energy, W_{ph}, of each photon: $P=\varphi W_{ph}$, hence

$$\phi = P/W_{ph} == 1000/331\times10^{-21} = 3.0\times10^{21} \quad \text{photons/m}^2\text{s}$$

Each photon liberates 1 electron (100% quantum efficiency), thus for 80% quantum efficiency 0.8x2.0×10^{21} electrons m^{-2}s^{-1} are circulated. Since the area is 10^{-2}m^2, the current (viz. the cell short circuit current) is

$$I_{sc} = \eta_{q\,eff}\times\phi\times Area\times q = 0.8\times3.0\times10^{21}\times10^{-2}\times1.6\times10^{-19} = 3.90 \quad \text{A}$$

ii. Since there is no internal resistance of the photodiode or load resistance, I_{sc}= 2.57 A. The open-circuit voltage is

$$V_{oc} = kT/q\times\ell\text{n}\,I_{sc}/I_o = 0.026\times\ell\text{n}\,3.90/10^{-10} = 0.7 \quad \text{V}$$

♣

Example 27.9: ***PV cell maximum power and efficiency***

A photo-diode has an area of 10 by 10 mm and is illuminated by monochromatic light with a wavelength of 800 nm and with a power density of 1000 W/m^2. At 300 K, the open circuit voltage is 0.683 V.

Assuming an ideal diode, with 100% quantum efficiency, find:

i. the reverse saturation current, I_o.
ii. the load resistance that allows maximum power transfer.
iii. the efficiency of this cell at maximum power transfer.

Solution

The power is $P = 1000\text{W/m}^2\times0.01\text{m}^2 = 0.1\text{W}$

The frequency that corresponds to light with 800 nm wavelength is

$$f = c/\lambda = 3\times10^8/800\times10^{-9} = 3.75\times10^{12} \quad \text{Hz}$$

i. At 300K, kT/q=25.8mV, whence

$$V_{oc} = kT/q\times\ell\text{n}\,I_{sc}/I_o \text{ thus}$$

$$I_{sc}/I_o = \exp 0.638/0.0258 = 314\times10^9$$

The photon flux φ is

$$\phi = P/W_{ph} = P/hf = \frac{0.01\text{W}}{6.62\times10^{-34}\times375\times10^{12}} = 400\times10^{15} \quad \text{photons/m}^2\text{s}$$

With 100% quantum efficiency, each photon liberates the emission of 1 electron, thus

$$I_{sc} = q\phi = 1.6\times10^{-19}\times400\times10^{15} = 0.064\text{A}$$

$$I_o = \frac{0.064}{314\times10^{9}} = 0.2\times10^{-12}$$ that is the reverse saturation current is 0.2pA

ii. The load voltage corresponding to the maximum power output is given by

$$\left(1+\frac{qV_m}{kT}\right)exp\left(\frac{qV_m}{kT}\right) = {I_{sc}}/{I_o} + 1 \approx {I_{sc}}/{I_o} = 314\times10^{9}$$

Numerically solving gives V_m=0.60V. The load voltage (the cell voltage) is

$$V_L = V_m = {kT}/{q}\times\ell\,\text{n}\left(\frac{I_{sc}-I}{I_o}\right)$$ whence

The load current *I* is given by

$$I_m = I = I_{sc} - I_o\exp\left(\frac{qV_m}{kT}\right) = 0.064 - 0.2\times10^{-12}\exp\left(\frac{0.64}{0.0259}\right) = 80.0\text{mA}$$

The load resistance for maximum power is therefore

$$R_L = {V_m}/{\text{I}_\text{m}} = \frac{0.60\text{V}}{80\text{mA}} = 7.5\Omega$$

iii. At maximum power, with load resistance 7.5Ω

$$P_L = V_m I_m = 0.6\text{V}\times80\text{mA} = 48\text{mW}$$

The cell efficiency is therefore

$$\eta = \frac{P_L}{P} = \frac{48\times10^{-3}}{0.1} = 48\%$$

♣

Example 27.10: *PV cell electron excitation*

A filter transmits without attenuation wavelengths between 600 and 1000 nm. What is the maximum bandgap voltage of a PV cell that will absorb all photons that passes through the filter?

Solution

Photons with energies from

$$W_{g1} = {hf}/{q} = {hc}/{\lambda q} = \frac{6.63\times10^{-34}\times3\times10^{8}}{1000\times10^{-9}\times1.60\times10^{-19}} = 1.24\text{eV}$$

to

$$W_{g2} = {hf}/{q} = {hc}/{\lambda q} = \frac{6.63\times10^{-34}\times3\times10^{8}}{750\times10^{-9}\times1.60\times10^{-19}} = 1.63\text{eV}$$

can all excite PV materials with a bandgap of less than 1.24eV, for example Si. No interaction results if the bandgap of the material is greater than 1.63eV

♣

Example 27.11: *Fuel cell voltage*

A photodiode with a bandgap energy of Wg=1.4eV is exposed to monochromatic radiation of 500 THz, with a
power density *P*= 500w/m^2. The active area of the device is 100 by 100 mm.

The ideal device has internal series resistance of 2 mΩ. The temperature is 298 K, at which the open-circuit voltage is 0.555 V.

i. Estimate the short-circuit current
ii. The power does the diode delivers to a 200mΩ load
iii. The efficiency of the cell when sourcing the 200mΩ load

Solution

i. The photon flux is

$$\phi = P/hf = \frac{500\text{W}}{6.63\times10^{-34}\times500\times10^{12}} = 1.52\times10^{21}\text{photons/m}^2\text{s}$$

The short circuit current is

$$I_{sc} = q\phi A = 1.6\times10^{-19}\times1.52\times10^{21}\times0.1^2 = 2.43\text{A}$$

The internal resistance of 2mΩ, causes a 4.8mV voltage drop, which not significant with respect to the open circuit voltage of 0.555V, so the short circuit current is not significantly affected.

ii. For an open circuit voltage of 0.555V:

$$V_{oc} = kT/q\,\ell n\left(\frac{I_{sc}}{I_o}+1\right) = 0.555V$$

$$\frac{1.38\times10^{-23}\times298}{1.6\times10^{-19}}\ell n\left(\frac{2.43}{I_o}+1\right) = 0.555V$$

which gives a reverse saturation current of I_o=1.02nA. The load voltage is

$$V_L = kT/q\,\ell n\left(\frac{I_{sc}-I}{I_o}\right) - IR_{\text{int}} = IR_L$$

That is

$$I\left(R_L + I_{\text{int}}\right) = kT/q\,\ell n\left(\frac{I_{sc}-I}{I_o}\right)$$

$$I\left(200\text{m}\Omega + 2\text{m}\Omega\right) = 0.0259\ell n\left(\frac{2.43-I}{1.02\text{nA}}\right)$$

Solving for *I*, by trial and error, gives a load current of *I*=2.32A, corresponding to a load voltage of V_L=2.32Ax0.2Ω=0.464V and a load power of P_L=2.32Ax0.464A=1.08W.

iii. The input power is 500W/m^{2}x0.01m^2=5W. The efficiency when sourcing a 200m Ω load is:

$$\eta = \frac{P_L}{P} = \frac{1.08}{5} = 21.7\%$$

Example 27.12: ***PV cell efficiency factors***

True or false. The efficiency of a photocell rises when:

1. The operating temperature rises.
2. The operating temperature falls.
3. The light power density rises.
4. The light power density falls.

Solution

False, True, True, False

Example 27.13: ***PV cell efficiency factors***

Five identical photocells connected in series feed a single-cell water electrolyser. The system operates at 300 K, and the photocells are exposed to a light power density that causes a photon flux of 2.5×10^{21} photons /s m^2 to interact with the device. Quantum efficiency is 100%.
For each photocell, the reverse saturation current, Io, is 0.4μA. and the series resistance is 10 mΩ. The active area of the diode is 100 by 100 mm. The electrolyser can be represented by a 1.6 V voltage source, in series with 100 mΩ resistance.

i. What is the hydrogen production rate in grams/day
ii. What photon flux is sufficient to start the electrolysis?

Solution

i. The circuit model of a photodiode is the one shown in the figure. When delivering a current, IL, it will develop a voltage, VL:

$$V_L = kT/q\,\ell n\left(\frac{I_{sc}-I_L}{I_o}+1\right) - I_L R_{\text{int}}$$

The voltage delivered by 5 identical photocells in series is 5 times larger, $5V_L$. This voltage is applied to an electrolyser whose circuit model is shown in the next figure. The combined circuit model equation is

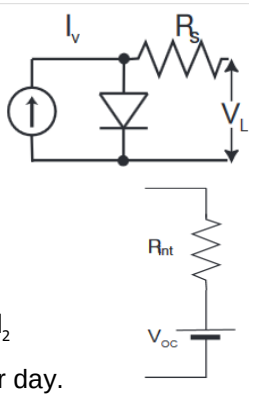

$$5\times\left[kT/q\,\ell n\left(\frac{I_{sc}-I_L}{I_o}+1\right) - I_L R_{\text{int}}\right] = I_L\times R_{ez\,\text{int}} + V_{ez}$$

where $I_{sc}=qA\Phi$=1.6x10^{-19}x10^{-2}x2.5x10^{21}=4A, thus

$$5\times\left[0.0259\ell n\left(\frac{4-I_L}{0.4\times10^{-6}}+1\right) - 0.01I_L\right] = 0.1\times I_L + 1.6$$

Numerical iteration yields I_L=2.43A.
The hydrogen production rate, N , is

$$N = I_L/qn_eN_o = \frac{2.43}{1.6\times10^{-19}\times2\times6.02\times10^{23}} = 1.26\times10^{-5}\ \text{moles/s of H}_2$$

This per second rate corresponds to 1.08 moles of H_2 per day or 2.16 grams of H_2 per day.

ii. As the photon flux is reduced, the current through the electrolyser reduces. The photon flux that causes $I_L\to0$ is at the limit of hydrogen production, so set I_L= 0 in

$$5\times\left[kT/q\,\ell n\left(\frac{I_{sc}-I_L}{I_o}+1\right) - I_L R_{\text{int}}\right] = V_{oc} = 5\times\left[0.0259\ell n\left(\frac{I_{sc}-0}{0.4\times10^{-6}}+1\right) - 0\times0.01\right] = 1.6$$

which yields I_{sc}=0.0887A. The photon flux needed to start electrolysis is

$$\phi_g = I_{sc}/qA = \frac{0.0887}{1.6\times10^{-19}\times10^{-2}} = 55\times10^{18}\quad\text{photons/s}$$

♣

Example 27.14: ***PV cell efficiency factors***

A fuel cell employs the gas reaction: A + B→AB

At STP, the thermodynamic data are

	ΔH_f	ΔS
	kJ/mol	J/K mol
A(g)	0	100
B(g)	0	150
AB(g)	-200	200

Find the reversible voltage of the fuel cell, where for each molecule of AB, 2 electrons flow in the load.

Solution

The enthalpy of formation ΔH_f of AB is 200kJ/mol.
The entropy of the reaction is 100+150=250 J/ K mol. So with 200 J/ K mol for the product, means 50 entropy units produce heat during the reaction, viz.

$$q = T\Delta S = 298.15\times50{,}000 = 14.91\ \text{kJ/mol of heat}$$

$$\Delta G = \Delta H - T\Delta S = -200-(-14.91) = -185.1\ \text{kJ/mol of product}$$

Since ΔG<0 the reaction is spontaneous and the reversible voltage (open circuit voltage) is

$$\Delta E = \Delta G/n_eq_eN_o = \frac{185.1\times10^3}{2\times1.6\times10^{-19}\times6.02\times10^{23}} = 0.960\text{V}$$

♣

Reading list

http://www.mpoweruk.com/
http://science.howstuffworks.com/solar-cell3.htm
http://photovoltaics.sandia.gov/
http://americanhistory.si.edu/fuelcells/index.htm
http://www1.eere.energy.gov
http://www.fctec.com/fctec_basics.asp
http://en.wikipedia.org/wiki/Solar_cell
http://www.pvresources.com/en/technologies.php
http://www.doitpoms.ac.uk/tlplib/index.php
http://www.fuelcells.org/info/

Problems

27.1 Consider the decomposition of H_2O_2 (hydrogen peroxide) at 298K and 1atm pressure according to:

$$2\ H_2O_2(\ell) \leftrightarrow 2\ H_2O(\ell) + O_2(g)$$

Substance	ΔG_f^o	ΔH_f^o	S^o
	kJ/mol	kJ/mol	J/ K.mol
$H_2O_2(\ell)$	-120.2	-187.6	109.5
$H_2O(\ell)$	-237.0	-285.8	69.4
$O_2(g)$	-	-	205

Find the
a) standard enthalpy of reaction.
b) standard entropy of reaction.
[-196.4 kJ; 125 J/K]

27.2. For the reaction in the previous question, find the
a) standard (Gibbs) free energy of reaction
b) the value of the (thermodynamic) equilibrium constant at 298 K, 1 atm
[-233.6 kJ; 8.85×10^{40}]

27.3. Carbon monoxide in the atmosphere slowly converts to carbon dioxide at normal atmospheric temperatures according to:

$$CO(g) + ½\ O_2(g) \leftrightarrow CO_2(g)$$

The standard enthalpy of reaction is -284 kJ and the standard entropy of reaction is -87 J/K. Estimate the temperature at which the equilibrium begins to favour the decomposition of CO_2. Assume that the enthalpy and the entropy of reaction are not affected by temperature.
[3260 K or 3300 K]

27.4. Indicate if TRUE or FALSE:

The entropy of a gas increases with increasing temperature.
The energy of a perfect crystal is zero at 0 K.
Spontaneous processes always increase the entropy of the reacting system.
All spontaneous processes release heat to the surroundings.
An endothermic reaction is more likely to be spontaneous at high temperatures than at low temperatures.
The entropy of sugar decreases as it precipitates from an aqueous solution.

[T F F F T T]

27.5. For each type of fuel cell below, what are the charge carrying species, i.e., electrolyte type?

(a) Polymeric exchange membrane
(b) Immobilised alkaline solution
(c) Direct methanol
(d) Phosphoric acid
(e) Molten carbonate
(f) Ceramic solid oxide

[H^+, OH^-, H^+, H^+, CO_3^{2-}, O^{2-}]

27.6. Which cells in question 27.5 are able to internally reform?

[High temperature, molten carbonate and solid oxide cells.]

27.7. The efficiency limit (voltage) of H_2 cells reduces as operating temperature is increased. Why are high efficiency systems often run at high temperatures?

[The heat produced can be more useful than the efficiency gained at lower temperatures. Running a system at a higher temperature allows the hot exhaust gasses to be utilised in a turbine-hybrid system, raising the overall efficiency of the system can be in excess of 80%.]

27.8. Give two reasons why fuel cells are not currently used in cars.

[(i) High temperature fuel cells are not easily portable and low temperature ones require hydrogen as the fuel in order to produce any useful power. Hydrogen is not yet a readily available fuel. It is also difficult to store.
(ii) Fuel cells also suffer from low reaction rates and therefore low power output.]

27.9. Why are nickel anodes used in SOFCs? How is it treated in order to aid bonding to YSZ?

[It is cheap and although it functions effectively, it flakes off unless mixed with zirconia.]

27.10. Give three ways to provide a mobile fuel cell with pure hydrogen.

[(i) Pure H_2 may be stored as used either under pressure, cryogenically, in a metal hydride, in a high surface area carbon nano-tube arrangement or even in glass nano-spheres.
(ii) Many fuels may be carried and reformed before use e.g. alcohols, alkali metal hydrides, ammonia, sodium borohydride, methane and even hydrazine.
(iii) Alternately the cell could be run directly on methanol.]

27.11 The following figure shows two *I-V* curves. One is for a PV cell with an equivalent circuit having no (infinite) parallel resistance.
What is the equivalent circuit parallel resistance of the other cell?

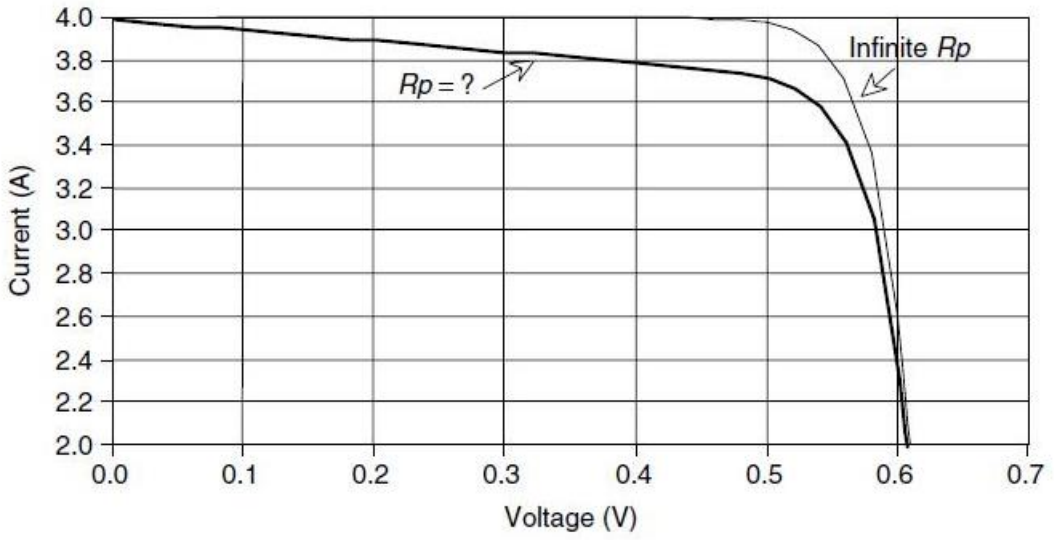

27.12 The following figure shows two *I-V* curves. One is for a PV cell with an equivalent circuit having no (zero) series resistance.
What is the equivalent circuit series resistance of the other cell?

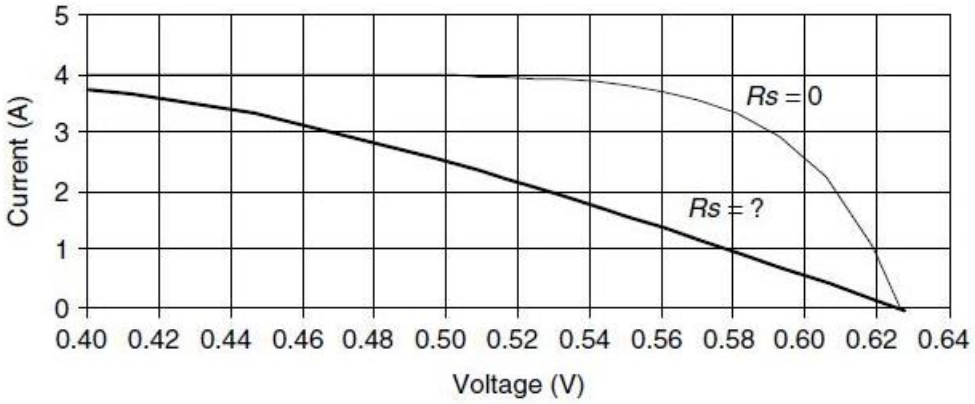

27.13 Estimate the cell temperature and power delivered by a 100W PV module under the following conditions. Assume 0.5%/°C power loss.

i. NOCT=50°C, ambient temperature=25°C, insolation=1 sun
ii. NOCT=45°C, ambient temperature=0°C, insolation=500W/m^2
iii. NOCT=45°C, ambient temperature=3°C, insolation=800W/m^2

Energy transformations for electrical or mechanical output

Fuel Cell:

Battery:

Heat Engine: